

Volume 2
Issue 2

Volume 02 Issue 02 N° ISSN 2253-0665 (2014)

Depot legal N° 5805-2012

MOMA

Models, Optimisation and Mathematical Analysis

Journal

Editor-In-Chief

Dr. Mostefa BELARBI

Edition comity

Abdelkader SENOUCI	University of Tiaret- Algeria
Abdelkader CHAIB	Univ. Centre of Tissemsilt – Algeria
Djamel TURKI	University of Tiaret- Algeria
Hayat DAOUD	University of Tiaret- Algeria
Sabrina AMAR	University of Tiaret- Algeria
Chahrazed ADDA	University of Tiaret- Algeria
Abdelhamid HARICHE	University of Tiaret- Algeria
Abdelmalek ABID	University of Tiaret- Algeria
Imane ZOUANE	University of Tiaret- Algeria

2014

Message of MOMA Journal Editor-In-Chief

This journal concerns both the national and international scientific community and will be primarily focusing on Models and Optimisation of Systems. Systems will be utilized in different applications for example, Web technologies, Information Systems, Decision Systems, Embedded Systems, Control-command Systems and Real-time Systems. Space of journal is also dedicated to mathematical analysis like functional spaces, polynomial computing etc.

The edited selected papers include classification with support vector machines, new quadratic programming algorithm, modeling of recommender systems through resource description framework, spectral analysis of ferrous metal based on neural networks, numerical modelling of the response hydromécanique around a tunnel (example of application: algiers metro), parametric study of the mechanical response around a tunnel (example of application: algiers metro), validating timing and scheduling marte's profils using event b: case study of a GPU architecture? A numerical investigation of the performance analysis of an electrorheological hydrostatic journal bearing, Local Search Heuristic for Multiple Knapsack Problem .

And finally numerical physics systems simulation electronic properties of sral2h2 for hydrogen storage, study of structural, electronic and optical properties of the chalcopyrite aggase2.

We would like to express our gratitude to everyone who has contributed towards the success of this edition.

Special thanks to the institution of Ibn khaldoun University of Tiaret to accept to support publication charges of the present issue.

Mostefa BELARBI
Editor-In-Chief of MOMA Journal

Table of Contents

Message of Editor-In-Chief

Classification with Support Vector Machines, New Quadratic Programming Algorithm

A.Chikhaoui, A. Mokhtari 01

Modeling of recommender systems through Resource Description Framework

S.Kharroubi , Y.Dahmani , O.Nouali 07

Spectral Analysis of Ferrous Metal Based on Neural Networks

A. TIFFOUR , M. BELARBI 15

Numerical Modelling of the Response Hydromécanique around a Tunnel

(Example of application: Algiers metro)

H.Ouabel 19

Parametric study of the mechanical response Around a Tunnel (Example of application:

Algiers metro)

H. Ouabel 26

Validating Timing and scheduling MARTE's profils using Event B: case study

of A GPU architecture

I. Zouaneb, M.Belarbi,Chouarfia Abdellah 30

A numerical investigation of the performance analysis of an electrorheological hydrostatic journal bearing

Abed N, Zahloul H 44

Local Search Heuristic for Multiple Knapsack Problem

BALBAL Samir, LAALAOUI Yacine, BENYETTOU Mohamed 50

Electronic properties of SrAl₂H₂ for hydrogen storage

K. Khodja, Y. Bouhadda 54

Study of structural, electronic and optical properties of the chalcopyrite AgGaSe₂

M.Azzouza, D.Kadria, B.Djeboura, D.Karouma, R Ascaria 59

Classification with Support Vector Machines, New Quadratic Programming Algorithm

¹A.Chikhaoui, ²A. Mokhtari,

¹University of Tiaret Algeria, ²University of Laghouat Algeria,
ah_chikhaoui@yahoo.fr, Aek_Mokhtari@yahoo.fr

Abstract-Support vector machines (SVM) are excellent tools for classification and regression. They seek the optimal separating hyperplan and maximal margin. The modeling results often lead to solving a quadratic programming problem. In this paper, we present a simple method to determine the hyperplan H that separates two classes of examples so that the distance between these two classes is maximal. This method is based on the geometric interpretation of the norm of a linear mapping. The result model of our algorithm modeling is a maximization of a concave quadratic program. This quadratic program is resolved by projection method. Example illustrates the method.

Keywords

Support vector machines, separating hyperplan, maximizing concave function, cosine, projection method.

1 Introduction

Learning to rank is an important problem in web page ranking information retrieval and other applications. Support Vector Machines (SVMs) are a powerful machine learning technique. Vapnik [7] showed how training a support vector machine for the pattern recognition problem leads to quadratic optimization problem (QP). The size of the optimization problem depends on the number of training examples. With 10000 training examples and more it becomes impossible to keep matrix data in memory. SVM^{Light} uses the decomposition idea of Osuna and al. ([7]) and decompose the problem into a series of smaller tasks. This decomposition splits the initial problem in an inactive and en active part. These algorithms may need a long training time. To tackle this problem, T. Joachims [5], uses a method for selecting the working set, successive “shrinking” of the optimization problem and incremental updates of the gradient (Joachims [6]). Burges form AT&T [1], has even developed a QP solver specifically for training SVM.

In this paper we introduce new support vector machines method in order to define a decision

surface separating two opposing classes of a training set of vectors.

This method associates a distance parameter with each vector of the SVM’s training set. The distance parameter is calculating as the shortest of distances from each vector of one class to the opposite class. The method determines initial separating hyperplan and its maximum margin, where the margin is defined as the shortest distances of the hyperplan from the closest points of the two classes. The optimal vectors to preselect as potential support vectors are those closest to the decision hyperplan. The vectors with the smallest distance are then selected as pivots.

To determine the optimal hyperplan, we will use the well-known result:

if f is a linear map from R^n into R defined by $f(x) = \langle a, x \rangle$, $a \in R^n$.

Then $\|a\| = d(0, H)$ where H is the hyperplan defined by $H = \{x \in R^n : \langle a, x \rangle = 1\}$.

The optimal hyperplan will be a boundary point of the set of feasible solutions which can be an extreme point.

2 Partition of examples \tilde{X}_+ and \tilde{X}_-

Suppose that separating hyperplan with maximum margin be written as $ax + b = 0$.

2.1 Formulation of the optimization problem

The inequalities $ax + b \geq 1$ and $ax + b \leq -1$ become $\frac{a}{2}x_+ + \frac{b}{2} \geq \frac{1}{2}$ and $\frac{a}{2}x_- + \frac{b}{2} \leq -\frac{1}{2}$, and the hyperplan is $\frac{a}{2}x + \frac{b}{2} = \frac{1}{2}$; i.e. $ax + b = 0$. As the couple (a, b) is set to a multiplicative coefficient,

the separating problem becomes then

$$\begin{cases} \inf \|a\|^2 \\ ax_+ + b \geq \frac{1}{2} \\ ax_- + b \leq -\frac{1}{2} \end{cases}$$

Suppose that \bar{x}_+ is support vector, $a\bar{x}_+ + b = \frac{1}{2}$

$$\Rightarrow b = \frac{1}{2} - a\bar{x}_+$$

Then $ax_+ + b \geq \frac{1}{2} \Leftrightarrow$

$$ax_+ + \frac{1}{2} - a\bar{x}_+ \geq \frac{1}{2} \Leftrightarrow a(x_+ - \bar{x}_+) \geq 0$$

$$\Leftrightarrow a(\bar{x}_+ - x_+) \leq 0 \quad \text{and}$$

$$ax_- + b \leq -\frac{1}{2} \Leftrightarrow ax_- + \frac{1}{2} - a\bar{x}_+ \leq -\frac{1}{2} \Leftrightarrow a(x_- - \bar{x}_+) \leq -1.$$

$$\text{Then } \begin{cases} \inf \|a\|^2 \\ a(\bar{x}_+ - x_+) \leq 0 \\ a(x_- - \bar{x}_+) \leq -1 \end{cases} = \begin{cases} -\text{Max}\{-\|a\|^2\} \\ a(\bar{x}_+ - x_+) \leq 0 \\ a(x_- - \bar{x}_+) \leq -1 \end{cases}$$

and consequently, the separating problem becomes

$$(P) = \begin{cases} \text{Max}\{-\|a\|^2\} \\ \Omega = \begin{cases} a(\bar{x}_+ - x_+) \leq 0, & x_+ \in X_+ \\ a(x_- - \bar{x}_+) \leq -1, & x_- \in X_- \end{cases} \end{cases},$$

$f(a) = \sum_{i=1}^n -a_i^2 = -\|a\|^2$ is concave, defined on

closed bounded convex of R^n , then the local maximum is global, but $\frac{\partial f}{\partial a_i}(a) = 0$ for all i ,

$$\Rightarrow 2a_i = 0, \quad a_i = a_i^* = 0.$$

The critical point $a^* = 0 \in R^n$ is not feasible solution, then the solution of the problem is the projection of $a^* = 0$ on Ω . This is a particular case of general optimization problem of concave quadratic programming, where

$$\alpha_i = 0, \beta_i = 1, a^* = -\frac{\alpha_i}{2\beta_i} = 0.$$

This problem of maximizing concave quadratic function under linear constraints has solved by Chikhaoui and all. [3]. It is noted that

$$P_{a(\bar{x}_+ - x_+)}(\mathbf{0}) = \mathbf{0}.$$

This was made possible through the form

$$\begin{cases} \frac{a}{2}x_+ + \frac{b}{2} \geq \frac{1}{2} \\ \frac{a}{2}x_- + \frac{b}{2} \leq -\frac{1}{2} \end{cases}, \text{ this minimize the computing}$$

time.

Increase in a margin.

Let (H) the separating hyperplan of wide margin of equation $ax + b = 0$.

We know that for all $x_+ \in X_+, x_- \in X_-$, we

$$\text{have } \begin{cases} \frac{a}{2}x_+ + \frac{b}{2} \geq \frac{1}{2} \\ \frac{a}{2}x_- + \frac{b}{2} \leq -\frac{1}{2} \end{cases}$$

$$\Rightarrow \begin{cases} ax_+ + b \geq \frac{1}{2} \\ -ax_- - b \geq +\frac{1}{2} \end{cases} \Rightarrow (ax_+ + b) + (-ax_- - b) \geq \frac{1}{2} + \frac{1}{2}$$

; from where

$$a(x_+ - x_-) \geq 1, \quad \forall x_+ \in X_+, \forall x_- \in X_-.$$

By the inequality of Cauchy Schwartz,

$$\frac{1}{\|a\|} \leq \|x_+ - x_-\|, \quad \forall x_+ \in X_+, \forall x_- \in X_-,$$

by passing to the lower bound, we obtain

$$\frac{1}{\|a\|} \leq \inf_{x_+ \in X_+, x_- \in X_-} \|x_+ - x_-\|.$$

Whence important proposal:

$$\text{Let } \tilde{H}_+ = \{x \in R^n : ax - a\bar{x}_+ = 0\},$$

$$\tilde{H}_- = \{x \in R^n : ax - a\bar{x}_- = 0\}.$$

Proposal:

The width of the strip is increased by the constant $K = \inf_{x_+ \in X_+, x_- \in X_-} \|x_+ - x_-\|$, and this is best constant.

Proof: Indeed, suppose x_+, x_- are two support vectors, i.e. $x_+ \in \tilde{H}_+, x_- \in \tilde{H}_-$;

$$d(x_+, \tilde{H}_+) = \frac{ax_+ + b}{\|a\|} = \frac{1}{2} \cdot \frac{1}{\|a\|},$$

$$d(x_-, \tilde{H}_-) = \frac{|ax_- + b|}{\|a\|} = \frac{1}{2} \cdot \frac{1}{\|a\|}$$

$$\Rightarrow d(x_+, \tilde{H}_+) + d(x_-, \tilde{H}_-) = \frac{1}{\|a\|}, \quad \text{and}$$

$$\frac{1}{\|a\|} \leq \inf_{x_+ \in X_+, x_- \in X_-} \|x_+ - x_-\| = K.$$

This is the best ever because in cases where $\tilde{X}_+ = \{x_+\}$ and $\tilde{X}_- = \{x_-\}$, then

$$\frac{1}{\|a\|} = \inf_{x_+ \in X_+, x_- \in X_-} \|x_+ - x_-\| = K; \quad \text{this completes the proof.}$$

We see that the margin width does not exceed $\|x_+ - x_-\|$.

This leads us to consider the separating hyperplan with the widest possible margin \tilde{H} .

2.2 Partition of X_+ and X_-

$$\text{Let } \inf_{x_+ \in X_+, x_- \in X_-} \|x_+ - x_-\| = \|\bar{x}_+ - \bar{x}_-\|,$$

$$\tilde{a} = \bar{x}_+ - \bar{x}_-,$$

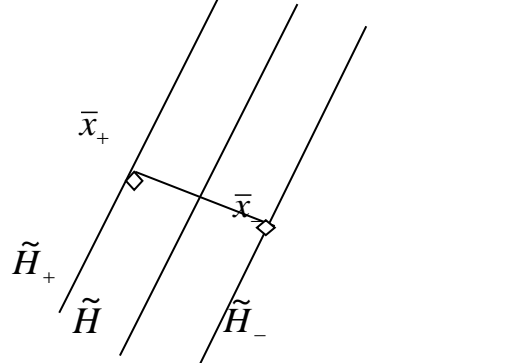
$$\tilde{H}_+ = \{x \in R^n : \tilde{a}x - \tilde{a}\bar{x}_+ = 0\},$$

$$\tilde{H}_- = \{x \in R^n : \tilde{a}x - \tilde{a}\bar{x}_- = 0\},$$

$$\tilde{H} = \left\{ x \in R^n : \tilde{a}x - \left(\frac{\tilde{a}\bar{x}_+ + \tilde{a}\bar{x}_-}{2} \right) = 0 \right\}$$

$$= \left\{ x \in R^n : (\bar{x}_+ - \bar{x}_-)x - \frac{(\bar{x}_+ - \bar{x}_-)(\bar{x}_+ + \bar{x}_-)}{2} = 0 \right\}$$

$$= \left\{ x \in R^n : (\bar{x}_+ - \bar{x}_-)x + \frac{\|\bar{x}_-\|^2 - \|\bar{x}_+\|^2}{2} = 0 \right\}$$



The existence of optimal separating hyperplan H , and construction of \tilde{H} define a partition of X_+ and a partition of X_- :

$$\tilde{X}_+ = \left\{ x \in X_+ : ax - a\bar{x}_+ < \frac{1}{2} \right\},$$

$$X_+ = \tilde{X}_+ \cup (X_+ / \tilde{X}_+)$$

$$\tilde{X}_- = \left\{ x \in X_- : ax - a\bar{x}_- > -\frac{1}{2} \right\},$$

$$X_- = \tilde{X}_- \cup (X_- / \tilde{X}_-)$$

If the hyperplans H and \tilde{H} separate the sets X_+ / \tilde{X}_+ and X_- / \tilde{X}_- and \tilde{H} is optimal.

$\tilde{X}_+ = \tilde{X}_- = \phi$ then $H = \tilde{H}$. Stop.

3 Finding Optimal separating hyperplan H : case $H \neq \tilde{H}$

The maximum margin separating \tilde{X}_+ and \tilde{X}_- is greater than or equal to the maximum margin separating X_+ and X_- because the optimal separating hyperplan H separates \tilde{X}_+ and \tilde{X}_- .

Suppose that the maximum margin between \tilde{X}_+ and \tilde{X}_- is strictly greater than that between X_+ and X_- , then this separating hyperplan is between H and \tilde{H} and hence it separates X_+ / \tilde{X}_+ and X_- / \tilde{X}_- . So this separating hyperplan separates X_+ and X_- with a wider margin than strictly greater than that to H . Contradiction, because H is optimal.

Proposition:

The optimal separating hyperplan of sets \tilde{X}_+ and \tilde{X}_- is optimal separating hyperplan for sets X_+ and X_- .

Proof: Denote by H^* optimal separating hyperplan of \tilde{X}_+ and \tilde{X}_- whose normal is a^* . There positive $\lambda_1!$ and $\lambda_2!$ such that $a^* = \lambda_1 a + \lambda_2 \tilde{a}$.

$$\text{In fact, } \begin{cases} \langle a, a^* \rangle = \|a\| \|a^*\| \cos \alpha \\ \langle \tilde{a}, a^* \rangle = \|\tilde{a}\| \|a^*\| \cos \beta \end{cases}$$

$$\begin{aligned} \langle a, \lambda_1 a + \lambda_2 \tilde{a} \rangle &= \|a\| \|a^*\| \cos \alpha \\ \Rightarrow \lambda_1 \langle a, a \rangle + \lambda_2 \langle a, \tilde{a} \rangle &= \|a\| \|a^*\| \cos \alpha \\ \Rightarrow \lambda_1 \|a\|^2 + \lambda_2 \langle a, \tilde{a} \rangle &= \|a\| \|a^*\| \cos \alpha. \end{aligned}$$

As well

$$\begin{aligned} \langle \tilde{a}, \lambda_1 a + \lambda_2 \tilde{a} \rangle &= \|\tilde{a}\| \|a^*\| \cos \beta \\ \Rightarrow \lambda_1 \langle \tilde{a}, a \rangle + \lambda_2 \langle \tilde{a}, \tilde{a} \rangle &= \|\tilde{a}\| \|a^*\| \cos \beta \end{aligned}$$

$$\Rightarrow \lambda_1 \langle \tilde{a}, a \rangle + \lambda_2 \|\tilde{a}\|^2 = \|\tilde{a}\| \|a^*\| \cos \beta. \quad \text{Then}$$

$$\begin{cases} \lambda_1 \|a\|^2 + \lambda_2 \langle a, \tilde{a} \rangle = \|a\| \|a^*\| \cos \alpha \\ \lambda_1 \langle \tilde{a}, a \rangle + \lambda_2 \|\tilde{a}\|^2 = \|\tilde{a}\| \|a^*\| \cos \beta \end{cases}$$

Where θ is the angle formed between hyperplanes H and \tilde{H} , as $H \neq \tilde{H}, \theta \neq 0$;

then $\cos \theta \neq 1$, and $\Delta = \|a\|^2 \|\tilde{a}\|^2 (1 - \cos^2 \theta). \quad \Delta > 0$

The system has a unique solution λ_1 and λ_2 .

Then suppose that the margin of H^* is strictly greater than that of H , as H and \tilde{H} separate X_+ / \tilde{X}_+ and X_- / \tilde{X}_- . i.e. a and \tilde{a} are solution of problem

$$\left\{ \begin{array}{l} \text{Max}_{\Omega} \{ -\|a\|^2 \} \\ \Omega = \begin{cases} a(-x_+ + \bar{x}_+) \leq 0 \\ a(x_- - \bar{x}_+) \leq -1 \\ \bar{x}_+ \in X_+ / \tilde{X}_+ \\ \bar{x}_- \in X_- / \tilde{X}_- \end{cases} \end{array} \right.$$

Ω' is bounded below convex, then $a^* \in \Omega'$.

The separating hyperplan H^* separates then X_+ and X_- whose margin is strictly greater than that of H . Contradiction, H is optimal by hypothesis.

Consequence:

To separate X_+ and X_- , just separate the sample \tilde{X}_+ and \tilde{X}_- . We then have a smaller number of constraints.

Example1.

$$X_+ = \left\{ (1,0), \left(2, \frac{3}{2}\right), (5,1), \right\}$$

$$X_- = \{(0,1), (-2,1), (-2,2),\}$$

Here,

$$\inf_{\substack{x_+ \in X_+ \\ x_- \in X_-}} (\|x_+ - x_-\|) = \|(1,0) - (0,1)\| = \sqrt{2};$$

$$x_+ = (1,0), \quad x_- = (0,1)$$

$$\tilde{a} = (x_+ - x_-) = (1,-1)$$

$$\tilde{H}_+ : (1,-1)x - (1,-1)(0,0) = 0$$

$$\tilde{H}_+ : x_1 - x_2 - 1 = 0$$

$$\tilde{H}_- : x_1 - x_2 + 1 = 0 \quad \tilde{H} : x_1 - x_2 = 0.$$

$$\left(2, \frac{3}{2}\right) \in \tilde{X}_+ \text{ car } 2 - \frac{3}{2} - 1 = -\frac{1}{2} < \frac{1}{2},$$

$$(5,1) \notin \tilde{X}_+ \text{ car } 5 - 1 - 1 = 3 > \frac{1}{2}$$

$$\Rightarrow \tilde{X}_+ = \left\{ (1,0), \left(2, \frac{3}{2}\right) \right\}$$

$$(-2,1) \notin \tilde{X}_- \quad \text{because}$$

$$-2 - 1 + 1 = -2 < -\frac{1}{2},$$

$$(-2,2) \notin \tilde{X}_- \quad \text{because}$$

$$-2 - 2 + 1 = 3 < -\frac{1}{2}$$

$$\Rightarrow \tilde{X}_- = \{(0,1)\}.$$

The constraint set Ω , of problem becomes

$$\begin{cases} a \left((1,0) - \left(2, \frac{3}{2}\right) \right) \leq 0 \\ a \left((0,1) - (1,0) \right) \leq -1 \end{cases} \quad \text{the solution is}$$

$$\begin{cases} 2a_{11} + 3a_{12} = 0 \\ a_{11} + a_{12} + 1 = 0 \end{cases} \Rightarrow \begin{cases} a_{11} = \frac{3}{5} \\ a_{12} = -\frac{2}{5} \end{cases}. \quad (H)$$

has the equation

$$\left(\frac{3}{5}, -\frac{2}{5}\right)(x_1, x_2) + \left(\frac{1}{2} - \left(\frac{3}{5}, -\frac{2}{5}\right)\right)(1,0) = 0,$$

$$H : \frac{3}{5}x_1 - \frac{2}{5}x_2 - \frac{1}{10} = 0.$$

4 Projection Method ([2])

Consider the problem quadratic result of our

$$\Delta = \frac{\|a\|^2 \langle a, \tilde{a} \rangle}{\langle \tilde{a}, a \rangle \|\tilde{a}\|^2} = \|a\|^2 \cdot \|\tilde{a}\|^2 - \langle a, \tilde{a} \rangle \langle \tilde{a}, a \rangle = \|a\|^2 \|\tilde{a}\|^2 - \|a\|^2 \|\tilde{a}\|^2 \cos^2 \theta$$

modeling:

$$(P) = \begin{cases} \text{Max}_{\Omega} \{-\|a\|^2\} \\ \Omega = \left\{ a \in \mathbb{R}^n, \begin{pmatrix} a(-x_+ + \bar{x}_+) \leq 0 \\ a(x_- - \bar{x}_-) \leq -1 \end{pmatrix}, x_+ \in \tilde{X}_+, x_- \in \tilde{X}_- \right\} \end{cases}$$

Since the function $f(x) = \sum_{i=1}^n -a_i^2 = -\|a\|^2$ is concave defined on a closed convex of \mathbb{R}^n , then the local maximum of f is global. But $\frac{\partial f}{\partial a_i}(a) = 0$,

$$\Leftrightarrow a_i = 0 \quad i=1,2,\dots,n$$

Critical point $(a_i^*)_i = 0$ for all $i=1,2,\dots,n$ is not feasible solution of problem (P) .

Then the solution of problem (P) is the projection of point $0 \in \mathbb{R}^n$ on Ω .

This is a particular case of more general problem of quadratic optimization:

$$f(a) = \sum_{i=1}^n \alpha_i a_i + \sum_{i=1}^n \beta_i a_i^2 \quad \text{with } \alpha_i \in \mathbb{R}, \beta_i < 0 \text{ for all } i,$$

under linear constraints.

In classification with SVM we have

$$a^* = \begin{pmatrix} -\alpha_i \\ 2\beta_i \end{pmatrix}_i \text{ with } \alpha_i = 0, \forall i \quad \beta_i = -1. \quad \text{For more}$$

details see [3]. We recall that if a concave function f defined on closed convex and that the critical point does not belong to convex, then the maximum of f is reached on a boundary point of closed convex. See [3].

The projection of point $0 \in \mathbb{R}^n$ on the hyperplan $a(x_- - \bar{x}_-) = -1$ is given by

$$P_{a(x_- - \bar{x}_-) = -1}(0) = 0 - \frac{1}{\|(x_- - \bar{x}_-)\|^2} (x_- - \bar{x}_-).$$

Example1

$$X_+ = \{(1,3), (1.5,4), (2,3), (3,3.5), (3,4)\}$$

$$X_- = \{(1,1.5), (1.5,1), (2,1), (2,2), (2.5,1.5)\}.$$

$$\inf_{\substack{x_+ \in X_+ \\ x_- \in X_-}} (\|x_+ - x_-\|) = \|(2,3) - (2,2)\| = 1;$$

$$x_+ = (2,3), \quad x_- = (2,2)$$

$$\tilde{a} = (x_+ - x_-) = (2,3) - (2,2) = (0,1)$$

$$\tilde{H}_+ : (0,1)(x_1, x_2) + \left(\frac{1}{2} - (0,1)(2,3) \right) = \frac{1}{2}$$

$$\Rightarrow \tilde{H}_+ : x_2 - 3 = 0$$

$$\tilde{H}_- : (0,1)(x_1, x_2) + \left(-\frac{1}{2} - (0,1)(2,2) \right) = -\frac{1}{2}$$

$$\Rightarrow \tilde{H}_- : x_2 - 2 = 0$$

$$\tilde{H} : (0,1)(x_1, x_2) + \left(\frac{-3-2}{2} \right) = 0$$

$$\Rightarrow \tilde{H} : x_2 - \frac{5}{2} = 0$$

Construction of \tilde{X}_+ and \tilde{X}_-

$$(1,3) \in \tilde{X}_+ \quad \text{because} \quad 3-3 \leq 0$$

$$(1.5,4) \notin \tilde{X}_+ \quad \text{because} \quad 4-3 \not\leq 0$$

$$(2,3) \in \tilde{X}_+ \quad \text{because} \quad 3-3 \leq 0$$

$$(3,3.5) \notin \tilde{X}_+ \quad \text{because} \quad 3.5-3 \not\leq 0$$

$$(3,4) \notin \tilde{X}_+ \quad \text{because} \quad 4-3 \not\leq 0$$

$$(1,1.5) \notin \tilde{X}_- \quad \text{because} \quad 1.5-2 \not\geq 0$$

$$(1.5,4) \notin \tilde{X}_+ \quad \text{because} \quad 4-3 \not\geq 0$$

$$(2,3) \in \tilde{X}_+ \quad \text{because} \quad 3-3 \leq 0$$

$$(3,3.5) \notin \tilde{X}_+ \quad \text{because} \quad 3.5-3 \not\geq 0$$

$$(3,4) \notin \tilde{X}_+ \quad \text{because} \quad 4-3 \not\geq 0$$

$$\text{Then } \tilde{X}_+ = \{(2,3), (1,3)\} \quad \tilde{X}_- = \{(2,2)\}$$

Constraints are:

$$\begin{cases} a((2,2) - (2,3)) \leq -1 & \Leftrightarrow a_2 \geq 1 \\ a((2,1) - (2,3)) \leq -1 & \Leftrightarrow a_2 \geq \frac{1}{2} \end{cases}$$

$$P_{a_2=1}(0) = 0 - \frac{-1}{1}(0,1) = (0,1) \quad \Rightarrow \|P_{a_2=1}(0)\| = 1$$

$$P_{a_2=\frac{1}{2}}(0) = 0 - \frac{-1}{1}(0,1) = \left(0, \frac{1}{2}\right) \quad \Rightarrow \|P_{a_2=\frac{1}{2}}(0)\| = \frac{1}{4}$$

The solution is $a = (0,1)$, because

$a = \left(0, \frac{1}{2}\right)$ is not feasible solution, and the optimal separating hyperplan is:

$$H : (0,1)(x_1, x_2) + \left(\frac{1}{2} - (0,1)(2,3)\right) = \frac{1}{2}$$

$$\Rightarrow x_2 - \frac{5}{2} = 0.$$

Remark: The feasible solution set of separating hyperplans is the half-space $a_2 \geq 1$ and the projection of 0 on this half-space is $(0,1)$. The set of feasible solutions do here no extreme point. It is interesting to study the nature of the set of separating hyperplans.

Example

$$X_+ = \left\{ \left(2, 2, \frac{1}{2}\right), (2, 3, 2), (3, 3, 1) \right\}$$

$$X_- = \left\{ \left(1, 0, \frac{1}{2}\right), (1, -1, 3) \right\}$$

$$\inf_{\substack{x_+ \in X_+ \\ x_- \in X_-}} \|x_+ - x_-\| = \|(2, 2, 0.5) - (1, 0, 0.5)\| = \sqrt{5}$$

$$x_+ = (2, 2, 0.5), \quad x_- = (1, 0, 0.5)$$

$$\tilde{a} = (x_+ - x_-) = (1, 2, 0)$$

$$\tilde{H} : (1, 2, 0)(x_1, x_2, x_3) - \frac{3}{2} = 0$$

$$\tilde{X}_+ = \left\{ \left(2, 2, \frac{1}{2}\right) \right\} \quad \tilde{X}_- = \left\{ \left(1, 0, \frac{1}{2}\right) \right\}. \text{ Here, in-}$$

side of band is empty. So $(\tilde{H}) = (H)$.

5 Conclusion

In this paper, we gave a geometric interpretation of the hyperplan that separates two classes linearly separable. In fact, the search algorithm to the optimum is nothing other than a particular case of general optimization problem:

$$\begin{cases} \sum_{i=1}^n \alpha_i x_i + \beta_i x_i^2, & \text{with } \alpha_i = 0, \beta_i = -1 \\ Ax \leq b \end{cases}$$

The nature of solution (extreme point or not) provides to better track the support vectors.

6 References

1. Burges C. J.C. 1998. A Tutorial on Support Vector machines for Pattern Recognition. *Data Mining and Knowledge Discovery*, 2(2): 121-167.
2. Chikhaoui A, Djebbar B., Bellabacci A, Mokhtari A., 2009. Optimization of a quadratic function under its Canonical form *Asian Journal of Applied Sciences* 2(6):499-510

3. Chikhaoui A, Djebbar B., and Mekki R., 2010. New Method for Finding an Optimal Solution to Quadratic Programming Problem, *Journal of Applied Sciences* 10(15):1627- 1631-2010. ISSN 1812-5654.
4. Chikhaoui A, Bellabacci A, Mokhtari A., 2012. New Algorithm for maximizing of linearly constrained convex quadratic programming. *IRECOS Vol 7*, ISSN 1828-6003.
5. Joachims T., 2003, Making Large-Scale SVM Learning practical, *Advances in kernel methods-support learning*. Page 169-184. MIT Press.
6. Joachims, T., Granka, L., Pan, Bing, Hembrooke, H., Radlinski, F., and Gay, G. Evaluating the accuracy of implicit feedback from clicks and query reformulations in web search. *ACM Transactions on Information Systems (TOIS)*, 25(2), April 2007.
7. Osuna, E., Freund, R. and Girosi, F. An improved training algorithm for support vector machines. In *Proceedings of the 1997 IEEE Workshop on Neural Networks for Signal Processing*, Eds. J. Principe, L. Giles, N. Morgan,
8. Vapnik, V.N., 1998, *Statistical learning theory*. John Wiley & Sons.
9. N.M., Deris S. and Chin K.K., 2003, A comparison of support vector machines training. *Jurnal Teknologi*, Vol 39, pp 45-56.
10. Wilson E., pages 276 – 285, Amelia Island, FL, 1997.

Modeling of recommender systems through Resource Description Framework

KHARROUBI Sahraoui¹, DAHMANI Youcef², NOUALI Omar³

¹Ibn Kahldoun University Tiaret, ALGERIA, sahraouikharoubi@gmail.com

²Ibn Kahldoun University Tiaret, ALGERIA, dahmeni_y@yahoo.fr

³Basic Software Laboratory, C.E.R.I.S.T, Ben Aknoun, ALGERIA, onouali@cerist.dz.

Abstract-Faced with problems of informational overload on a dynamic, distributed and heterogeneous web, current research aims to design and develop recommender systems that are mainly based on techniques of information filtering. In this paper, we propose a hybrid modeling of recommendation systems by formalizes resources description framework (RDF), while based on the integration of elements of the Dublin Core (DC) describing resources and the vocabulary Friend of A Friend (FOAF) describing the users. A hybridization procedure was introduced into the function of similarity calculation. The empirical tests on various real data sets (Book-Crossing, FoafPub) showed satisfactory performances in relevance and precision.

Keywords

Dublin Core; friend of a friend; information filtering; recommendation; social network; user profile.

I. Introduction

Taking into account the excessive mass of the data in various forms, as well as the multiplicity of the services through the Web, access to relevant information become more difficult, in spite of its availability it is lost in the mass. In recent years, there have been many research works in various fields such as e-Business, e-Education, music and video[4,7,14,24] interested in the development of information filtering approach's as being the basic mechanism for recommender systems (RS), thus and in order to filter the interesting information with the user expectations. Large companies and Websites integrate the techniques of filtering in its servers, such as NetFlix, Amazon, CDNow, ebay, MovieLens... etc [9].

Among the most recent tracks, those which explores semantic information [3, 11,12,18] to take advantage of meta-data and implicit information, and others are based on ontologies to conceptualize a specific domain and automate tasks that can improve the performance of RS[23,26].

As part of this work, we adopted Resource Description Framework (RDF) syntax to describe the various components of the system. Firstly, we presented the resources through the basic elements of Dublin Core (DC). In the same way, we select-

ed the properties necessary for the description of the users with the Friend Of A Friend (FOAF) vocabulary. Secondly, and in order to preserve the crucial characteristic of collaborative filtering, we took into account the user's evaluations to group them according to their interests. Moreover, for the process of recommendation, we propose a hybrid function of similarity calculation. By practices of Web 2.0 like DC and FOAF which are regarded as recommendations of the W3C1, we thought of putting these systems open and interoperable and to avoid concentrating on a specific field and closed approaches, the observed tests of experiments section are encouraging.

The rest of paper is structured as follows; section 2 presents a state of the art describing the categories of RS and their methods. In section 3, we introduce in details the modeling suggested of the items and users in RDF and adopted vocabularies. The section 4 devoted to the phase of implementation and experiments complemented by a discussion of the results. In the end, we conclude our work with a conclusion and perspective.

State of the art

Traditionally, information filtering is divided into several categories and sub-categories, depending on the approach used and algorithms adopted by each approach. Essentially, there are [14, 24] contents based filtering also called cognitive filtering, collaborative filtering, also called social filtering, and hybrid filtering. In the first category, the approach achieves a prediction based on a comparison between the themes identified in the user profile and those identified in the documents [15].

In the second category which interesting and widely studied by developers, we find users based methods, where the prediction is calculated with the active user u_a on the basis of evaluations history of the most similar users (user community) to active user, and items based methods where the prediction is calculated on the basis of similarity

¹ <http://www.w3.org>

of the items (item community) thus offer the advantage in term of the control of the items and the calculation which can hold an offline [2]. Finally, hybrid methods are adopted to combine the advantages of each method. Breese and al. [13, 15] classify the algorithms according to the data charged in memory for calculates prediction: memory based where the algorithm handles the totality of the data and model based where the algorithm handles only part of data what allows a time-saver.

The second generation of RS collects the advantageous features of content-based filtering and collaborative filtering to improve the efficiency and overall performance [20]. Many commercial, educational and informational sites integrates RS in their servers such as Tapstry [4] for the management of E-mail, GroupLens [14] for the recommendation of the articles, Newspaper of Usnet, MovieLens for movies, Amazon for CD, books and other products [9], VERSIF for new technologies, Delicous for recommending websites...etc. Current research in this field aims to develop a semantic RS, based primarily on semantic descriptions of the user profiles and/or of the items and the implementation of taxonomies, or ontologies to improve the performance and accuracy of these systems [12, 18]. We have shown in previous research the benefit of integrating semantic information and optimization by SVD (Singular Value Decomposition). Other research is concerned in RS adaptable to the contexts and takes into account various factors related to the field of application [21, 26], others focus on the development of RS based on trusted networks [5, 10, 19].

However, these systems still suffer from some shortcomings such as Cold start [1] where there's little information about a new user or item which has just joined the system; the problem of Scalability [22] due to the high number of system elements that generate a combinatorial complexity of calculation in order to generate an online recommendation for users; and also the problem of Sparsity [25] resulting from the absence of sufficient data for the calculation of similarities even the formation of communities, as well as coverage issues and selectivity [16]. In this paper, we proceeded to a standard vision and modular for the modeling of the system, each component is formalized by an appropriate RDF vocabulary, the values of the properties compose a base of knowledge for an accomplishment and implementation, the following section explains the basic concepts of this representation.

Proposed approach

1. RDF modeling

Resource Description Framework (RDF)², is a data model for the description of various types of resources (person, web page, movie, service, book ...etc.). It treats the data and its properties and the relationship between them, in other words it is a formal specification by meta-data. A RDF document is a set of triplet <subject, predicate, object> where the subject is the resource to be described, the predicate is the property of this resource and the object it is the value of this property or present another resource. For a proper identification, the resources and the predicates are anchored by URIs (Uniform Resource Identifier), in our study we are interested in web resources that are identified by URLs (Uniform Resource Locator as subset of URIs).

Often, the syntax of such a document is based on the XML markup (structure, encoding, internationalization, character sets... etc), it is always possible to present a RDF document by a labeled directed graph.

Example

The book " Semantic Web for the Working Ontologist " written by Dean Allemang on July 5, 2011, in RDF / XML Syntax:

```
<?xml version="1.0"?>
<rdf:RDF
  xmlns:ss="http://workingontologist.org/"
  xmlns:rdf="http://www.w3.org/1999/02/22-rdf-syntax-ns#"
  xmlns:xsd="http://www.w3.org/2001/XMLSchema#"
  xmlns:rdfs="http://www.w3.org/2000/01/rdf-schema#"
  >
  <rdf:Description
    rdf:about="http://www.amazon.fr/Semantic-Web-Working-Ontologist-Effective/dp/0123859654/">
    <ss:written_by
      rdf:resource="http://www.cs.bu.edu/fac/allemand/">
    </rdf:Description>
    <rdf:Description
      rdf:about="http://www.amazon.fr/Semantic-Web-Working-Ontologist-Effective/dp/0123859654/">
      <ss:hasTitle >Semantic Web for the Working Ontologist </ss:hasTitle >
    </rdf:Description>
```

² <http://www.w3.org/TR/2004/REC-rdf-syntax-grammar-20040210/>

```
<rdf:Description
rdf:about="http://www.amazon.fr/Semantic-Web-
Working-Ontologist-Effective/dp/0123859654/">
<ss:hasDate >July 5, 2011 </ss:hasDate >
</rdf:Description>
</rdf:RDF>
```

N.B: there is a web validation service³ for check and visualize the triples of the data model and the associated graph for RDF documents.

Among the goals of RDF is to specify the semantics of Web resources by treatment of the associated meta-data and providing interoperability between applications that exchange information. Improves the efficiency and accuracy of search engines, e-business, social networks ...etc.

The RDF model is shared, open and modular, thus, by declaring namespaces which refer to other vocabularies such as DC or FOAF and to integrate them into a single RDF document.

2.1 Item's representation

A social RS consists of resources "items", the user's profiles and the history which memorizes the interactions of the users (rating) about item's recommended. In addition, each item is identified by a set of specific attributes like URI or ISBN or generals like color, form, date... etc.

A. Dublin Core Vocabulary

Dublin Core (DC)⁴ is a set of simple and effective elements to describe a wide variety of web resources, the standard version of this format includes 15 elements of which semantics has been established by an international consensus coming from various disciplines recommended by W3C. The objective of DC is to standardize the meta-data in order to control and facilitate the use and the interoperability of the various types of resources. These elements are gathered in three categories those which describe the contents (Cover, Description, Type, Relation, Source, Subject) and those which describe the individual properties (Collaborator, Creator, Editor, Rights) and others for instantiations (Date, Format, Identifier, Language), the current version is known as 1.1, validated in 2007 and revised in 2009 by DCMI (Dublin Core Metadata Initiative)⁵.

B. Description of the items by DC

The core of RS is to form properly the communities, according to well determined criteria, in our research we propose to form the items by taking

of account the qualified DC meta-data QDCMI. We define the set of items as follows:

$$I = \{(i_1^1, i_1^2, \dots, i_1^p), (i_2^1, i_2^2, \dots, i_2^p), \dots, (i_m^1, i_m^2, \dots, i_m^p)\}$$

where i_k^j represent the j^{eme} property for item k which is identified by its URI and is specified by its qualified.

We group items by degree of similarity, so I_1 the set of properties assigned to the i_k item and I_2 is the set of properties assigned to the i_l item then the degree of similarity between i_k and i_l by cosine measurement is given by:

$$\text{sim}(i_k, i_l) = \frac{\sum_{j \in I_1 \cap I_2} i_k^j i_l^j}{\sqrt{\sum_{j \in I_1} (i_k^j)^2} \cdot \sqrt{\sum_{j \in I_2} (i_l^j)^2}} \quad (1)$$

The items are grouped according to the similarity of their DC properties.

2.2 User's Representation

The objective of RS is to deliver the relevant resources to the user, which needs a good making of it profile. In our study we took into account the contribution of social networks [5, 10] for the construction of the communities. The choice of criteria is necessary for assigning a user to a particular community [16], currently the most common practice based on syntax RDF is the use of the FOAF [6, 8].

A. FOAF vocabulary

FOAF (Friend Of A Friend)⁶, is an RDF vocabulary for describing in structured manner a person and his relationships. FOAF file is specific to each person and can contain various information (*mbox, name, gender, family_name, Given name, Home Page, weblog, dateOfBirth, interst, accountName, Knows, ...etc.*). We adopt this representation to describe the user's profiles of our SR. We profited of modularity of RDF, these profiles can be enriched by other vocabularies referenced through namespaces such as DC (for a description of a resource), BIO (for describing biographical information) Menow (to describe the current status of a person), relationship (describe the type of relationship with someone) ...etc. Example: FOAF user profile

```
<rdf:RDF
xmlns:rdf="http://www.w3.org/1999/02/22-rdf-
syntax-ns#">
```

³ <http://www.w3.org/RDF/Validator/>

⁴ <http://dublincore.org>

⁵ <http://dublincore.org/documents/dcq-rdf-xml/>

⁶ <http://www.foaf-project.org>

```

xmlns:rdfs="http://www.w3.org/2000/01/rdf-
schema#"
xmlns:foaf="http://xmlns.com/foaf/0.1/"
xmlns:dc="http://purl.org/dc/elements/1.1/"
xmlns:bio="http://purl.org/vocab/bio/0.1/"
xmlns:menow="http://schema.menow.org/#"
xmlns:rel="http://purl.org/vocab/relationship/"
xmlns:doac="http://ramonantonio.net/doaw/0.1/"
xmlns:geo="http://www.w3.org/2003/01/geo/wg
s84_pos#
....
<foaf:Person rdf:nodeID="UserA123">
<foaf:name>xxx</foaf:name>
<foaf:family_name>xxy</foaf:family_name>
<foaf:homepage
rdf:resource="http://www.pageperso.com"/>
<foaf:dateOfBirth>YYYY-MM-
DD</foaf:dateOfBirth>
<foaf:gender>Male</foaf:gender>
<foaf:interest
rdf:resource="http://dbpedia.org/page/Artificial_
intelligence"/>
<foaf:interest
rdf:resource="http://dbpedia.org/page/Associatio
n_football"/>
<doac:Experience>
<doac:title>Web      Development
DB</doac:title>
<doac:location>SIM Labs</doac:location>
<doac:date-starts>2010-09-19</doac:date-
starts>
<doac:date-ends>2013-03-18</doac:date-
ends>
</doac:Experience>
<foaf:OnlineAccount
rdf:about="http://www.youtube.com/user/UserA1
23">
</foaf:OnlineAccount>
<foaf:knows>
<foaf:Person
rdf:about="http://www.../foaf.rdf">
<foaf:name>UserB456</foaf:name>
</foaf:Person>
</foaf:knows>
....
<foaf:Person>
</rdf>

```

We note that we have various vocabularies joined together for the description of any type of user in a standard and structured way.

B. User's Community

The representation of the user profile by vocabulary FOAF has enabled us to build communities according to various descriptions (*weblog, interest, knows, geo, relationship,...*), thus and for a new user, the system can easily assign it to a close community starting from its FOAF file what decreases the problem of cold start in RS.

Let U be the set of users $U = \{u_{F1}, u_{F2}, \dots, u_{Fn}\}$ and $F = \{f_1, f_2, \dots, f_m\}$ the set of the foaf descriptions for these users.

Knowing that $u_{F1} = \{f_1^1, f_2^1, \dots, f_l^1\}$ and $u_{F2} = \{f_1^2, f_2^2, \dots, f_k^2\}$ where $l \leq m$ and $k \leq m$

Thus, the foaf similarity sim_f between two users u_{F1} and u_{F2} by the measurement of cosine are given by the relation:

$$sim_f(u_{F1}, u_{F2}) = \frac{\sum_{j \in u_{F1} \cap u_{F2}} f_j^1 \cdot f_j^2}{\sqrt{\sum_{j \in u_{F1}} (f_j^1)^2} \cdot \sqrt{\sum_{j \in u_{F2}} (f_j^2)^2}} \quad (2)$$

The result of this process makes it possible to form the users according to their foaf common properties.

2. Recommendation engine

The RS are articulated on three crucial processes [4, 7, 14], evaluation of the recommendations by the users, the formation of the communities which depends on similarity measures and the process of recommendation which depends on the values of the predictions calculated by the system. In our study which is leaning on the hybrids RS, where we used three types of similarity to generate recommendations.

2.1 Combined similarity

To have increasingly relevant predictions, we proposed a combined similarity while holding in account RDF as being a building block of the semantic Web, and we use standard vocabularies DC (for the description of the items) and the FOAF (for the description of the user profiles). The formula of combined similarity is given by the relation:

$$sim_c = \alpha sim_{dc} + \beta sim_f + \gamma sim_r \quad (3)$$

Where $\alpha, \beta, \gamma \in [0, 1]$ are parameters adjusted by the system according to a satisfaction degree.

- sim_{dc} resulting from paragraph 1.1, is the similarity based on the elements of DC, is the most important part of our

approach, because of the availability of data and the diversity of criteria for the formation of the communities.

- sim_f resulting from paragraph 1.2, is the similarity based on FOAF profiles of the users and also it is interesting to overcome the cold start problem by the assignment of the new user at a close community through the means of its FOAF profile.

- sim_r the rating similarity, in order to keep the principle of collaboration in RS, we considered the history of user's evaluations, by the items based approach adopted by the majority of the current systems such as (Amazon, Netflix,...etc.), [15, 26] thus the similarity by evaluation between

two items i_p and i_q according to the correlation of Pearson is given by:

$$sim_r(i_p, i_q) = \frac{\sum_{k=1}^m (r_{k,p} - \bar{r}_p) \cdot (r_{k,q} - \bar{r}_q)}{\sqrt{\sum_{k=1}^m (r_{k,p} - \bar{r}_p)^2 \cdot (r_{k,q} - \bar{r}_q)^2}} \quad (4)$$

Where $k = 1..m$: List of the users ratings items i_p and i_q .

$r_{k,p}$: Rating value of the user K for the item p.

\bar{r}_p : Average of the evaluation of the item p.

2.2 Prediction calculation

It selects the most similar items (the S closer neighbors) for the current item, then it generates the prediction value for item i_k through the rating feedback of the current user has for the S similar items:

$$p_{a,k} = \frac{\sum_{t=1}^S (r_{a,t} \cdot sim_c(i_k, i_t))}{\sum_{t=1}^S sim(i_k, i_t)} \quad (5)$$

Where $r_{a,t}$: rating value of the current user has on the i_t similar item.

S: size of the most similar items.

2.3 Recommendation task

This step is performed automatically and the generation of the list of items which comprises the recommendation values assigns the highest prediction (N-top list), as an item is deemed to be relevant (recommended by the system) if the pre-

dition value is greater than a threshold δ .

$$\begin{cases} i_k \text{ recommended} & \text{if } p_{a,k} \geq \delta \\ i_k \text{ not recommended} & \text{otherwise} \end{cases}$$

IV. Experimentation

This section is devoted to the experimental results of our hybrid approach on real data sets. For evaluation and comparison, we implemented two other traditional basic approaches: user-based approach and an item based approach, on an Intel Core i5-3570K 3.4 GHz machine with 6 Gigabyte of RAM and a 1Tera Byte capacity of hard disk.

1. Datasets

Our proposal is based on modeling in RDF, it is more general and takes any data source respecting RDF syntax. For demonstration we exploited two datasets:

- *Book-Crossing dataset*⁷, collected for research purposes by Cai-Nicolas Zeigler in 2004 starting from the famous site Amazon.com, this set includes 278.858 users providing 1.149.780 votes to 271.379 books. To prove our reasoning in §3 we extended the BX-book table containing ISBN, title, author by DC properties inspired always of the same site, such as Subject, Description, Publisher, Date... etc. Thus, in order to taking into account the principle of collaborative filtering we took the history of users evaluations in the calculated of the similarity sim_r by the use of the BX-Rating-set table.
- *foafPub dataset*⁸, it is a set of data extracted from the FOAF files collected during the fall of 2004, has 7118 FOAF documents received from 2044 sites and distributed under the Creative Commons license (v2.0). We used SPARQL requests to import foaf properties, for example to have the value of a property p binding two people one applies the query:

```

PREFIX foaf: <http://xmlns.com/foaf/0.1/>
PREFIX rdf:  <http://www.w3.org/1999/02/22-
rdf-syntax-ns#>
SELECT mbox1, ? mbox2
WHERE
( ?person1 foaf:mbox ?mbox1 )
( ?person1 rdf:type foaf:Person )
( ?person1 foaf:p ?person2 )
( ?person2 foaf:mbox ?mbox2 )
( ?person2 rdf:type foaf:Person )
    
```

⁷ <http://www.informatik.uni-freiburg.de/~ctieglter/BX/>

⁸ <http://ebiquity.umbc.edu/resource/>

2. Step

We deployed an XML parser for the extraction of DC and FOAF complementary properties, all RDF models are exploited by SPARQL9 engine of the framework Jena-2.6.4 and to extract the essential properties we create SPARQL queries through java classes, then we provide to store data in tables, and we have defined several functions to standardize and collect these heterogeneous properties, the tables are converted into Matlab files in order to deduce matrices of similarities between items and/or users and to visualize the plots of the results. 75% of datasets are devoted to the training phase and 25% for the test.

3. Metrics

To evaluate our approach, we proceeded to the selection of MAE metric, very popular and specific for RS also two other metrics (recall and precision) inspired from information retrieval [1, 17].

- A. *MAE*: mean absolute error, calculates the mean absolute difference between predicted p_i calculated by the system and their real score e_i

$$|E| = \frac{\sum_{i=1}^n |e_i - p_i|}{N}$$

N : Number of items rated by the user.

- B. *Recall*: is the proportion of relevant items returned by the algorithm over the total number of existing relevant items,

$$R = \frac{N_{pr}}{N_p}$$

- C. *Precision*: is the proportion of the relevant items among all those returned by the system.

$$P = \frac{N_{pr}}{N_r}$$

These three metrics measure the error, efficiency and quality of RS.

4. Results and discussion

In this section, we have the experimental results on the real datasets (§1.). Figure 1 shows the results of the three algorithms which we implemented, user-based, items based and that of our proposal.

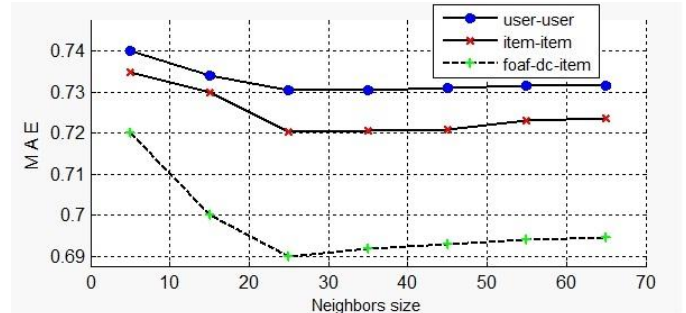
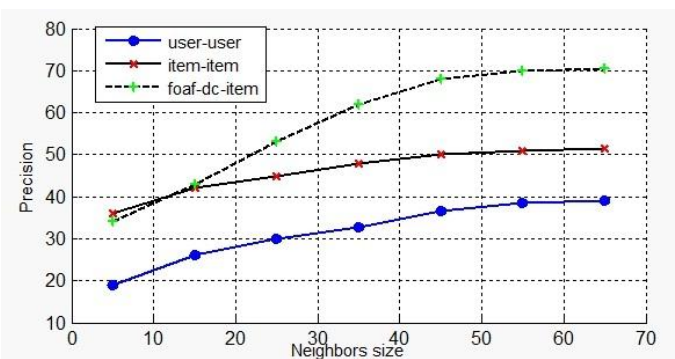


Figure 1. Comparison of prediction error

Near the neighborhood of size 25, the metric MAE records the values of 0.73, 0.72 and 0.69 respectively for these three algorithms. This remarkable improvement is founded on the one hand, of the incorporation of the DC properties and those of FOAF formalism, as additional and complementary sources of data, that leads to a good determination of communities, also appeased the sparsity problem, on the other hand, the adoption of the hybrid approach of the similarities between items and users thus between the evaluations given by the users (§ 3.2.1), prove the result obtained MAE=0.69, our process led to the improvement of the quality and the performance of the prediction.



⁹ <http://www.w3.org/TR/2013/REC-sparql11-query-20130321/>

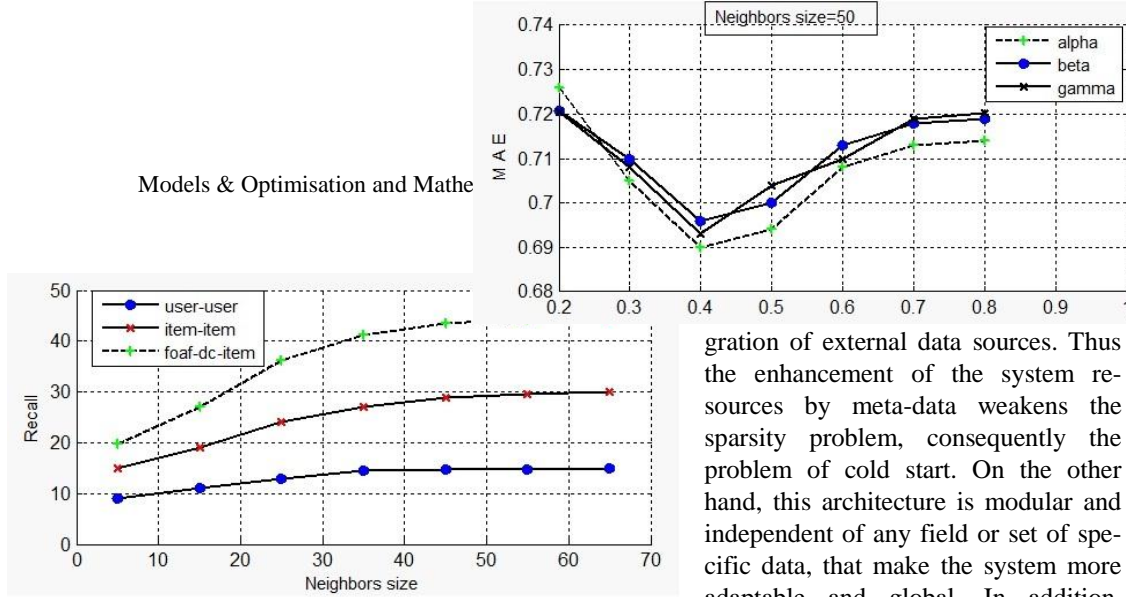


Figure 2. Performance of prediction- Recall

In the same way, beside a size of 50-60 the recall rate reaches 45% for the suggested approach (Figure 2), 15% and 30% for the two other algorithms based-user and based items respectively.

Figure 3. Performance of prediction- Precision

The same observation was noted for the rate of precision where we recorded a rate of 70% for our approach DC and FOAF against a rate of 28% and 41% for the algorithm based-user and based items beside 55 neighbors.

Figure 4. Impact of combination of parameters (alpha, beta, gamma)

A fourth experiment is to vary the three parameters α , β and γ of the formula (3) to see the impact of each parameter on the prediction value, we proceeded to vary a parameter α for example and the other two taken equal so that $\alpha = 1 - (\beta + \gamma)$ and $\beta = \gamma$, we repeated the same process for the two other parameters β and γ .

We note that the error is weak in interval 0.35 and 0.45 (figure 4), which explains the importance of hybridization by taking into account the meta-data of resources to completed miss data in order to achieve satisfactory results.

V. Conclusion and outlook

In this paper, we proved the need for formalizing the components of a RS by rules recommended and well structured. Our approach is essentially based on a description in purely RDF vocabularies through DC (ISO158360) and FOAF to ensure interoperability with other applications. Based on the advantage of using URIs for the unique identification of resources and relationships between resources, in order to avoid ambiguity and the namespace advantage for extensibility and inte-

gration of external data sources. Thus the enhancement of the system resources by meta-data weakens the sparsity problem, consequently the problem of cold start. On the other hand, this architecture is modular and independent of any field or set of specific data, that make the system more adaptable and global. In addition,

combination of similarities which we adopted shows the improvement of the coverage and accuracy of prediction function. A future reasoning considered the manner of filtering only the useful properties and granted them with adequate weights.

VI. References

- [1] A. I. Schein, A. Popescul, L. H. Ungar, and D. M. Pennock, "Methods and metrics for cold-start recommendations," in Proceedings of the 25th Annual International ACM SIGIR Conference on Research and Development in Information Retrieval (SIGIR '02), 2002.
- [2] B. M. Sarwar, G. Karypis, J. A. Konstan and J. Riedl, "Item based collaborative filtering recommendation algorithms," in *Proceedings of the 10th International Conference on World Wide Web (WWW '01)*, pp. 285–295, May 2001.
- [3] C. Jie, W. Zhiang, Y. ZHUANG, M. Bo and Y. Zeng "A Novel Collaborative Filtering Using Kernel Methods for Recommender Systems." *Chinese Journal of Electronics* Vol.21, No.4, Oct. 2012.
- [4] D. Goldberg, D. Nichols, B. M. Oki and D. Terry, "Using collaborative filtering to weave an information tapestry" *Communications of ACM*, vol. 35, no. 12, pp. 61–70, 1992.
- [5] D. Zhou, H. Ma, C. Liu, R. Michael and L. Shatin. "Recommender Systems with Social Regularization." *WSDM'11, February 9–12, 2011*, Hong Kong, China. Copyright 2011 ACM 978-1-4503-0493-1/11/02, 2011.
- [6] FOAF specification available at <http://xmlns.com/foaf/spec/20100809.html>
- [7] G. Adomavicius and A. Tuzhilin, "Toward the next generation of recommender systems: a survey of the state-of-the-art and possible extensions," *IEEE Transactions on Knowledge and Data Engineering*, vol. 17, no. 6, pp. 734–749, 2005.
- [8] G. Astrand Grimnes, P. Edwards, and A. Preece. "Learning Meta-Descriptions of the FOAF Network."
- [9] G. Linden, B. Smith and J. York, "Amazon.com recommendations: item-to-item collaborative filtering," *IEEE Internet Computing*, vol. 7, no. 1, pp. 76–80, 2003.
- [10] H. Ma, I. King, and M. R. Lyu. "Learning to recommend with social trust ensemble." In Proc. Of *SIGIR '09*, pages 203–210, Boston, MA, USA, 2009.
- [11] H. Oufaida and O. Nouali "Exploiting Semantic Web Technologies for Recommender Systems A Multi View Recommendation Engine", Copyright © 2009, Association for the Advancement of Artificial Intelligence.

- [12] H.F. Khosravi and M. Nematbakhsh. "A Semantic Recommendation Procedure for Electronic Product Catalog" *World Academy of Science, Engineering and Technology* 22, 2008.
- [13] I. Guy, N. Zwerdling, D. Carmel, I. Ronen, E. Uziel, S. Yagev, and S. Ofek-Koifman. "Personalized recommendation of social software items based on social relations". In *Proc. of RecSys '09*, pages 53–60, New York, USA, 2009.
- [14] J. A. Konstan, J. Riedl, A. Borchers and J. L. Herlocker. "Recommender systems: a GroupLens perspective. In Recommender Systems". Papers from 1998 Workshop. Technical Report WS-98-08. AAAI Press, 1998.
- [15] J. Breese, D. Heckerman and C. Kadie, "Empirical analysis of predictive algorithms for collaborative filtering," in *Proceedings of the 14th Conference on Uncertainty in Artificial Intelligence (UAI '98)*, 1998.
- [16] L. Abrouk, D. Gross-Amblard and Nadine Cullot "community detection in the collaborative web". *International Journal of Managing Information Technology (IJMIT)* Vol.2, No.4, November 2010.
- [17] M. R. McLaughlin and J. L. Herlocker, "A collaborative filtering algorithm and evaluation metric that accurately model the user experience," in *Proceedings of 27th Annual International ACM SIGIR Conference on Research and Development in Information Retrieval (SIGIR '04)*, pp. 329–336, Sheffield, UK, 2004.
- [18] N. Ziegler, "Semantic Web Recommender Systems." *Proc. of the joint ICDE/EDBT Workshop*. (2004).
- [19] P. Bedi, H. Kaur and S. Marwaha. "Trust based recommender system for semantic web". In *Proc. Of IJCAI'07*, pages 2677–2682, 2007.
- [20] R. Burke, "Hybrid recommender systems: survey and experiments," *UserModelling and User-Adapted Interaction*, vol. 12, no. 4, pp. 331–370, 2002.
- [21] S. Kim, Y. J. Kwon, "Effective Context-aware Recommendation on the Semantic Web." *International Journal of Computer Science and Network Security*, v.7, pp. 154-159. (2007).
- [22] S. Schelter, C. Boden and V. Markl "Scalable Similarity-Based Neighborhood Methods with MapReduce" *RecSys'2012, September 9-13, 2012 Dublin Irlan*. Copyright 2012 ACM 978-1-4503-1270-7/12/09, September 2012.
- [23] S. Shishehchi, S. B. Yashar, N. Azan and S.A. hahrul, "Ontological Approach in Knowledge Based Recommender System to Develop the Quality of E-learning System", *Australian Journal of Basic and Applied Sciences*, 6(2): 115-123, 2012 ISSN 1991-8178.
- [24] S. Xiaoyuan and T. M. Khoshgoftaar "A Survey of Collaborative Filtering Techniques", *Hindawi Publishing Corporation Advances in Artificial Intelligence* Volume 2009, ID 421425.
- [25] Z. Huang, H. Chen and D. Zeng, "Applying associative retrieval techniques to alleviate the sparsity problem in collaborative filtering" *ACM Transactions on Information Systems*, vol. 22, no. 1, pp. 116–142, 2004.
- Z. Yu, and al. "Ontology-Based Semantic Recommendation for Context-Aware E-Learning". *Proc. of the 4th Conference on Ubiquitous Intelligence and Computing*, v.4611, Berlin: Springer, pp. 898-907. (2007).

Spectral Analysis of Ferrous Metal Based on Neural Networks

A. TIFFOUR and M. BELARBI
mbelarbi@mail.univ-tiaret.dz/ a.tiffour54@gmail.com
Ibn Khaldoun University, Tiaret, Algeria

Abstract-This study concerns electro-magnetic signals modelling. The main proposes of the present paper consists of the specification spectral analysis of radiation emitted in heterogeneous environment. Comparative study is presented between polynomial Lagrange and neural networks modelling. We show that neural networks give best results when it is experimented to establish concentration elements of ferrous metallic elements.

Keywords

component; formatting; spectral analysis, neural networks, algorithmic complexity, Lagrange approximation.

VII. Introduction

Our research study consists of establishing signal processing system which allows to convert data during analysis of ferrous sample using spectrophotometer using real data and using percentage of chemical elements present in the analysed sample..

As basis of our research we use standardised samples where the chemical composition is known and certified by laboratories using spectroscopy chemical analysis [2]

The purposes of the present study is the modelling of electro-magnetic signals using numerical models [1] [4], in order to establish and improve the use of spectral analysis of radiation emitted in heterogonous environment. In modelling, neural networks have emerged as powerful tool that has been applied by various researchers [5].

This study is applied to the production industry of metal and « font » which require strong competence in the field of ferrous metal analysis.

Therefore, in order to improve physical and chemical quality of the production (elasticity, hardness,..., etc.), the metallurgists need to know chemical composition of the metal to deal with. Therefore, it exist several systems of structural scruting of matters. Spectral analysis is among the more efficient methods which allows to detect the presence of different chemical elements in the analysed samples, the results of measure are done with four digits precision. For example we can speak about chemical elements the most im-

portant during metal processing like: C, Si, Mn, P, S, Al, Ni, Mo, Cr, Cu, V, Mg, Ti etc.

The principle of spectral analysis is based mainly on diffraction the light emitted by sample of production during processing, extracted from the furnace and solidified. This diffraction produces spectra with visible colours characterising each of elements present in the sample. The intensity of each of these colours is rigorously et respectively proportional to the concentration of each of these elements constituting the analysed metal.

The used equipment consists of a spectrophotometer, this equipment is based on the diffraction of the light emitted by a sample to be analysed. This sample which we transmitted an electrical arc. The white light obtained is diffracted by optical system which generates several rays with different colours. Each of these colours correspond to the frequency and the intensity of each of chemical elements present in the sample and by percentage of the concentration (%).

These rays are obtained by sensors and converted on electrical tensions using filters computed and calibrated in order that each one can react exclusively to frequency associated to its design. Consequently, each element is characterised by electrical signal with unique frequency. This signal is measurable and its amplitude is proportional to concentration of the used chemical element. At the end, these signals are recorded and converted into binary code and transmitted into numerical processing unity (PC). There fore we can visualise the concentration of the analysed sample.

The paper is presents as follows: Section 2 describes the acquisition system: spectrophotometer and PC relation. Section 3 gives the principles of neural network model used in the study. Section 4 presents the results of software based on neural network and comparison with Lagrange method.

VIII.DESCRPTION OF THE SYSTEM

The system is constituted by two main parts:

- a) Part one : the spectrophotometer : which is electronical and optical equipment which

main function is the conversion of optical signal to voltage.

b) Part two : the Computer processing software which controls and commands of the spectrophotometer and the data processing ,

As example of classical methods there exists polynomial Lagrange method of N-1 degree The curve modelled by dx and dy segments. These classical methods have advantages and inconvenient.

Our contribution consists of establishing software processing of data obtained as voltages proportional to elements presents in the analysed sample.

During this study we show that the range of errors of classical methods which have bad effect during analysis. Specially, when we use extrapolation of results or if the analysis result value is comprised between two far points in etaloned curve.

At last, we try to prove that we can improve the result precision of the studied system using new method like neural network described in the next section.

IX. NEURAL NETWORK MODELLING

The neural network model has deterministic kind with real computed output using sigmoid function. The architecture is constituted by successive layers with input layer and output layer. The model use gradient retro-propagation algorithm. This algorithm is used through the learning of the model. We can see results obtained during learning [see annexe]

1. Computing the output of the first hidden layer

$$k=1$$

$$y_{kj} = \sum_{j=0}^{NS(k)-1} \sum_{m=0}^{NS(k-1)-1} w_{kjm} \cdot X_{i,m}$$

with :

$k=1$: indicate the number of the layer (in this case the first hidden layer)

J: the number of the cell of the layer k

m: the number if the cell of layer k-1

i : indice of the vector of I/O (X_i, C_i) ,

(with X_i the values of the axis of abscissa and C_i the values of the axis of ordinates)

NS (k): gives the number of cells of the layer k

2. Computing the output of the other layer

$$k \neq 1$$

$$y_{kj} = \sum_{k=2}^{NC-1} \sum_{j=0}^{NS(k)-1} \sum_{m=0}^{NS(k-1)-1} w_{kjm} \cdot y^{(k-1), m}$$

with :

NC : Number of layers (Input layer + Output Layer + hidden layers)

X. RESULTS INTERPRETATION

Working with adequate configuration of our neural network which is specific to each of graphs which we studied. After learning of Neural Network, we obtain results in the form of modelling graphs. We compare our results with the graph generated by polynomial of Lagrange (green colour in the graphs(Annexe). This comparison shows the disadvantages of classical method which was enable to extrapolate the graph out of values of the standardised samples and also for far points.

Whereas, the graphs modelled by neural networks (blue in the graphs) follows the progression of the values of standardised samples and extrapolate perfectly the graph out of some points.

For each element, the intensities obtained by analysis versus the correspondent concentrations (%)

Table 1 : Neural Network Configuration

Element	Epsilon	Input Layers	Hidden Layers	Output Layers
Phosphore	01	1	1 60 cell	1
Carbone	0,31 E	1	3 layers 8 Cells	1
Manganese	1.2 E-04	1	5 Layers 7 cells	1

Nickel	2.3	1	5 Layers 7 cells	1
Silicium	2.3	1	4 Layers 8 cells	1

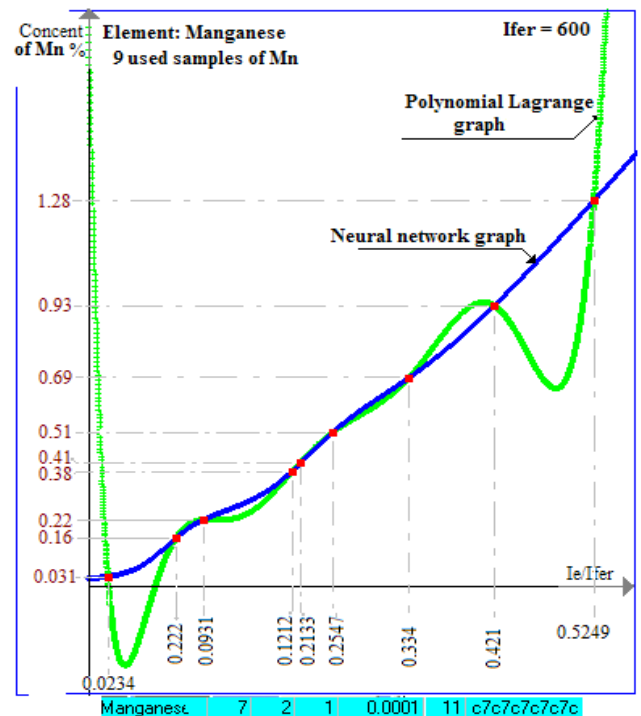
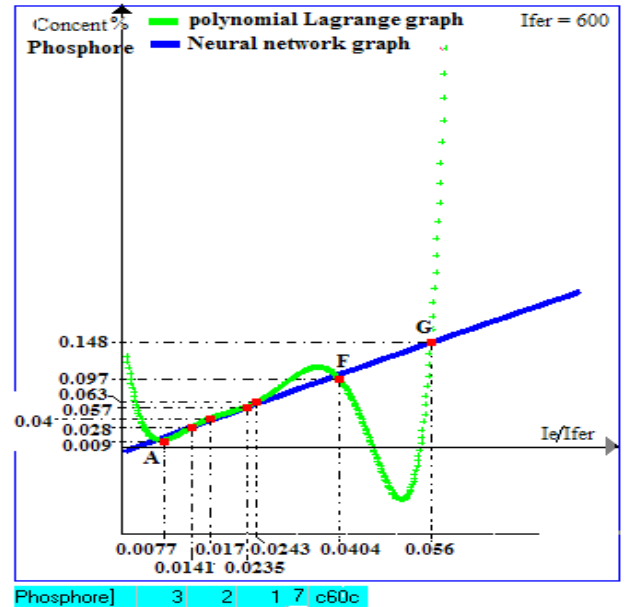
XI.CONCLUSION

The main purpose of this paper consists of presenting comparison study between polynomial Lagrange method and neural network applied to ferrous metal detection. We showed that Neural Network Model gives good performances for spectral analysis.

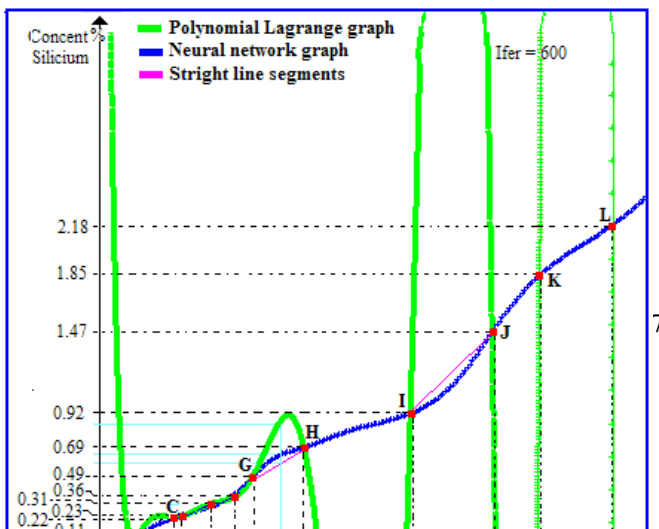
As future work, we think about extending the method to non – ferrous metal. In the present study we limit our selves to six elements and it seems interesting to experiment other elements and consequently produce rules for neural network configuration.

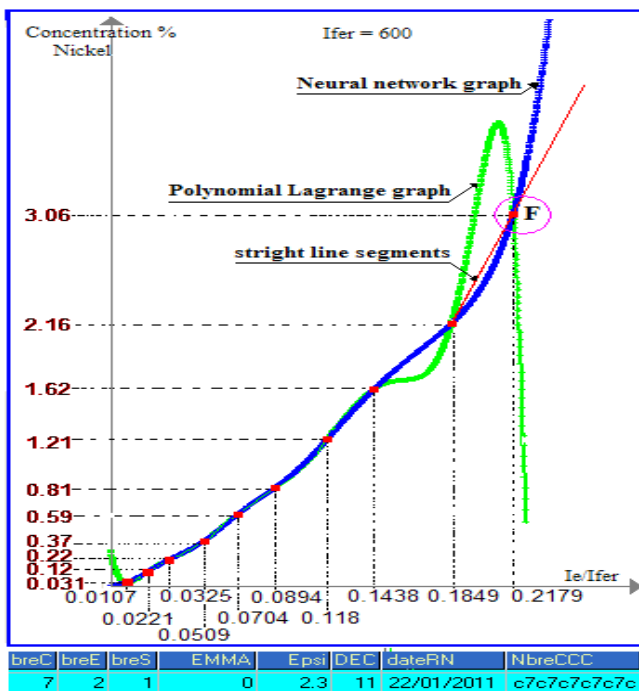
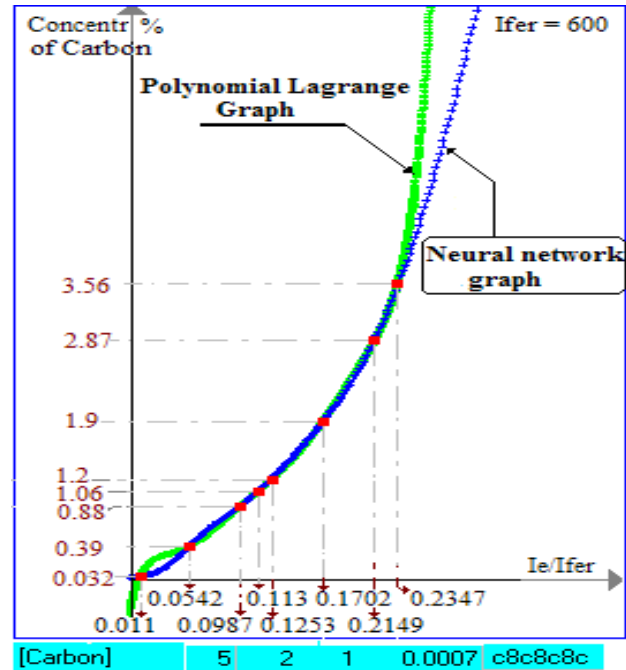
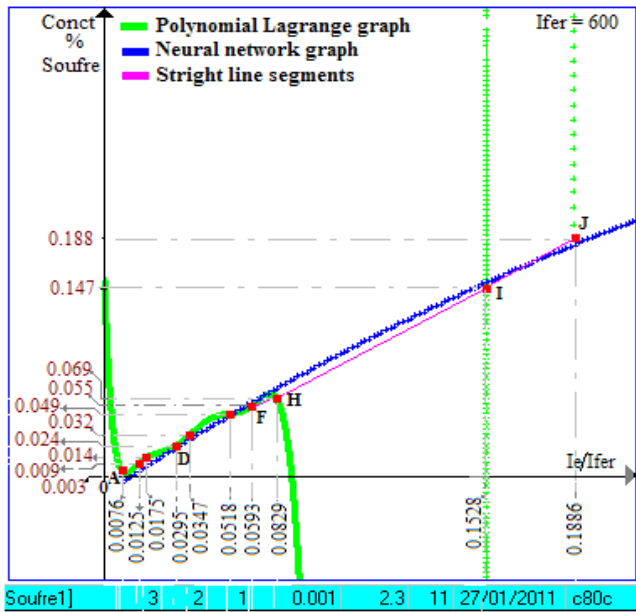
VI. REFERENCES

- [1] N. MURATA : Network information criterion : determining the number of hidden units of an artificial network model . archives 1992
- [2] M. BAGHDAD and K. GHARABI : “Modelling and simulating of polynomial Lagrange method for ferrous metal using spectral analysis” Report of end of cycle Project, University of Tiaret – June 2009.
- [3] H. RAR : “Detecting system and fluorescence measure “ report of end of Cycle, University of Quebec – March 2006.
- [4] F. ELIE : Design and implementation of system using neural network for identifying and characterizing transient signals of wheezing kind”. Thesis dissertation, University of Orleans – France, Dec. 1997.
- [5] B. Bhattacharyya, D. Dey, S.Munishi : “ A correlation Based system identification technique for a class of power converter”. Applied soft computing Journal, May 2010.



ANNEXE : CURVES OF ELEMENTS





Numerical Modelling of the Response Hydromécanique around a Tunnel (Example of application: Algiers metro)

Houari Ouabel, doctoral student in Civil Engineering, University of Tlemcen, Algeria
ouabelhouari@yahoo.fr

Abstract-*Tunneling at shallow depth can induce ground movements that may cause deformation and in extreme cases of severe damage to surface structures this work deals bibliographic analysis and numerical modeling of the hydro mechanical response around a tunnel. a numerical analysis of the effect of excavation of a tunnel towards a low multiple-stage structure centered over the axis of a tunnel. The study is performed using the computer code Plaxis 8.2 which is based on the finite element method (FEM) in plane strain. The analysis applies to a real case in this instance the Algiers metro, excavation was conducted using the New Austrian Method (NMA) taking account of deconfinement.*

Our objective in this work is to estimate numerically the different movements caused by the construction of a tunnel at shallow depth (vertical and horizontal as well as pressure dissipation and soil consolidation movement.

Keywords

Tunnel, the Algiers Metro, consolidation, coupled hydro-mechanical finite element method. Free surface, settlement, PLAXIS 8.2

The digging of underground is nowadays one of the most suitable for the construction of infrastructure road and rail transport solutions, and drinking water and sanitation networks with major cities of the world have a growing need .

One of the major problems associated with these structures is formed by the movement induced by the work floor. These works are, for both economic and functional, usually constructed shallow reasons, movements

they cause, can damage the existing structures on the surface.

This problem is even more important in the presence of compressible soils. Settlements due to construction of the book are in the most important cases and they develop over time, sometimes for long periods of time after completion. These deferred deformations mainly concern the consolidation of fine soils that occurs over time by expulsion of excess pore water occupying the voids in the massif..

1. INTRODUCTION

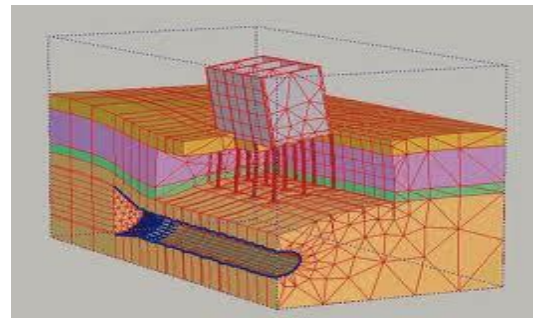
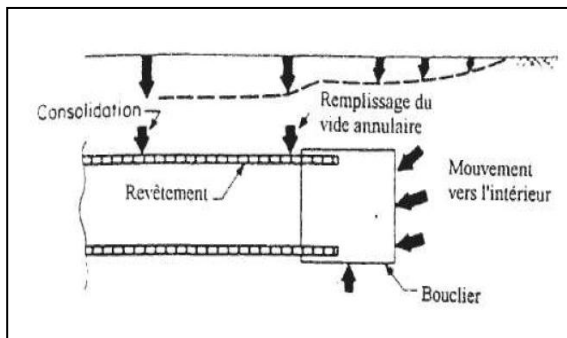
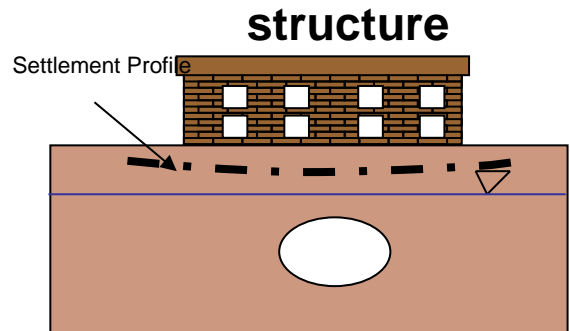


Fig.1: problematic

2. Mesh and numerical model

Given the complexity of movement resulting from tunnelling, it seems necessary for the determination of these movements have a reliable computational tool for the numerical simulation of this extremely delicate behavior.

Our contribution is a proper use of a computer code PLAXIS 8.2 finite element is a program in two dimension finite element specifically designed for analyzes performed deformation and stability for differing type of application in geotechnical

This last is made up of 04 modules summarize the almost unique approach to solving the problem of civil engineering namely:

- The input data program (**Input**)
- The calculation program (**Calculations**)
- The program results (**Output**)
- The program curves (**Curves**)

This code was used for modelling a digitally the case of Algiers metro in particular cutting calcu-

lation was selected in the test section hamma garden

The results can be through this program PLAXIS are many

It is clear that the choice of a mesh enormously influenced the results we selected only the optimal mesh shown in Fig.2 the 1st forward calculation and second by giving against the deformation of the mesh into account the existence of a structure on the surface

Note that a movement of soil occurred at the natural surface, so that e at the excavation

The deformed mesh shows clear ing the existence of a basin of settlement caused by the construction of the tunnel

Here has been some shortening the tunnel lining; this is due to the differing phases of construction such as excavation, filling the annular space, the paving

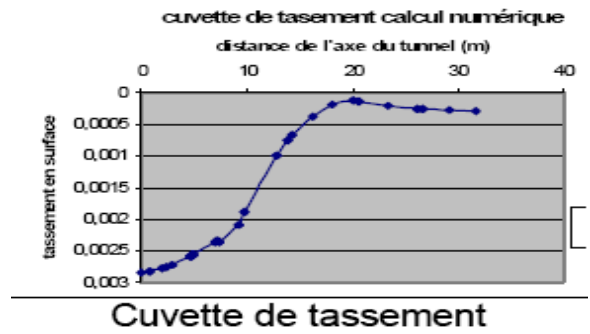
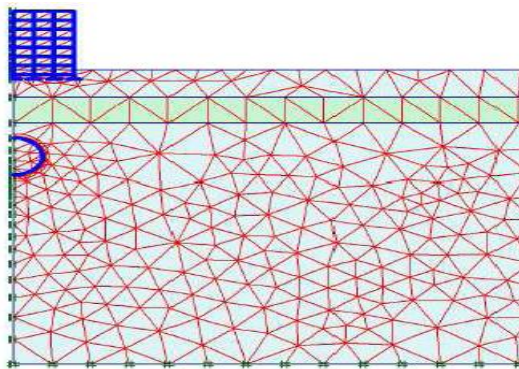


Fig.2: deformed mesh

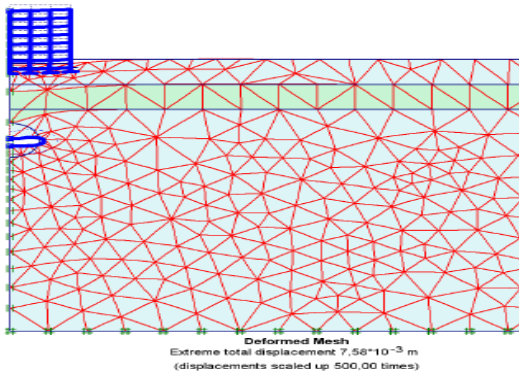
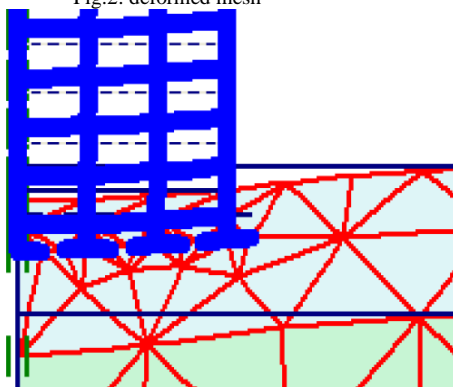


Fig.2: deformed mesh



3. Vertical displacement

The fig.3 shows the distribution of vertical displacement is in shade or color curves iso value

Thereafter we consider cuts in the horizontal direction (surface and above the tunnel) (key point called tunnel) we note that the key vertical displacement is greater than the surface

4. horizontal movements

In Simulator way we analyze the distribution of horizontal displacement Nuance color and iso value curve

We have shown in a vertical section the evolution of these last we note that the Horizontal displacement is almost zero below the tunnel

5. Evolution of pore pressure in the massive

Up to this point we have to mention the mechanical parameter, as engineer changing the pi implies emblem on the principle of Terzaghi bishop or a change in the effective stress which gives a mechanical effect that is why we presented the evolution of pi in time with differing section

Over time it decreased pi therefore water overpressure induced by the excavation are completely dissipated

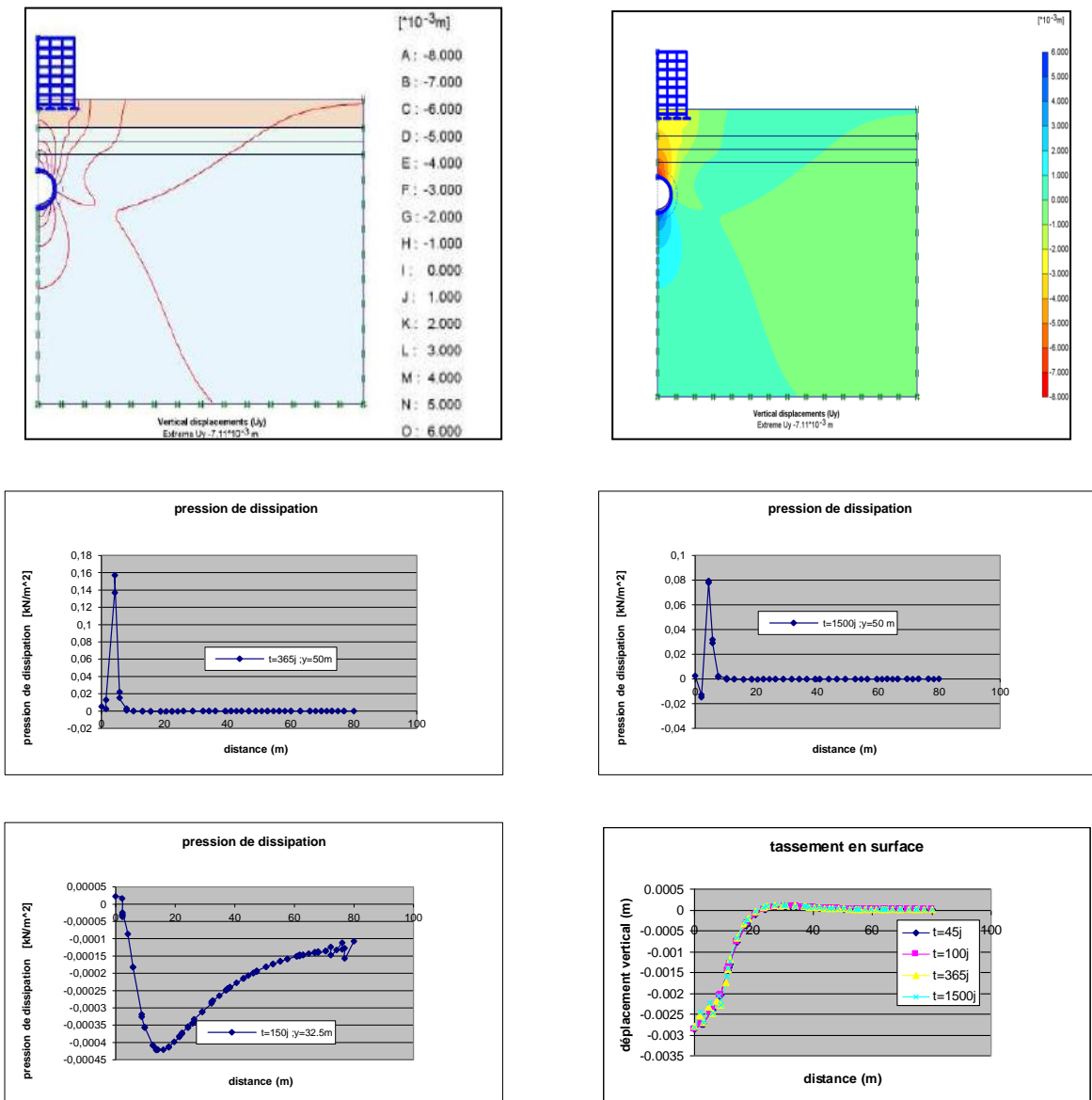


Fig.3: Vertical displacement

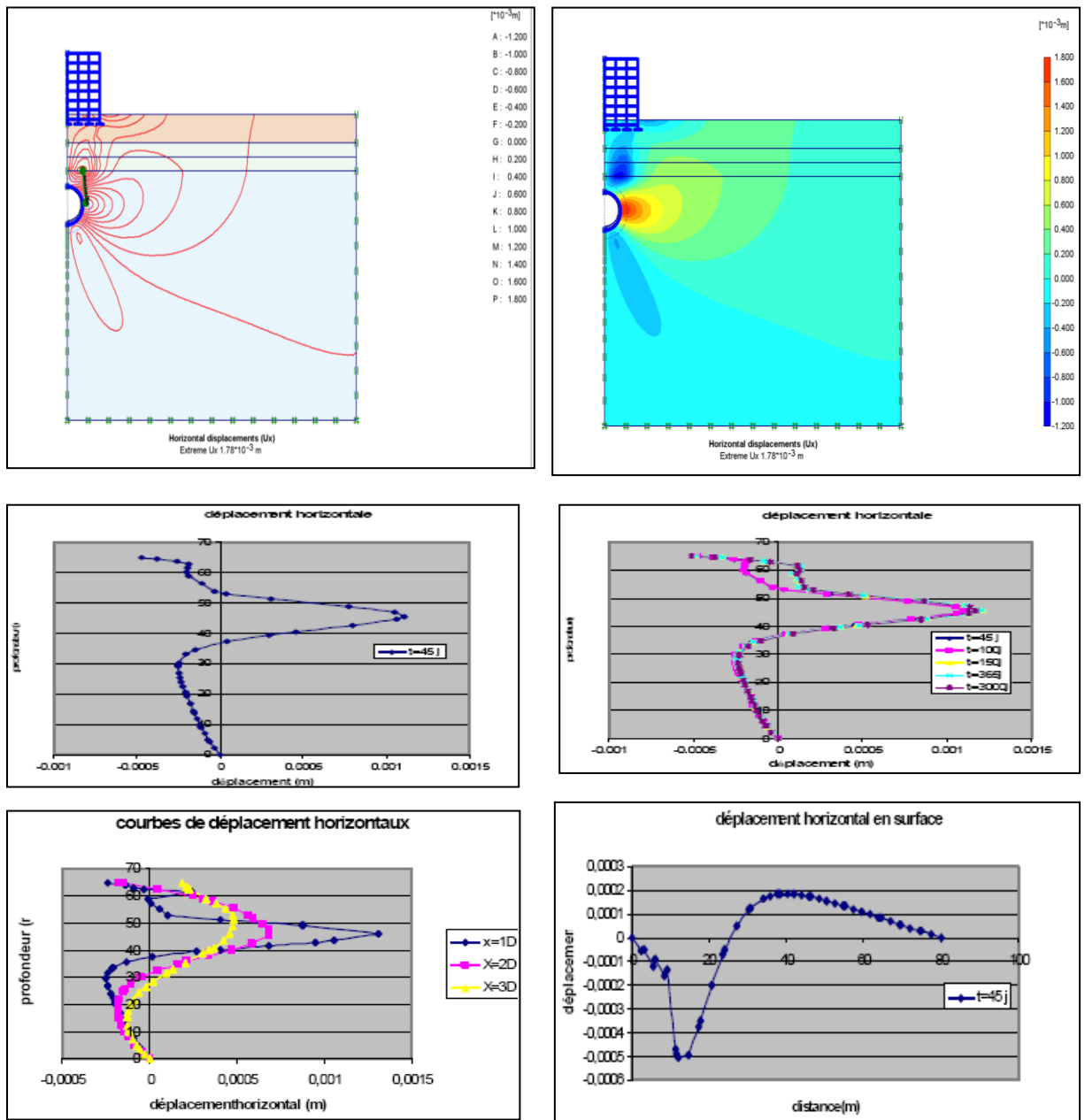


Fig.4: Horizontal Movements

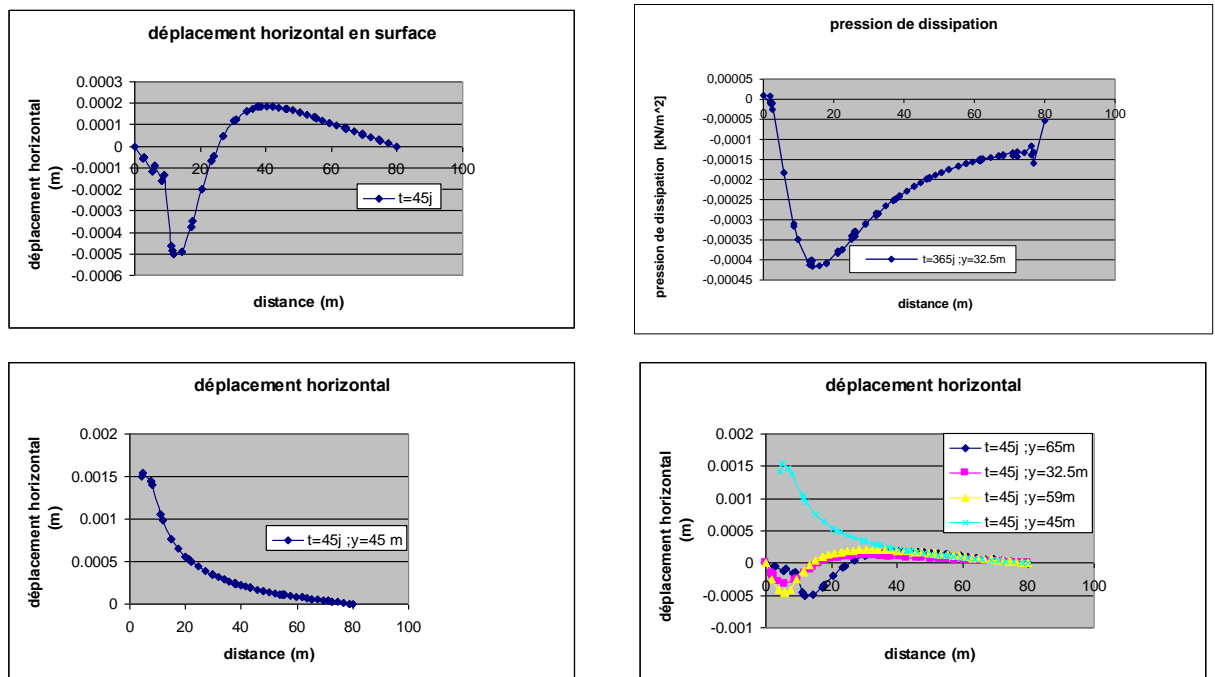


Fig.4: Horizontal Movements

Conclusion

The use of computer code Plaxis has enabled us to make a two-dimensional analysis of this phenomenon based on the finite element method and the results obtained are comparable to those obtained by other codes (Melanie), and measures in situ

The choice of parameters used in the finite element is very important, taking into account that the variation curves of the mechanical characteristics of the soil represent the means values of the measurements

Hydromechanical behavior of soils in tunnelling Take into account the phenomenon of tunnelling interaction with other structures on the surface and in depth such as masonry buildings, pipelines and underground pipes, deep foundations, tunnel existing study of a real example of reference Algiers metro study of consolidation around the tunnel and the influence of time on the appearance of long term settlements

7. Bibliographical references:

1-N, Dolzhenko (2002). Experimental and numerical modeling of two-dimensional underground urbain.réalisation bi trials axial and oedometer on the analog ground taylor-Schneebeli, PhD thesis, INSA Lyon

6.

2-D DIAS. (1999). Strengthening gauge tunnels by bolting. Numerical study and application to a real case in urban areas. PhD thesis, INSA Lyon

3-K, TERZAGHI, Peck, Mesri. Soil Mechanics in Engineering Practice 1940.534 pages

4-K, Terzaghi. (1943). Theoretical soil mechanics, 526 pages

5 - K, Terzaghi. Theoretical Soil Mechanics (New York, 1943) 278.

6- M. A. BIOT, *J. Appl. Phys.* 12 (1941) 155.

7- C. W. CRYER.a comparison of the three-dimensional consolidation theories of biot and terzaghi (1962)

8-I, BENAMAR (19-12-1996). Study of delayed effects in deep tunnels, PhD of the National School of Bridges and Roads, 205pages

9-M, Zouhair Babchia, J-P, Magnan. Numerical analysis of the behavior of massive clay, LPC N° 140 October 1986

10-H, Mroueh (27-05-1998). Tunnels in urban areas and numerical modelling interaction widening existing structures, PhD Central School of Lille, 132 pages

11-J-P, Magnan & L LEPIDAS. Parametric study of horizontal displacements of soft soil under the embankment during construction, GT42 July 1990

12-M, MRAD. (2005). modelling of the hydromechanical behavior of unsaturated expansive soils, PhD Thesis of National School of Geology, Nancy, 342 pages

13-A, ZADJAOUI (2000). Bibliographic analysis and numerical modeling of flow around tunnels. Magisterial memory, Department of Civil Engineering, Faculty of Engineering, University aboubakr Belkaid tlemcen. (Algeria).

14-M, ATWA. (1996). numerical analysis of water flow and soil consolidation around tunnels in clay, Doctoral Thesis of the National School of Bridges and Roads, 492 pages.

15-M, Ould AMY. (1990). Numerical modelling of flows and deformations in earth dams constructed on soft soils, PhD

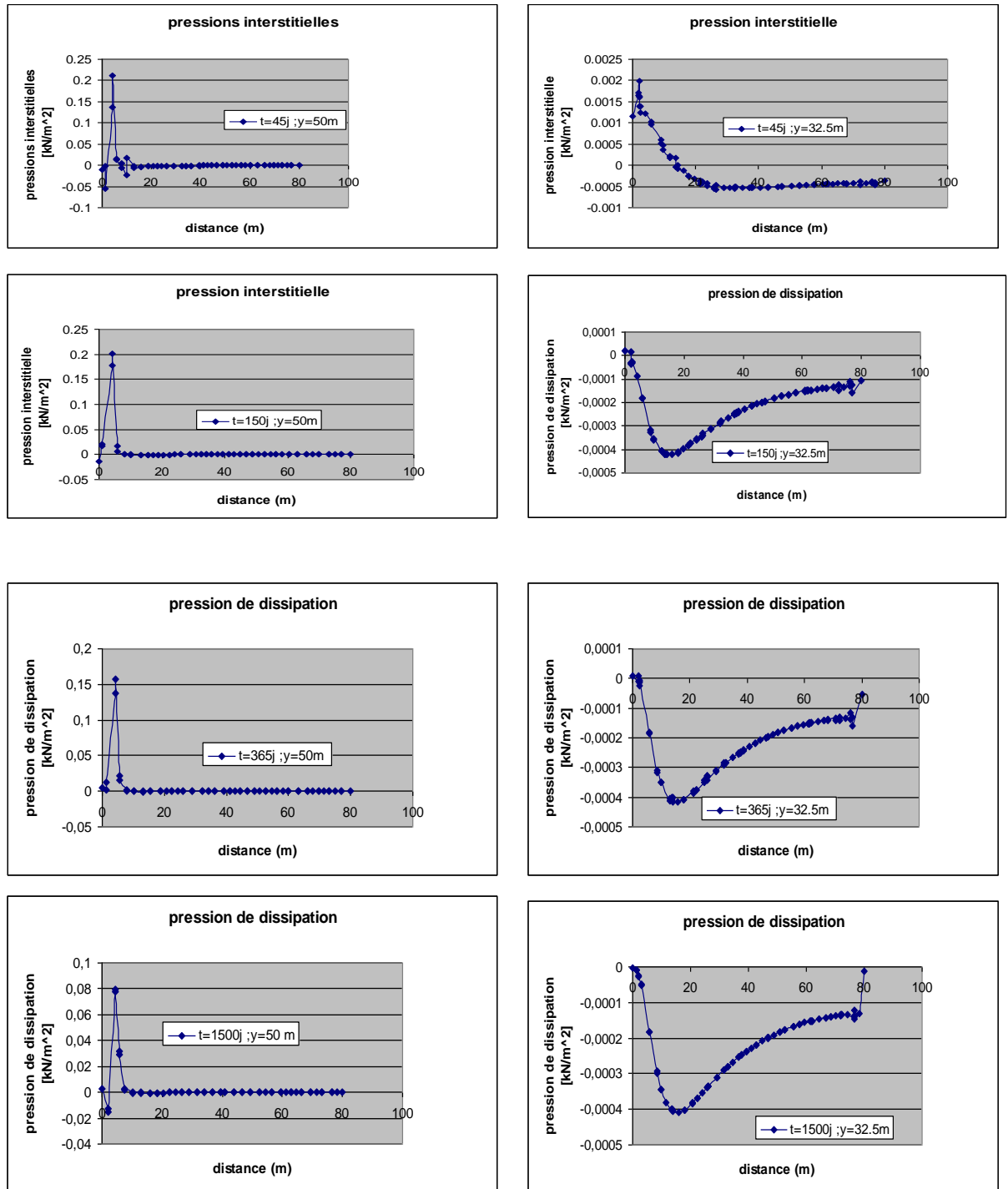


Fig.5: Evolution of pore pressure in the massive

Parametric study of the mechanical response Around a Tunnel (Example of application: Algiers metro)

Houari Ouabel, doctoral student in Civil Engineering, University of Tlemcen, Algeria
ouabelhouari@yahoo.fr

Abstract-*Tunneling at shallow depth can induce ground movements that may cause deformation and in extreme cases of severe damage to surface structures this work deals with the setting of the hydro mechanical response around a tunnel. a numerical analysis of the effect of excavation of a tunnel towards a low multiple-stage structure centered over the axis of a tunnel. The study is performed using the computer code Plaxis 8.2 which is based on the finite element method (FEM) in plane strain. The analysis applies to a real case in this instance the Algiers metro, excavation was conducted using the New Austrian Method (NMA) taking account of deconfinement.*

Our objective in this work is to make a parametric study of geometric parameters differing and so the geotechnical parameter mesh position and lap

Keywords

Tunnel, the Algiers Metro, consolidation. Finite element method. Settlement, PLAXIS 8.2

1. INTRODUCTION

The digging of underground is nowadays one of the most suitable for the construction of infrastructure road and rail transport solutions, and drinking water and sanitation networks with major cities of the world have a growing need.

One of the major problems associated with these structures is formed by the movement induced by the work floor. These works are, for both economic and practical reasons, usually constructed shallow movements they cause, can damage the existing structures on the surface.

2. Mesh and numerical model

Given the complexity of movement resulting from tunneling, it seems necessary for the determination of these movements have a reliable computational tool for the numerical simulation of this extremely delicate behavior.

Our contribution is a proper use of a computer code PLAXIS finite element 8.2 is a program in two dimension finite element specifically designed for analyzes performed deformation and

stability for differing type of application in geotechnical

This last is made up of 04 modules summarize the almost unique approach to solving the problem of civil engineering namely:

The input data program (Input)

The calculation program (Calculations)

The program results (Output)

The program curves (Curves)

This code was used for modelling a digitally the case of Algiers metro in particular cutting calculation was chosen in the section hamma- garden test

The results can be thanks to this program are many PLAXIS

It is clear that the choice of a mesh enormously influenced the results we selected only the optimal mesh shown in Fig.2 the 1st forward calculation and second by giving against the deformation of the mesh into account the existence of a structure on the surface (cup packing)

Note that a ground movement occurred at the natural surface, so that e at the excavation The deformed mesh ment clearly shows the existence of a basin compaction caused by the construction of the tunnel

There has been some shortening the tunnel lining; this is due to the differing phases of construction such as excavation, filling the annular space, the paving

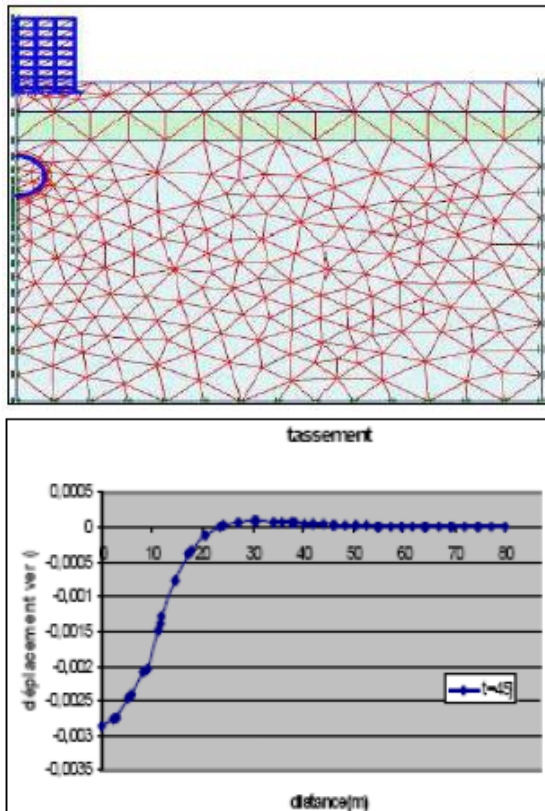


Fig.1 deformed mesh and cup of settlement

3. Parametric study:

3.1 The influence of geometric and geotechnical parameters

In this section, we studied the influence of the pro splitter and the diameter of the tunnel as well as some mechanical characteristic of the field as the coefficient of land, friction angle, Poisson's ratio, modulus of elasticity, on movement across the solid

3.1.1 The influences of geometric parametric

Influence depth to study the influence of the ratio of the tunnel on ground motion, we performed calculations for three different relationship

We plotted the cup packing for these differing depths in the end better see the différence that can undergo compaction by varying the ratio

Figure .2 below include the value of settlement found through our simulation, as well as the value of the width of the bowl

It is clear, that ratio increases more than the movement increases, this may be explained by the fact that the surface settlements are strong

relationship with the convergence of the ground level to the excavation, and the radial movement around the tunnel is influenced by the variation of the ratio (the

radial displacement increases by increasing the ratio, panet, 1995) which leads to a vault effect less important on the contour of the excavation, and the settlements the same report were plotted for different values of key report similar findings were obtained

The purpose of a parametric study is to draw at the end of the study of charts to guide the user in his work by facilitating the task to its first approximations

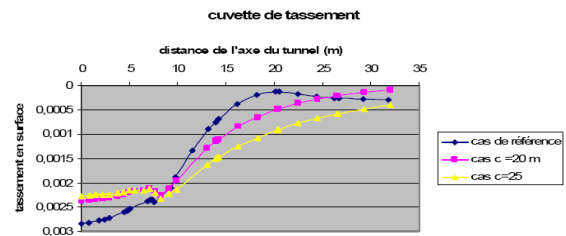


Figure A.2: Variation of depth

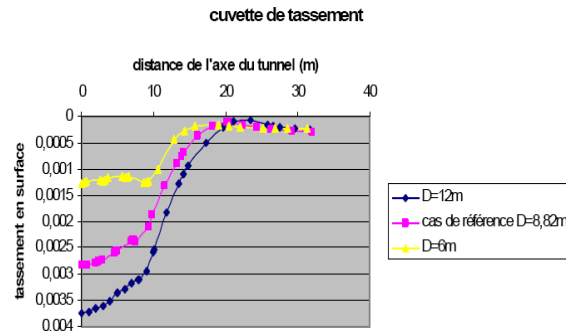


Figure.3: variation of the diameter

3.1.2 Influence of geotechnical parameters of the land

3.1.2.1 Coefficient of land at rest (ko)

To see the influence of geotechnical parameters of the land on soil behavior vis-à-vis the tunneling, we studied the influence of parameter ko to see the influence of the anisotropy of the initial stresses three cases been studied with coefficient values of land resting+ 0, 2.+ 0.4

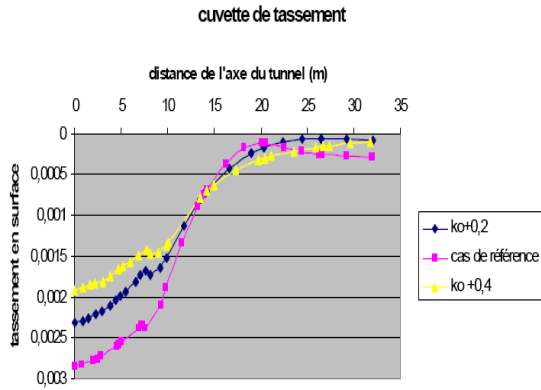


Figure.4: Coefficient of land at rest (k_0)

There through Figure.4 the surface settlements are influenced by the coefficient of land at rest, in fact, there is a reduction in the maximum surface settlement when k_0 augment

However, lateral movement does not seem to be affected, which allows us to say that the influence of the coefficient of land at rest is important on the final results of the settlement, these results were confirmed by some authors Mroueh (1998) Dolzhenko (2002), Robeert (2005)

3.1.2 .2 soil friction angle:

The angle of internal friction is a solid friction in a skeleton grains order to study the influence of this angle on the behavior of land undergoing excavation; we performed two calculations for the results found were prepared as next the curves

The variation of the angle of friction affects the maximum settlement and seems not to influence the width of the bowl, in fact, there is a reduction in the amplitude of the maximum settlement when the friction angle is about and when there is an increase in the settlement there is also a significant increase in horizontal displacements

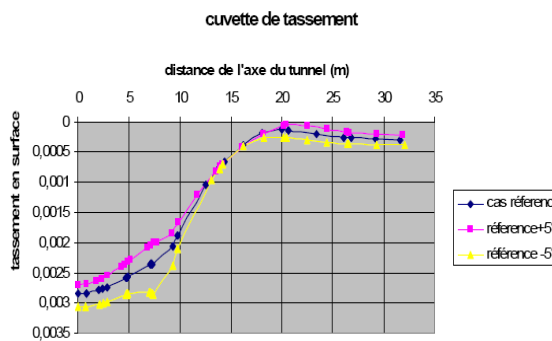


Figure.5: variation of the angle of friction of the soil

3.1.2.3 Poisson's ratio:

The Poisson's ratio characterizing the elastic behavior of the material in order to study the influence of Poisson's ratio on the behavior of soils, we performed two calculations with values of Poisson's ratio

The results for these values have allowed us to conclude that this parameter does not substantially affect the magnitude of settlements, in fact, the use of equations of the mmc.

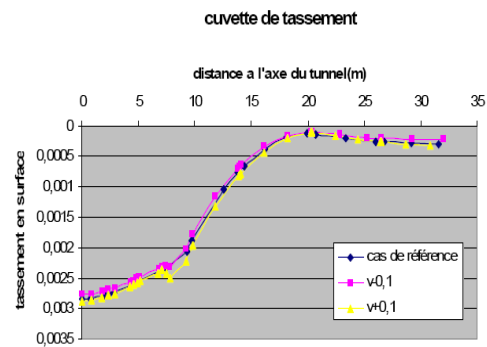


Figure.6: variation of Poisson's ratio

3.1.2.4 Soil Stiffness (E):

Soil stiffness was changed to three calculations due to analyze soil movements vis-à-vis Changing this parameter The results from these calculations show that the maximum settlements are affected by the change in stiffness soil, their amplitudes decrease by increasing this module

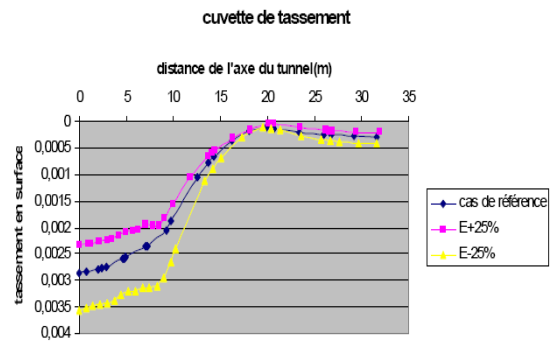


Figure.7: variation of soil stiffness (E)

These results we seem obvious that the increase in the modulus of elasticity and stiffens the floor therefore are reduced settlements

3.1.2.5 Mesh

Modification of this parameter The results from these calculations show that the maximum set-

lements are affected by the variation of the model grid, their amplitudes decrease with decrease in the mesh

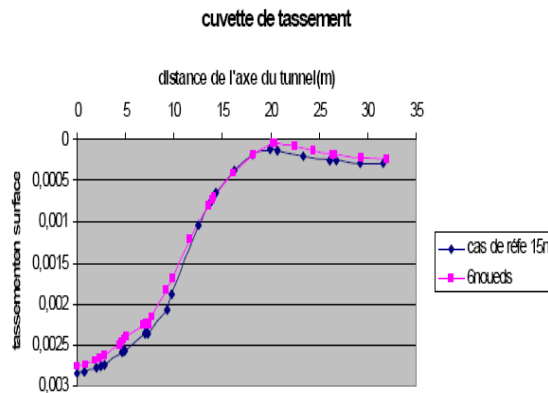


Figure.8: variation of mesh

3.1.3.6 change in position of the Nappe

The change of this parameter indicates that the maximum subsidence are affected by the variation of the position of the web will increase when the amplitudes of the position away from the web natural surface

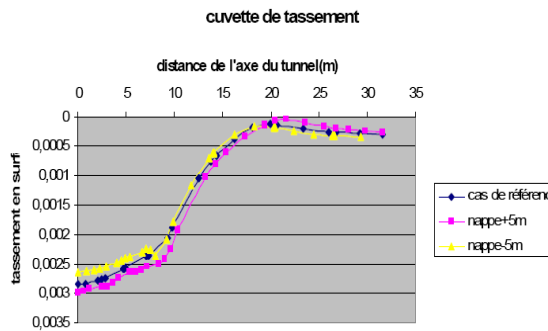


Figure.9: change in position of the Nappe

4. Conclusion:

According to the parametric study on the influence of rheological parameters, it was noted that the geotechnical parameters have an obvious influence on the behavior of soils especially in settlements where the need for a proper determination of these parameters,

The most influential parameters are Poisson's ratio, Young's modulus and the friction angle and the parameter mesh type and position of the water

on the influence of digging a tunnel on the possible appearance of settlements due to the presence of a surface structure, the effect is significant and preliminary studies should consider this type of work during the various phases to correctly size the structure

5. Bibliographical references:

- 1-N, Dolzhenko (2002). Experimental and numerical modeling of two-dimensional underground urbain.réalisation bi trials axial and oedometer on the analog ground taylor-Schneebeli, PhD thesis, INSA Lyon
- 2-D DIAS. (1999). Strengthening gauge tunnels by bolting. Numerical study and application to a real case in urban areas. PhD thesis, INSA Lyon
- 3-K, TERZAGHI, Peck, Mesri. Soil Mechanics in Engineering Practice 1940.534 pages
- 4-K, Terzaghi. (1943). Theoretical soil mechanics, 526 pages
- 5 - K, Terzaghi. Theoretical Soil Mechanics (New York, 1943) 278.
- 6- M. A. BIOT, *J. Appl. Phys.* 12 (1941) 155.
- 7- C. W. CRYER.a comparison of the three-dimensional consolidation theories of biot and terzaghi (1962)
- 8-I, BENAMAR (19-12-1996). Study of delayed effects in deep tunnels, PhD of the National School of Bridges and Roads, 205pages
- 9-M, Zouhair Babchia, J-P, Magnan. Numerical analysis of the behavior of massive clay, LPC N° 140 October 1986
- 10-H, Mroueh (27-05-1998). Tunnels in urban areas and numerical modelling interaction widening existing structures, PhD Central School of Lille, 132 pages
- 11-J-P, Magnan & L LEPIDAS. Parametric study of horizontal displacements of soft soil under the embankment during construction, GT42 July 1990
- 12-M, MRAD. (2005). modeling of the hydromechanical behavior of unsaturated expansive soils, PhD Thesis of National School of Geology, Nancy, 342 pages
- 13-A, ZADJAOUI (2000). Bibliographic analysis and numerical modeling of flow around tunnels. Magisterial memory, Department of Civil Engineering, Faculty of Engineering, University aboubakr Belkaid tlemcen. (Algeria).
- 14-M, ATWA. (1996). numerical analysis of water flow and soil consolidation around tunnels in clay, Doctoral Thesis of the National School of Bridges and Roads, 492 pages.
- 15-M, Ould AMY. (1990). Numerical modelling of flows and deformations in earth dams constructed on soft soils, PhD Thesis of the National School of Bridges and Roads, 275 pages.

Validating Timing And Scheduling Mar- te's Profils Using Event B: Case Study Of A Gpu Architecture

Imane ZOUANE, Mostefa BELARBI, Chouarfia Abdellah
LIM Research Laboratory, University of Ibn khaldoun Tiaret, Algeria
i_zouaneb@yahoo.fr, belarbimostefa@yahoo.fr

Abstract-*System on chip multi calculator (CPU and GPU) is a promoted filed to parallelize application thanks to the multi-core GPU architecture. GPUs (Graphic Processing Unit) ensure the parallelism on the chip and discharge the Central Processing Unit (CPU). The specification of scheduling and timing on GPUs had been always a research problematic. MARTE is an efficient semi formal tool for specification thanks to the several diagrams of UML and the new profiles provided by MARTE which treats the software, hardware and scheduling of the specified SoC. But it still none valid specification because it isn't proved. That's why we propose to couple MARTE with the formal method Event B to have a valid and proved specification and to validate the task scheduling on the GPU. After having a valid specification a second phase of executable code generation from Event B specification is essential to execute parallel applications on the GPU. CUDA is an efficient programming language on GPUs because it offers new tools for parallel programming.*

Index Terms

GPU, MARTE, Scheduling, Timing Event B, Refinements, Code generation, CUDA.

1. INTRODUCTION

A System on Chip (SoC) is a total electronic system integrated on one chip. A SoC can be constituted of a CPU, a memory (DRAM), a bus and a specialized unit of processing according to the SoC's function. In the last years the Graphic processing Unit (GPU) started to be essential in SoCs. GPUs permit to execute parallel tasks on the SoC.

To specify SoCs we need specialized tools such as UML¹⁰/ MARTE (Modeling and Analysis of Real-Time and Embedded Systems) which offer a support to cover all the phases of SoC development and to specify hardware and software SoC's aspects. But this specification misses the mathematic improves because it's informal so it can't be considered valid. To solve this problem the proposed solution is to couple the UML/MARTE

with a formal tool to have a sure specification based on mathematic notions and successive refinements.

We are interested to coupling UML/MARTE to the formal method B-event which is an extension of B method. Many works have proposed approaches to translate UML diagrams to B specification. The work made by Laleau [1] proposes a tool of automatic generation of class and state-transition diagram to B abstract machines Using OCaml language in Rose Programming Environment. But he found some limits of semantics of the concepts which cause the user intervention to complete the generated specification. Then Ledang [2] proposed an approach to translate the compartment diagrams because according to him the previous works have interested just to static diagrams. He has concentrated on collaboration diagram by considering it as layers of objects. He proposed the notion of calling-called to link between layers and generated abstract machines. We can say that Ledang [2] has created an effective tool to translate UML compartment diagrams to B specification. In addition, to complete his works, Ledang [3] has created a tool named ArgoUML+B which permit to generate B specifications from UML diagrams. This tool has given good results in the field of UML translation to B specification and it has been developed using Java to avoid limits founded in Laleau's work[1]. Based on this works we propose an approach of coupling UML/MARTE to B-event specification to have proved and verified specification thanks to B-event.

After specifying our SoC we need to generate an executable code on GPU from the MARTE specification using the proved Event B specification as an intermediate. Model Driven Engineering (MDE) proposes an approach to generate executable code from a model throw successive transformations of the semi-formal specification. In this field several works have been proposed by

¹⁰UML: Unified Modeling Language

Wendell [4][5] to generate OpenCL¹¹ code from a GPU MARTE specification in order to provide a tool of code generation for none specialized in parallel programming to develop their applications. Wendell proposed an MDE approach of specification, modeling and generation of OpenCL applications. A first specification has been done using UML/MARTE and ARRAYOL of GPU architecture and the Conjugate Gradient algorithm, then a successive transformations using MOF/QVT (Meta-Object Facility Query/View/Transformation) result an executable OpenCL code on GPU.[4] Another work which studies a H.263 video compression (Downscaling) application where a preliminary MARTE specification of the downscaler has been done using Gaspard2. Then an OpenCL valid code has been generated from Gaspard2 specification.[5] We are going to generate a pre-code CUDA (Compute Unified Device Language) from UML/MARTE specification but after transforming this later into Event B specification to guarantee its validity.

This paper is divided into several sections, section 2 defines MARTE specification. The section 3 gives a brief description of Event B. In section 4 we describe GPU's architecture. Then we present our proposition of GPU specification in section 5 and we treat a study case of GPU specification using UML/MARTE, coupling MARTE with Event B and extracting a CUDA code of vector addition algorithm using Event B refinements. Finally we present our conclusion and some perspectives.

2. MARTE

The MARTE (Modeling Analysis Real Time Embedded systems) profile is an extension of UML to complete the missing tools of embedded systems modeling. MARTE was created by "ProMarte" consortium for OMG (Object Management Group) users. [6] MARTE is composed of four packages: foundations, design model, analysis model and annexes. Each package contains several profiles which permit specifying, modeling, analyzing and verifying an embedded

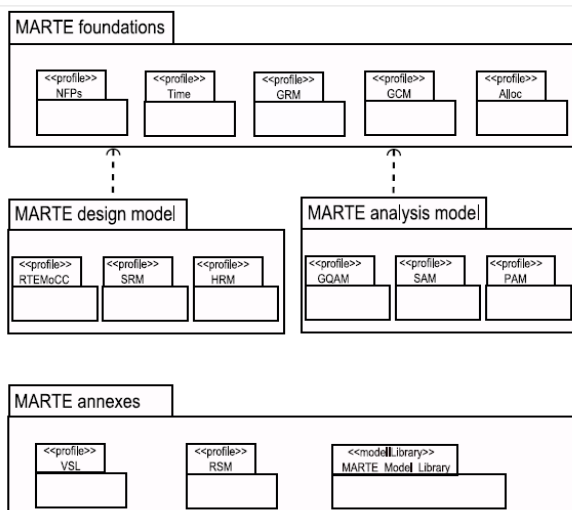
real time system.

Fig 1. MARTE architecture

MARTE has improved the UML specification because:

- It distinguishes the hardware part from the software part using Hardware Resource Modeling (HRM) profile and Software Resource Modeling (SRM) profile.
- It permits to allocate the software application on the hardware resources thanks to Allocation profile (Alloc).
- It permits timing and scheduling modeling.
- It permits performance and scheduling analysis using Performance Analysis Modeling (PAM) profile and Schedulability Analysis modeling (SAM) profile.

Several works have used MARTE profile for system modeling especially real time embedded system thanks to its efficient tools (profiles). We mention the work of remote controlled robot specification [7] where they used MARTE for real time constraints modeling. They stereotyped the classes with *SchedulableResource* stereotype in class diagram and they added *timing observation (reference)* in sequence diagram to illustrate the timing constraints of remote controlled robot system. Another paper where they dealt with time specification in an automotive system of an ignition control and knock correction in the case of four stroke engine. In a 4-stroke engine a cycle is composed of four phases: Intake, Compression, Combustion and Exhaust. This phases were represented by a timing diagram to illustrate the timing properties in addition to the MARTE notions of *TimedEvent* and *TimedProcessing* used in the state-transition diagram.[8] The MoPCom approach which is a co-design methodology to generate VHDL codes has also used MARTE to describe real-time properties and perform the platform modeling. In addition to UML diagrams, the MARTE profiles SRM, HRM and Alloc have been essential in the process of VHDL code generation.[9] MARTE was also a base of a methodology approach for high level modeling and model+code generation for embedded real time systems. The methodology consist of specifying a system with UML and MARTE profile then the specification become a source to model and code generation of real time components and scheduling analysis. [10] MARTE became an essential element in real time embedded systems specification because it offers a multitude tools (profiles)



for modeling time constraints, scheduling and performance of systems.

3. EVENT B

Event B is an enriched extension of the formal method B created by J. R Abrial [11] for system specification, design and coding. It is based on Set theory and it specifies the system by abstract machines, operations and successive refinements which permit to prove, to verify and to validate the specified system.

Event B is based on MODEL notion which describes the labeled transaction of the system. A MODEL is composed of a static part which contains the states, its invariants and its properties and a dynamic part containing transitions (events). A MODEL has a name, variants, invariants and Events. A MODEL is completed by a formalism called the CONTEXT. It plays an important role in MODEL parameterization and instantiation. A CONTEXT has also a name, Sets, Invariants.[12][13] Each MODEL can reference a CONTEXT and many refinements which concretes models and contexts as it is shown in the figure 2.

The Event B method is efficient because it uses tools like Atelier B¹² and the platform RODIN (Rigorous Open Development Environment for Complex Systems). This platform is a tool to develop and to prove Event B specification under Eclipse environment. [12] The main objective of RODIN is to create a methodology and supporting open tool platform for cost-effective, rigorous development of complex, dependable software systems and services. [14]

4. GPU ARCHITECTURE

Graphic Processing Units have a high performance processors dedicated to graphics processing. Originally, GPUs were oriented to accelerating graphics rendering functionality. Lately they are used to perform different kinds of general purpose computations in a parallel way to minimize application’s runtime.[15]

GPU is a multi-core architecture used to enhance intensive computing and to discharge the CPU. A GPU is composed of a Global memory (DRAM) and a set of Streaming Multiprocessor (SM). Each SM is constituted of a set of Streaming Processor (SP) and each SP is linked to a local memory (Register memory). And the SPs of SM are linked to a shared memory. The multi-core architecture of GPU ensures its efficiency in its capacity of computing. [16]

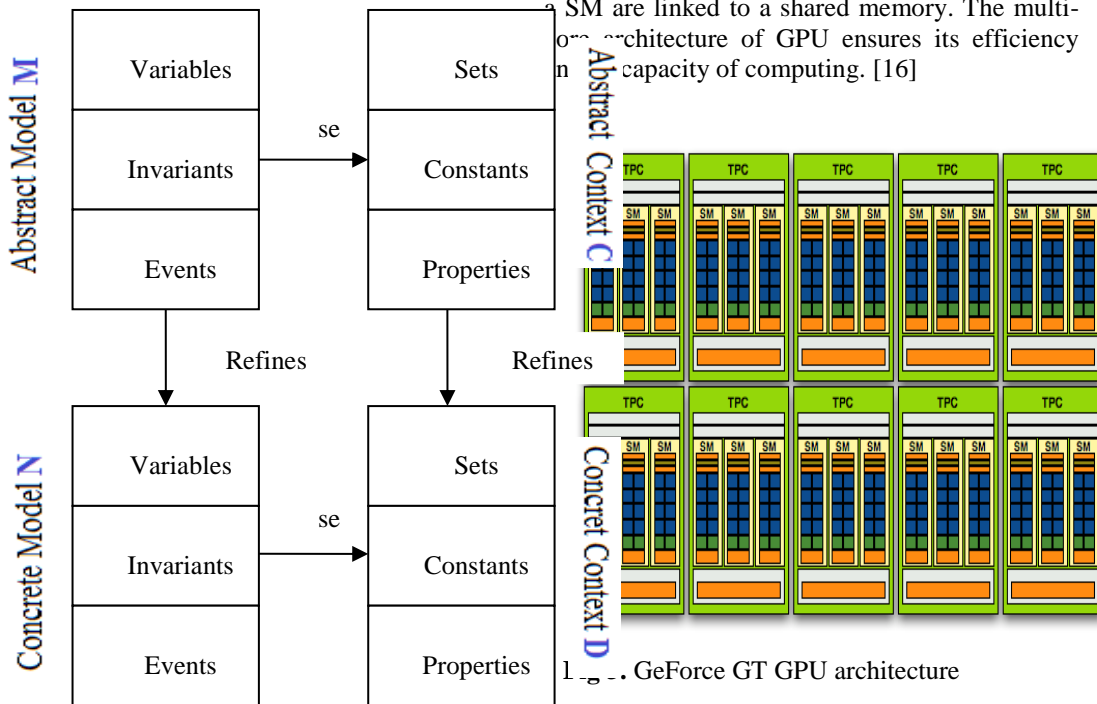


Fig 2. Refinements of models and contexts

1. ... GeForce GT GPU architecture

In Nvidia architecture tasks are executed using SIMD (Single Instruction Multiple data) blocs written in CUDA. [17] CUDA (Compute Unified

¹² Atelier B is a tool that permit operational use of the method B : <http://www.atelierb.eu>

Device Architecture) provides a set of software libraries, an execution environment and a multitude drivers for different languages of programming (C,C++,...). CUDA is an extension of C language for programming on NVIDIA GPU. The computations on a GPU are programmed as *kernel* functions. A kernel program describes the execution of a serial *thread* on a GPU. The kernel is launched by the host CPU with specified numbers of blocks and threads, where a *block* represents a set of a certain number of threads, and all blocks in that kernel launch have the same numbers of threads. The total number of threads is the number of blocks times the number of threads per block. [18] Since there is a number of processing units on GPU a solution of scheduling is needed to organize the execution on GPU.

5. PROPOSED APPROACH VIA A CASE STUDY

Our main objective is to specify a GPU with different tools and to generate a valid executable code.

We propose to use UML diagrams and MARTE profile to specify a SoC with:

- i. Hardware Resource Modeling (HRM) to specify the SoC components,
- ii. Software Resource Modeling (SRM) for modeling the applications that will be executed on the SoC.
- iii. Allocation (Alloc) profile to allocate the software on the hardware components.
- iv. **Timing profile** for time constraints modeling.
- v. **Schedulability Analysis Modeling (SAM)** for scheduling modeling and analysis.

After specifying our SoC with MARTE profile we propose to couple it with Event B specification to make it valid, sure and proved with Event B rigorous tools. We have proposed a set of rules for transformation of MARTE models into Event B specification.

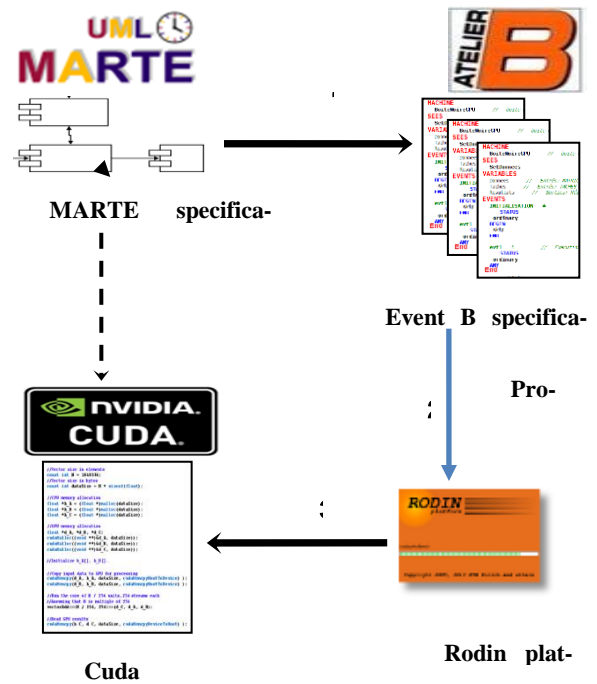


Fig 4. Proposed approach of SoC specification

Once a valid, sure and correct specification of SoC has been carried out, it could be exploited to generate an executable code to be run on the SoC hardware resources (CPU/GPU). We propose to do a set of refinements of Event B specification to generate a parallel executable code written in CUDA language which is rich of parallel implementation on NVIDIA GPU architectures.

To test our approach we used a case study of GPU architecture. We are going to specify a GPU architecture using MARTE and Event B with an application (*Vector addition*) which will be executed on GPU architecture.

5.1. GPU specification

5.1.1 GPU architecture

We are using a GeForce GT 210 GPU to implement our case study. It is composed of 16 CUDA cores. The relation between internal GPU components is illustrated in the component diagram where each component is stereotyped by MARTE stereotypes for each type component (hwcomponent, hwRam, hwBus, hwComputingResource,...).

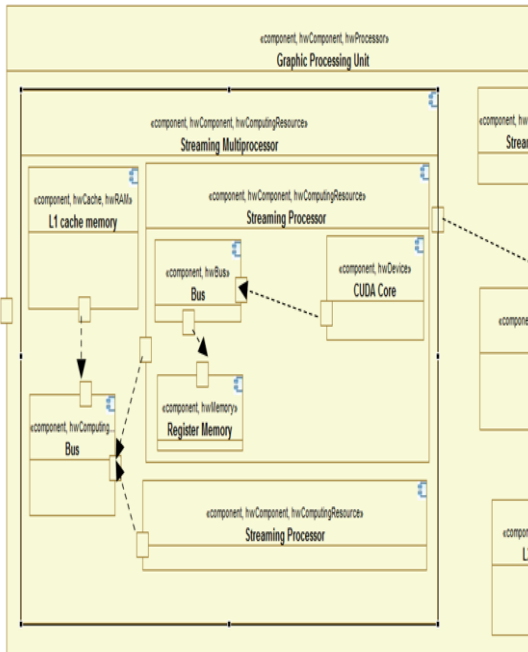


Fig 5. Component diagram of GPU architecture

The properties of GPU component are illustrated by a GPU class where all the GPU details are presented.

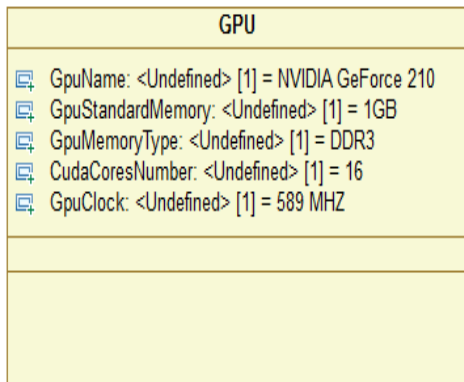


Fig 6. GPU class

5.1.2 Link between hardware architecture and software architecture

In order to treat the parallel execution of applications on GPUs we have chosen a simple algorithm of Arrays addition.

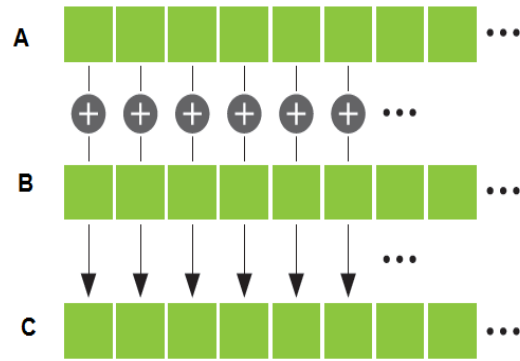


Fig 7. Vector Addition

The sequential algorithm of **Vector addition** of two vectors A, B (of N dimension) resulting a vector C is illustrated thereafter. It is necessary to run through a loop to execute the addition operation. So the time spent in executing vector addition is doubled.

Algorithm Vector Addition

Input:
A,B: array [1..N] d'entier

Output: C

Begin
i: entier
for (i=0 à N ; i++)
 C[i]= A[i]*B[i] ;
Endfor
End

To optimize the runtime the vector addition algorithm can be executed in a parallel way on GPU architecture thanks to its multi-cores. Each addition operation of an element C[i] is calculated in a CUDA core basing the element A[i] and the element B[i]. [19] In this case the execution of vector addition follows these steps:

- Vector A loading on the CPU;
- Vector B loading on the CPU;
- Data (vector A, vector B) transfers from CPU into GPU;
- Calculating C: kernel parallel execution on GPU which is illustrated in the next algorithm;
- Data transfers (vector C) from GPU into CPU;
- Vector C display.

```

Algorithm Kernel


---


Input: A,B
Output:C
Begin
    int nmb_r_bloc,nmb_r_thread,affect;
    affect=nbre_bloc/nbre_thread;
    if (affect >=0) then
        Execute (Vector-addition (C[1], C[2],...,
C[N]));
    endif
End


---


Vector-Addition (C[i])
Begin
    C[i] = A[i]+B[i] ;
End

```

The elements C[i] are considered as blocs and executed in a parallel way using the A[i] and B[i] elements.

We specified the vector addition using MARTE profile then we allocated the application on the hardware architecture (CPU/GPU).

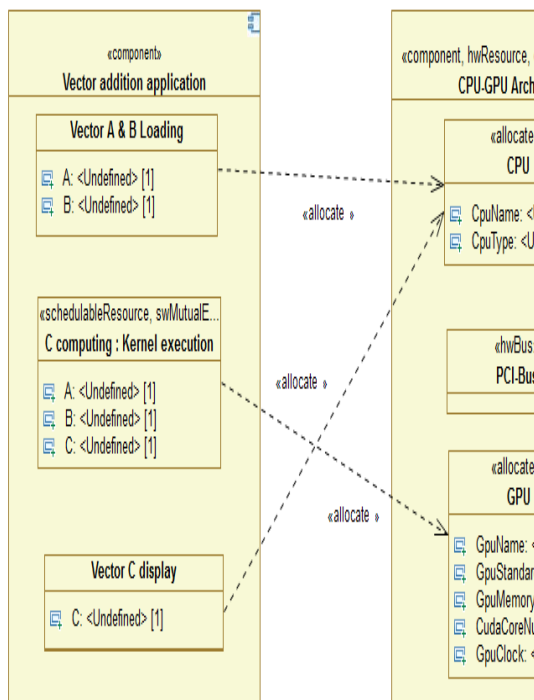


Fig 8. Allocation of vector addition application on hardware architecture

When a kernel is launched on GPU architecture only this kernel is executed, the other kernels will wait until it finishes to be executed. This notion is

represented using MARTE stereotypes (swSchedulable, swMutualExclusion)

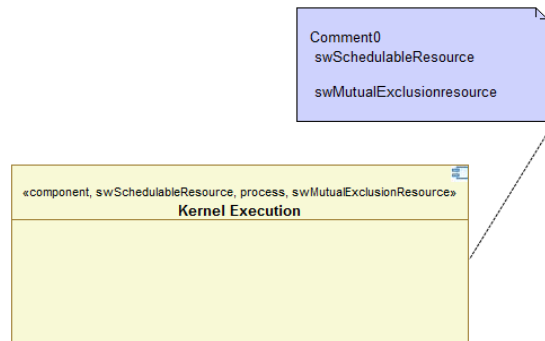


Fig 9. Kernel execution stereotypes

5.1.3 State-transition diagram

When a task is launched a preliminary test is executed on the CPU to affect the task to the right processor. If it is a repetitive one it will be considered as a kernel which is going to be executed many times on the GPU-(SIMD) Single Instruction Multiple Data. If it is a sequential task, it will be run once on the CPU. The state transition events are **TimedEvent** and the state-transition of task execution is stereotyped by **Timedprocessing** stereotype.

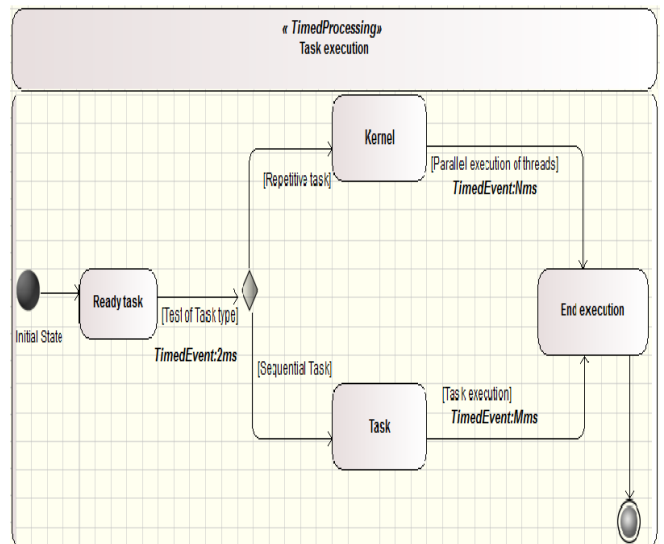


Fig 10. State-transition diagram of task execution

5.1.4 Timing diagram

When the Vector addition is launched the parameters (Vector A and Vector B) will be transferred into the GPU and the function of vector addition will be a kernel. Then on the GPU the

kernel will be divided into blocs that will be executed in a semi-parallel way. Each bloc executes one operation of addition, then it is affected to the result vector C.

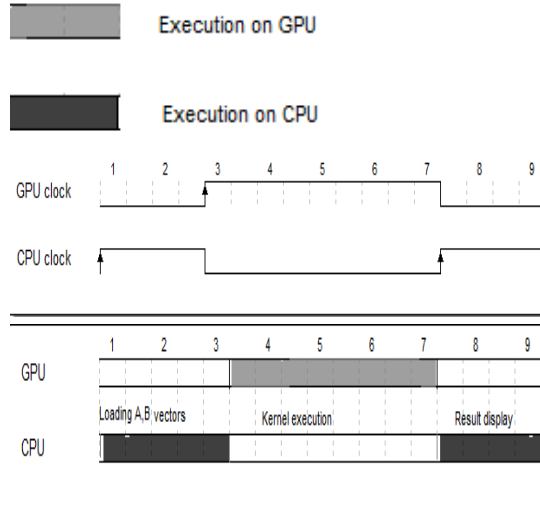


Fig 11. Timing diagram of vector addition on GPU

5.1.5 Sequence diagram

The process of vector addition is represented by a sequence UML diagram.

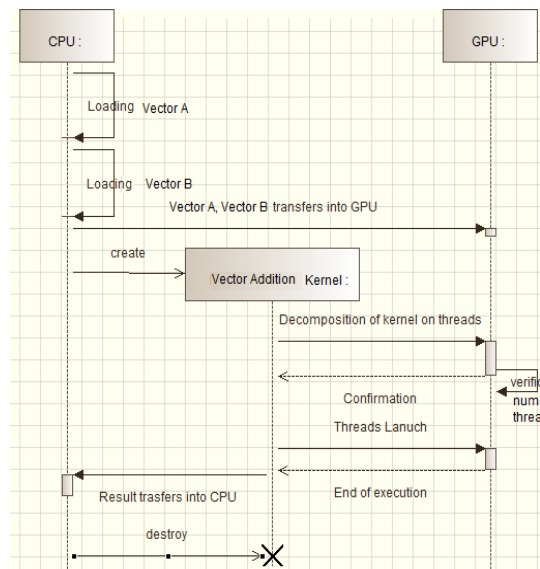


Fig 12. Sequence diagram of vector addition

5.2 Coupling MARTE with Event B

The approach of UML/MARTE transformation into Event B consists of representing the aspects of an application by UML/MARTE diagrams

then they must be transformed into Event B specification and proved by Rodin. This technique uses MARTE as a start point for modeling oriented object models then they are proved and validated by Event B tools. Event B gives a correct semantic of the Graphic UML/MARTE models.

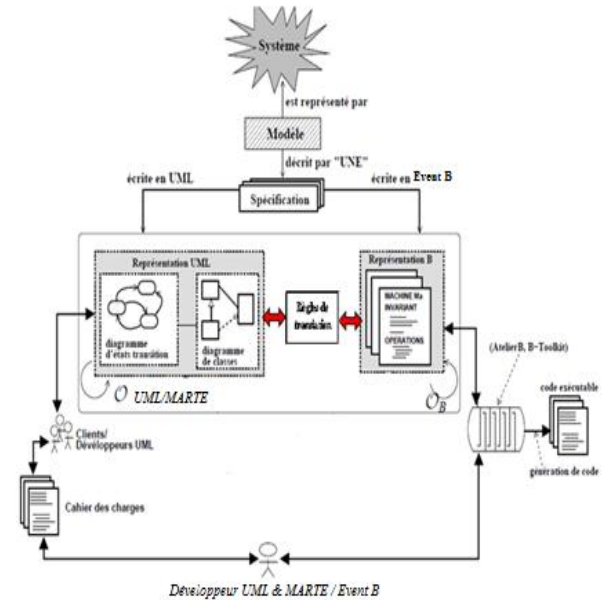


Fig 13. Process of MARTE transformation into Event B

5.2.1 MARTE profiles' Instantiation

At the beginning we did a preliminary phase of MARTE's specification instantiation of MARTE Timing and scheduling profiles to Event B context from MARTE definition.

```

CONTEXT
  Timing-profile
SETS
  Timing_stereotypes
CONSTANTS
  TimedEvent
  TimedProcessing
  EventDuration
AXIOMS
  axm1 : EventDuration ∈ N1
  axm2 : TimedEvent ∈ Timing_stereotypes
  axm3 : TimedProcessing ∈ Timing_stereotypes
  axm4 : Timing_stereotypes ≠ ∅
END
    
```

CONTEXT
 Scheduling-profile

SETS
 Scheduling_stereotypes

CONSTANTS
 SWSchedulableResource
 SWSMutualExclusionResource

AXIOMS
 axm1 : SWSchedulableResource ∈ Scheduling_stereotypes
 axm2 : SWSMutualExclusionResource ∈ Scheduling_stereotypes
 axm3 : Scheduling_stereotypes ≠ ∅

END

5.2.2 Rules of MARTE specification transformation into Event B

In order to transform MARTE models into Event B specification we proposed a set of rules based on the state-transition, class diagram and Allocation diagram:

Rule 1: A class X is transformed into a Machine X.

Rule 2: The properties of class X are the variables of Machine X.

Rule 3: Each Machine X has a ContextX that defines its variables.

Rule 4: The states of state-transition diagram (of class X) are constants in the context ContextX.

Rule 5: The events of state-transition diagram are the events of Machine X.

Rule 6: The software Machines share the same context.

Rule 7: The operations of a class X are the events of the corresponding Machine X.

Rule 8: The hardware machine refines the software machines.

Applying these rules on the GPU MARTE specification we conclude the following Event B specification illustrated by a schema (cf.Fig).

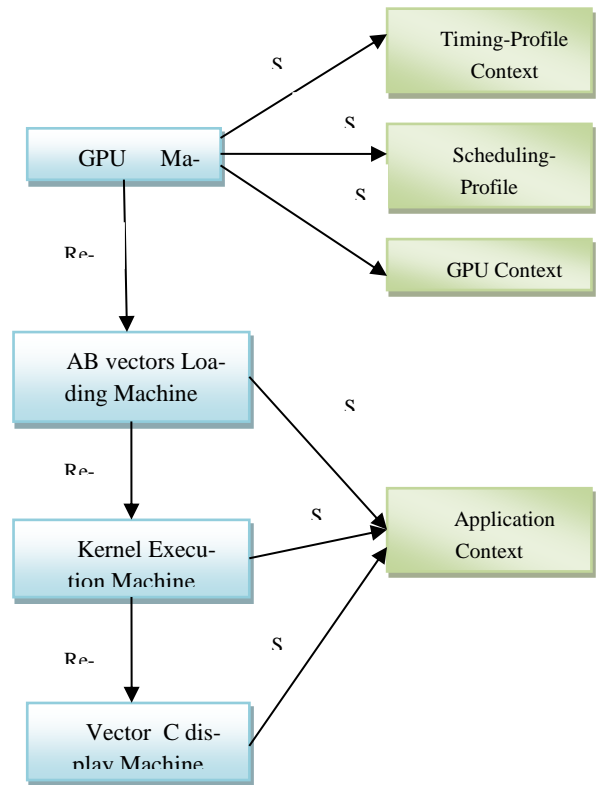
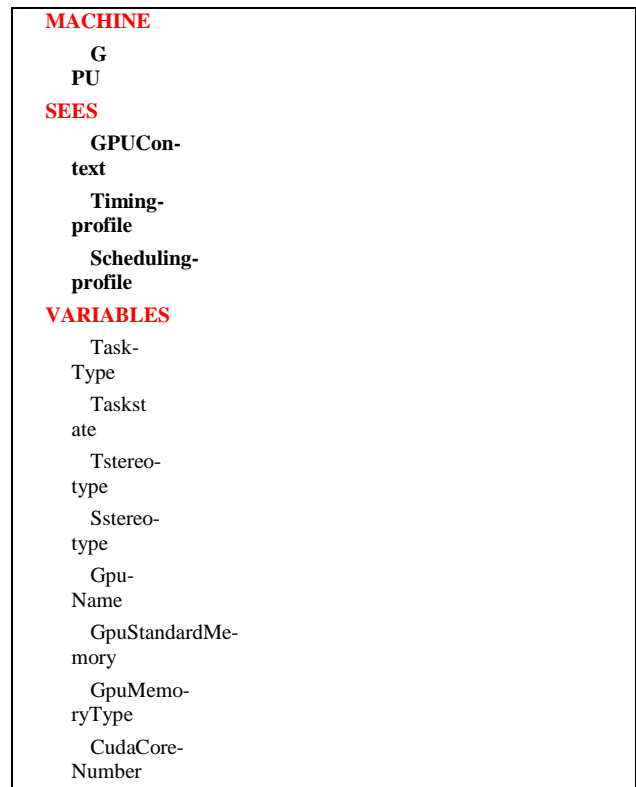


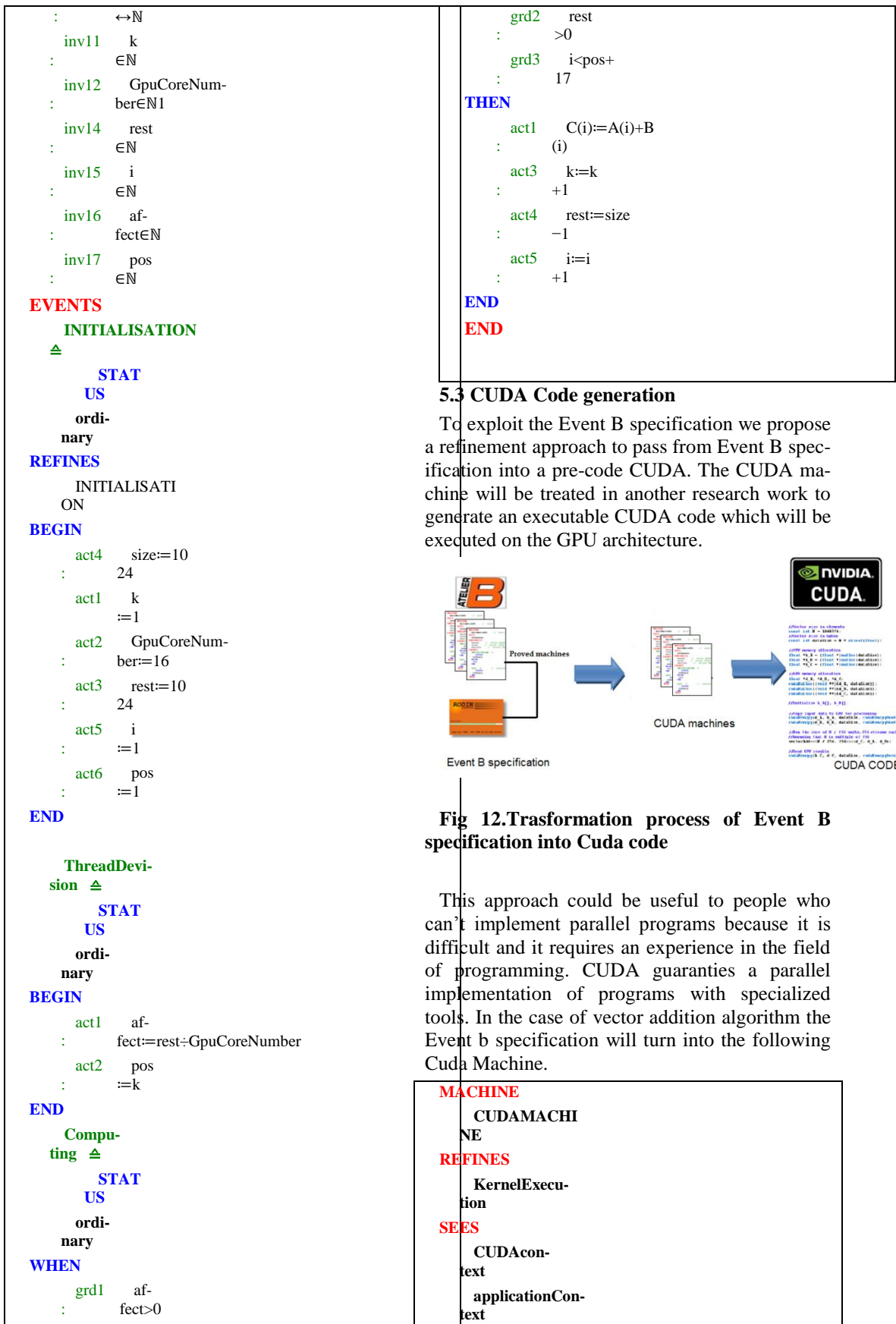
Fig 14. Resultant machines of transformation

The transformation of GPU class result a GPU machine using scheduling and timing profiles:



<pre> Gpu- Clock evdura- tion INVARIANTS inv9 Task- : Type ∈ TASKtype inv2 Taskstate ∈ State : ate inv10 Tstereo- : type ∈ Timing_stereotypes inv11 Sstereo- : type ∈ Scheduling_stereotypes inv13 GpuStandardMemo- : ry ∈ N1 inv14 CudaCoreNum- : ber ∈ N1 inv15 Gpu- : Clock ∈ N1 inv16 Gpu- : Name ∈ Gpunamesetgpu inv17 GpuMemo- : ryType ∈ MemoryType inv18 evdura- : tion ∈ N1 EVENTS INITIALISATION ≙ extended STAT US ordi- nary BEGIN act11 Sstereo- : type := SwSchedulableResource act10 Tstereo- : type := TimedProcessing ac 3 Task- : Type := TR act4 Taskstate := ReadyTa : sk act12 Gpu- : Name := GeForce210 act13 GpuMemo- : ryType := DDR3 act14 CudaCoreNum- : ber := 16 act15 Gpu- : Clock := 589 act16 GpuStandardMemo- : ry := 1 END TestE- vent ≙ STAT US or in </pre>	<pre> ary ANY Tas kT Tst ate WHERE grd1 TaskT= : TR grd3 Tstate=ReadyTa : sk THEN act1 Taskstate := Ker : nel act2 Sstereo- : type := SwSchedulableResource act3 Tstereo- : type := TimedEvent act4 evdura- : tion := 2 END Execu- tion ≙ STAT US ordi- nary ANY Tst ate WHERE grd1 Tstate = Ker : nel THEN act6 Taskstate := ExecutionE : nd act3 Sstereo- : type := SwMutualExclusionResource act4 Tstereo- : type := TimedEvent act7 evdura- : tion := 30 END END </pre>
	<p>For the application there are three machines refined from GPU machine which are presented in the next part:</p>

<p>MACHINE</p> <p>VectorABLoading</p> <p>REFINES</p> <p>G</p> <p>PU</p> <p>SEES</p> <p>applicationContext</p> <p>VARIABLES</p> <p>si</p> <p>ze</p>	<pre> : *k act5 k:=k : +1 END END </pre>
<p>INVARIANTS</p> <p>inv1 size\in</p> <p>: $\mathbb{N}1$</p> <p>inv7 k</p> <p>: $\in \mathbb{N}$</p> <p>inv12 A\in1..size</p> <p>: $\rightarrow \mathbb{N}$</p> <p>inv13 ran(A)=ran(Array)</p> <p>: ay)</p> <p>inv14 A$\in$$\mathbb{N}$</p> <p>: $\leftrightarrow \mathbb{N}$</p> <p>inv15 B$\in$1..size</p> <p>: $\rightarrow \mathbb{N}$</p> <p>inv16 ran(B)=ran(Array)</p> <p>: ay)</p> <p>inv17 B$\in$$\mathbb{N}$</p> <p>: $\leftrightarrow \mathbb{N}$</p> <p>EVENTS</p> <p>INITIALISATION</p> <p>\triangleq</p> <p>STAT</p> <p>US</p> <p>ordinary</p> <p>BEGIN</p> <p>act1 size:=10</p> <p>: 24</p> <p>act4 k</p> <p>: :=1</p> <p>END</p> <p>TableLoading \triangleq</p> <p>STAT</p> <p>US</p> <p>ordinary</p> <p>WHEN</p> <p>grd1 k<size</p> <p>: +1</p> <p>THEN</p> <p>act3 A(k)</p> <p>: :=k</p> <p>act4 B(k):=k</p>	<p>MACHINE</p> <p>KernelExecution</p> <p>REFINES</p> <p>VectorABLoading</p> <p>VARIABLES</p> <p>si</p> <p>ze</p> <p>r</p> <p>est</p> <p>GpuCoreNumber</p> <p>af-</p> <p>fec</p> <p>p</p> <p>os</p> <p>INVARIANTS</p> <p>inv1 size\in</p> <p>: $\mathbb{N}1$</p> <p>inv2 A\in1..size</p> <p>: $\rightarrow \mathbb{N}$</p> <p>inv3 ran(A)=ran(Array)</p> <p>: ay)</p> <p>inv4 A$\in$$\mathbb{N}$</p> <p>: $\leftrightarrow \mathbb{N}$</p> <p>inv5 B$\in$1..size</p> <p>: $\rightarrow \mathbb{N}$</p> <p>inv6 ran(B)=ran(Array)</p> <p>: ay)</p> <p>inv7 B$\in$$\mathbb{N}$</p> <p>: $\leftrightarrow \mathbb{N}$</p> <p>inv8 C$\in$1..size</p> <p>: $\rightarrow \mathbb{N}$</p> <p>inv9 ran(C)=ran(Array)</p> <p>: ay)</p> <p>inv 0 C$\in$$\mathbb{N}$</p>



<p>VARIABLES</p> <p>de- ceA</p> <p>de- viceB</p> <p>de- ceC</p> <p>si ze</p> <p>Transfer- Mem</p> <p>CudaMal- loc</p> <p>af- fect</p> <p>GpuCore- Number</p> <p>r est</p> <p>p os</p> <p>Cudafr ee</p> <p>INVARIANTS</p> <p>inv1 de- : ceA ∈ 1 · · size → N</p> <p>inv2 de- : viceB ∈ 1 · · size → N</p> <p>inv3 de- : ceC ∈ 1 · · size → N</p> <p>inv8 Transfer- : Mem ∈ TRANSFERDATATYPE</p> <p>inv10 size ∈ : N1</p> <p>inv11 ran(deviceA)=ran(Arr : ay)</p> <p>inv12 ran(deviceB)=ran(Arr : ay)</p> <p>inv13 ran(deviceC)=ran(Arr : ay)</p> <p>inv14 de- : ceA ∈ N ↔ N</p> <p>inv15 de- : viceB ∈ N ↔ N</p> <p>inv16 de- : ceC ∈ N ↔ N</p> <p>inv18 i : ∈ N</p> <p>inv19 k : ∈ N</p> <p>inv20 rest : ∈ N</p> <p>inv21 GpuCoreNum- : ber ∈ N</p> <p>inv22 pos</p>	<p>: ∈ N</p> <p>inv24 Cudafree ∈ CudaFr : ee</p> <p>inv25 CudaMal- : loc ∈ Malloc</p> <p>EVENTS</p> <p>INITIALISATION</p> <p>△</p> <p>STAT</p> <p>US</p> <p>ordi- nary</p> <p>REFINES</p> <p>INITIALISATI ON</p> <p>BEGIN</p> <p>act3 size:=10 : 24</p> <p>act4 i : :=1</p> <p>act5 k : :=1</p> <p>act6 rest:=10 : 24</p> <p>act7 GpuCoreNum- : ber:=16</p> <p>act8 pos : :=1</p> <p>act9 CudaMal- : loc:=nonalloc</p> <p>END</p> <p>CudaAlloca- tion △</p> <p>STAT</p> <p>US</p> <p>ordi- nary</p> <p>BEGIN</p> <p>act1 CudaMal- : loc:=malloc</p> <p>act2 Cudafree:=nonFr : ee</p> <p>END</p> <p>CudaCPUtoGPUtras- ferts △</p> <p>STAT</p> <p>US</p> <p>ordi- nary</p> <p>WHEN</p> <p>grd1 CudaMal- : loc=malloc</p> <p>THEN</p> <p>act1 de- : ceA:=A</p> <p>act2 de- : viceB:=B</p>
---	--

```

    act3  Transfer-
    :      Mem:=HostToDevice
END

ThreadDivision ≙
    STAT
    US
    ordi-
    nary
BEGIN
    act1  af-
    :      fect:=rest-GpuCoreNumber
    act2  pos
    :      :=k
END

CudaKernelLaunchADD ≙
    STAT
    US
    ordi-
    nary
WHEN
    grd1  af-
    :      fect>0
    grd2  rest
    :      >0
    grd3  i<pos+
    :      17
THEN
    act1  de-
    :      viceC(i):=deviceA(i)+deviceB(i)
    act2  k:=k
    :      +1
    act3  i:=i
    :      +1
    act4  rest:=size
    :      -1
END

CudaGPUtoCPUtransfers ≙
    STAT
    US
    ordi-
    nary
BEGIN
    act1  C:=devic
    :      eC
END

CudaFree
    ≙
    STAT
    US
    ordi-
    nary
WHEN

```

```

    grd1  rest
    :      ≤0
THEN
    act1  Cudaf-
    :      ree:=Free
END

END

```

After having refined our vector addition algorithm into a CUDA machine, our goal is to generate a valid CUDA code that guarantees the parallelism implementation on GPU architecture.

6. CONCLUSION

The paper suggests new approaches of specification and implementation of GPU SOC basing on MARTE models. The first approach consists on validating the proposed MARTE specification with the formal tool Event B. The second approach proposes to refine the event B specification to have a pre-Code CUDA.

The proposed approaches need to be improved by new rules. As a perspective we want to implement our approaches with automatic generation tools to apply our proposed rules of MARTE transformation into Event B specification and to validate task scheduling on the GPU architecture with formal tools such as Event B. Another perspective is to generate an executable code from the refined pre-code machine CUDA.

7. REFERENCES

- [1] R. Laleau and A. Mammar, "An Overview of a Method and its support Tool for Generating B Specifications from UML NotationsC, In The 15th IEEE Int. Conf. on Automated Software Engineering, Grenoble (France), September 11-15, 2000.
- [2] H. Ledang and J. Souquière, "Formalizing UML Behavioral Diagrams with B", In the Tenth OOPSLA Workshop on Behavioral Semantics: Back to Basics, Tampa Bay, Florida (USA), October 15, 2001.
- [3] H. Ledang, J. Souquière & S. Charles, "ArgoUML+B : un outil de transformation systématique de spécifications UML en B", LORIA - Université Nancy 2, 2003.
- [4] Antonio Wendell de O. Rodrigues & all. "A Modeling Approach based on UML/MARTE for GPU Architecture ", In the The Computing Research Repository (CoRR), May 2011.
- [5] Antonio Wendell de O. Rodrigues, Frédéric Guyomarc'h and Jean-Luc Dekeyser, "Programming Massively Parallel Architectures using MARTE: a Case Study", In the Second Workshop on Model Based Engineering for Embedded Systems Design (M-BED 2011), 2011.
- [6] Madeleine Faugère, Thimothée Bourbeau, Robert De Simone and Sébastien Gérard, "MARTE: Also an UML Profile for Modeling AADL Applications", In the 12th IEEE International Conference on Engineering Complex Computer Systems (ICECCS 2007), 2007.

- [7] Naoufel MACHTA M. Taha BENNANI Samir BEN AHMED, "MODELISATION ORIENTEE ASPECTS DES SYSTEMES TEMPS REEL", In the 8th International Conference of Modelisation and Simulation (MOSIM 10), Hammamet (Tunisie), 2010.
- [8] C. Andre, F. Mallet, M-A. Peraldi-Frati, "A multiform time approach to real-time system modeling Application to an automotive system ", Int. Symp. on Industrial Embedded Systems, Lisboa, Portugal, pp 234-241, Jul 2007.
- [9] Jorgiano Vidal, Florent de Lamotte, Guy Gogniat, Philippe Soulard, Jean-Philippe Diguët, "A co-design approach for embedded system modeling and code generation with UML and MARTE", Int Conf Design, Automation, and Test in Europe - DATE , Nice (France), pp. 226-231, 2009.
- [10] Julio L. Medina and Alejandro Pérez Ruiz, "High level modeling for Real-time applications with UML & MARTE", the 25th Euromicro Conference on Real-Time Systems (ECRTS'13), Paris, France, pp 13-16, July 2013.
- [11] J.R Abrial, "The B-book: Assigning programs to meanings", 1996.
- [12] C. Métayer, J.-R. Abrial, L. Voisin. "Event-B Language", May 2005.
- Architectures nouvelles de machines, Fribourg : Switzerland, pp 1-11, 2008.
- [18] Reiji Suda and Da Qi Ren, "Accurate Measurements and Precise Modeling of Power Dissipation of CUDA Kernels toward Power Optimized High Performance CPU-GPU Computing", In International Conference on Parallel and Distributed Computing, Applications and Technologies, pp 432-438, Higashi Hiroshima, Japan 2009.
- [19] Jason Sanders, Edward Kandrot. "CUDA par l'exemple ", Pearson Education France, 2011.
- [13] Yamine AIT-Ait-Ameur & all. "Vérification et validation formelles de systèmes interactifs fondées sur la preuve : application aux systèmes multi-modaux." IN Journal d'Interaction Personne-Système, Vol. 1, No. 1, Art. 3, Septembre 2010.
- [14] Joey Coleman, Cliff Jones, Ian Oliver, Alexander Romanovsky, and Elena Troubitsyna, "RODIN (Rigorous Open Development Environment for Complex Systems)".
- [15] Sylvain Collange, Yoginder S. Dandass, Marc Daumas, and David Defour, "Using Graphics Processors for Parallelizing Hash-Based Data Carving", In *HICCS*, Hawaii International Conference on System Sciences, pp 1-10, 2009.
- [16] Peter N. Glaskowsky. "NVIDIA's Fermi: The First Complete GPU Computing Architecture", 2009: http://www.nvidia.com/content/PDF/fermi_white_papers/P.Glaskowsky_NVIDIA'sFermi-First_Complete_GPU_Architecture.pdf
- [17] Sylvain Collange, Marc Daumas, David Defour & Régis Olivés, "Fonctions élémentaires sur GPU exploitant la localité de valeurs", In SYMPosium en

A numerical investigation of the performance analysis of an electrorheological hydrostatic journal bearing

Abed N. and Zahloul H.

Department of Mechanical Engineering,
Univ. Chlef, Algeria
Asma.raven@gmail.com

Bouزيدane A. and Nemchi Amina
Department of Mechanical Engineering,
Univ. Tiaret, Algeria
Ahmed.bouزيدane@gmail.com

Abstract— This work describes a theoretical study concerning the performance characteristics of an electrorheological hydrostatic journal bearing. The hydrostatic journal bearing consists of four hydrostatic bearing flat pads fed by capillary restrictors. A negative electrorheological (NER) fluid is a Newtonian fluid with a viscosity which decreases when an electric field is applied, and which can restore its property when the field is removed. A reversible change in viscosity occurs in milliseconds with application of an electric field. Therefore, these fluids are suitable for the real-time control of vibration and vibration damping. A linear modeling was performed in order to study the performance characteristics of a capillary compensated four-pad hydrostatic journal bearing in order to investigate the effect of negative electrorheological fluids and static eccentricity ratio on carrying load capacity, flow, and the dynamic characteristics (stiffness and damping) of an electrorheological hydrostatic journal bearing. An electrorheological fluid consists of a suspension of micron-sized particles dispersed in a dielectric liquid. The discussion of results includes some thoughts on future trends. The results presented in this work are expected to be quite useful to the bearing designers.

Keywords—*Electrorheological fluid, Hydrostatic bearing, Squeeze film lubrication, Newtonian fluids, Reynolds equation, Journal bearing dynamics.*

Introduction

In rotating machinery, more performance enhancement is in demand in terms of speed and accuracy. However, these machines face to a vibration problems caused by mass imbalance, bearing defect, and shaft misalignment, especially in high speed rotating machinery. For subject of vibration suppress, there are three kind of control: passive, active and semi active. The hydrostatic squeeze film damper HSFD is a kind of bearing damper that has been used in the process industry to reduce vibration. It generates its damping force capability in reaction to dynamic journal motions squeezing a thin film of lubricant in the clearance between a stationary housing and a whirling journal. However, for rotors operating at

rotational speed beyond critical speeds, a semi-active control to reduce vibrations is favourable in terms of stability and performance [1]. Smart hydrostatic squeeze film damper using an electrorheological fluid ER as a smart material is effective in reducing rotor vibration when the rotor passes through the critical speed.

An electrorheological fluid consists of micron-sized particles dispersed in dielectric liquid. Under the action of electric field, the particles in the ER suspension are polarised and the interaction between the resulting dipoles causes the particles to form fabricated structure aligned with the electric field. A gel-like phase is obtained at zero shear rate which is broken only when imposing a shear stress greater than a threshold value (the yield stress). The rapid transformation (in milliseconds) of the ER fluid from a liquid phase to a solid phase leads to a dramatic and reversible change in its rheological properties (viscosity, yield stress, shear modulus, etc.), where the apparent viscosity increases by factor as high as 10^5 [2-5].

Since the innovation of the ER fluid in 1947 by Winslow [6], attention has been paid in order to increase the rheological properties induced by electric field [2-7]. This effect is termed the positive ER effect. Wen et al (2003) [8] have reported the giant electrorheological effect in a suspension of nano-particles, where the yield stress up to 130 kpa.

In 1995, Boissy et al [9] found in their studies that the apparent viscosity of the ER suspension decreases as the external electric field increases. This phenomenon is totally opposite to the positive ER effect, and termed the negative ER effect.

Negative ER effect could be used in the industry when a controllable decrease of the viscosity is expected. The advantage of the viscosity change of negative ER fluids is that the behavior remains Newtonian [10]. Various other systems were also found to display the negative ER effect [11-15]. Kimura et al (1998) [12] studied the ER effect in

several UPPG (urethane-modified polypropylene glycol) /DMS (dimethylsiloxane) blends, they found that the sign positive or negative and the strength of the ER effect can be controlled by changing the temperature and viscosity ratio of UPPG and DMS. Lobry and Lemaire (1999) [13] obtained a decrease of the viscosity in a suspension making use of Quincke rotation: the spontaneous rotation of insulating particles (PMMA) suspended in a weakly conducting liquid when the system is submitted to a DC electric field. They found for the first time that an apparent zero viscosity is attained. This system can be tuned in a negative range when the system is submitted to a DC field, or in a positive range where the external field frequency is increased for few hundred Hertz. Mitsumata and Sugitani (2004) [14] showed that the negative ER effect is influenced by the swelling of the particles. Cetin et al (2012) [15] investigated the properties of the negative ER effect in a suspension of colinamite and polyindene dispersed in silicone oil. They found that the negative ER response was converted to a positive one by addition of non-ionic surfactant and they showed that these materials have the potential to be used for vibration damping when doped with appropriate surfactants.

Because of their fast response time and controllable shear viscosity, many ER devices have been reported and patented such as clutches, shock absorber [16], damping devices [17], micro fluidic chips [18], haptic devices [19], etc. One very promising application is the use of ER fluids for vibration control of high speed lubricated rotor bearing systems, based on the electrical alteration of stiffness and damping. Nikolajsen and Hoque (1990) [20] were first to investigate the performance of ER squeeze film damper and to recognize its efficiency. Pecheux et al (1996) [21] investigated numerically a shaft bearing assembly with a squeeze film damper using negative electrorheological fluid in order to control the dynamic behaviour of the shaft. They showed that it could be possible to monitor the damping of a squeeze film damper. Ahn et al (1998) [22] described a controllable squeeze film damper that uses liquid crystal LC as a lubricant in rotating machines which can produce anisotropic damping forces in the horizontal and vertical directions. Liquid crystal is an ER fluid that the Newtonian viscosity can be varied by the applied of electric or magnetic field strength. They showed that the liquid crystal is successfully applied to the SFD for the stabilisation of rotating system and the damping force can be controlled by the externally applied field. Nikolakopoulos and Papadopoulos (1998) [23] presented an experiment in a high speed journal bearing

with small radial clearance, lubricated with ER fluid. They showed that ER fluids have a substantial effect on the dynamic characteristics of journal bearing operating at high shear rates, even using material with the small yield stress (150 pa) in realistic bearing configuration. Yao et al (1999) [24] studied theoretically and experimentally the application of a new disk type to the vibration suppression of a rotor system. They found that the ER damper can suppress large vibration amplitudes around the critical speed. Seungchul et al (2005) [1] investigated the design and application of an electrorheological fluid damper to semi active vibration control of high speed rotor systems. Bouzidane and Thomas (2007) [10] investigated the dynamic behaviour of a rotor supported by a new hydrostatic journal bearing, and fed with a negative electrorheological fluid. They found that in order to reduce vibratory response of the rotor excited by an imbalance, it is sufficient to use a fluid with a high viscosity in order to obtain a high damping, however, the NER fluid can be activated when operating at speeds higher than critical speed without increasing rotor vibration. On the other hand, using a negative electrorheological fluid (NER) is very efficient when the force transmitted to the base must be reduced. When the rotor operates close to the critical speed, the electric field has not to be activated in order to obtain a high damping. When the excitation speed is higher than 1.4 times the critical speed, the electric field must be activated in order to reduce damping.

The objective of this study is to investigate the static and dynamic behaviour of a four pad hydrostatic journal bearing fed with a negative electrorheological fluid. We present a linear modeling in order to study the effect of the negative electrorheological fluid on carrying load capacity, flow and the dynamic characteristics (stiffness and damping).

Description of hydrostatic journal bearing

In this study, the hydrostatic journal bearing is composed of four identical plane hydrostatic bearing pads, with indices 1, 2 and 3 refer to the characteristics of the upper, left, lower and right hydrostatic bearing pads, respectively (Fig. 1).

Each pad fed with a negative electrorheological fluid by a recess, which is supplied by an external pressure P_s through a capillary restrictor-type hydraulic resistance.

The calculation of hydrostatic journal bearing characteristics is obtained by considering the hydrostatic journal bearing as the juxtaposition of three hydrostatic bearing flat pads. We assume that the fluid flow is incompressible, laminar, isothermal, and steady state.

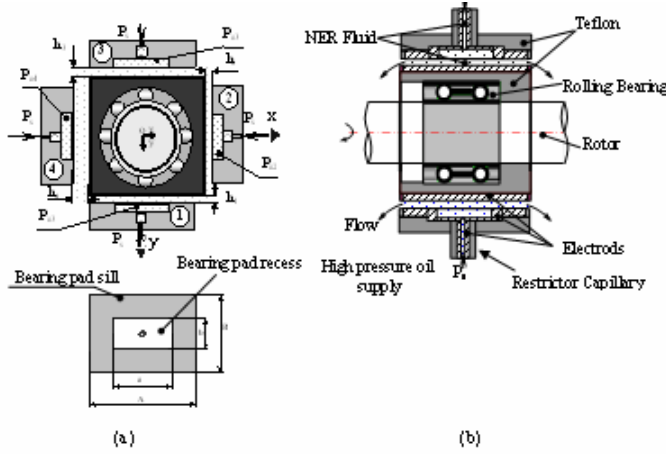


Fig. 1: Hydrostatic journal bearing characteristics

Reynolds equation

The Reynolds equation allows the computation of the distribution pressure $P_i(X_i, Z_i)$. This equation can be solved numerically by applying the centered finite differences method, or analytically in case of particular assumption of infinitely long journals. If we assumed that there is no slip between the fluid and pad bearing, the boundary conditions associated with the speed will be as follows (Fig. 2):

On bearing pad: $U_{1i} = 0; V_{1i} = 0; W_{1i} = 0$

On journal: $U_{2i} = 0; V_{2i} = \dot{h}_i; W_{2i} = 0$

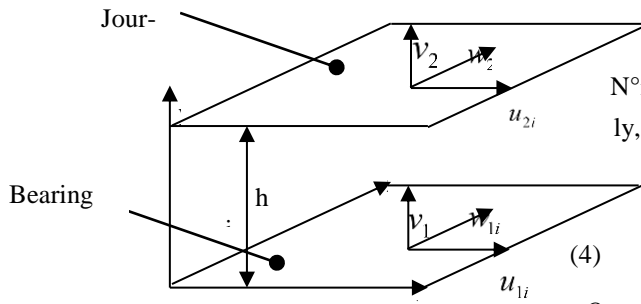


Fig.2. Boundary conditions of hydrostatic journal bearing.

Where U_{1i}, V_{1i} and W_{1i} are the speeds of the surface of the bearing pad $N^{\circ}i$ and U_{2i}, V_{2i} and W_{2i} are the speeds of the surface of the journal.

With these boundary conditions, and for assumption of incompressible, laminar, isoviscous and inertialess fluid flow free of cavitations, the Reynolds equation may be written as:

$$\frac{\partial}{\partial x} \left[\frac{h_i^3}{\mu} \left(\frac{\partial P_i}{\partial x} \right) \right] + \frac{\partial}{\partial z} \left[\frac{h_i^3}{\mu} \left(\frac{\partial P_i}{\partial z} \right) \right] = 12 \dot{h}_i \tag{1}$$

Where $0 \leq x \leq A$ and $0 \leq z \leq B$, P_i is the hydrostatic pressure field of the hydrostatic bearing pad $N^{\circ}i$, h_i is the film thickness of the hydrostatic bearing pad $N^{\circ}i$, \dot{h}_i is the squeeze velocity of the hydrostatic bearing pad $N^{\circ}i$, and μ is the fluid viscosity.

It assumed that the pressure in the recess is constant and equal to P_{ri} and the ambient pressure is null. Thus the boundary conditions of equation (1) are:

$$P_i(0 \leq x \leq A, z = 0) = 0,$$

$$P_i(x = 0, 0 \leq z \leq B) = 0,$$

$$P_i(x_1 \leq x \leq x_2, z_1 \leq z \leq z_2) = P_{ri}$$

Recess pressure

The recess pressure for each hydrostatic bearing pad is obtained by resolving the flow continuity equation.

$$Q_{ri} = Q_{si} \tag{2}$$

Where $Q_{si} = Q_{xi} + Q_{zi} + Q_{vi}$

(3)

Q_{ri} is the flow through an orifice hydraulic resistance, Q_{xi} and Q_{zi} are the fluid flow of the hydrostatic bearing pad $N^{\circ}i$ in the x_i and z_i directions, respectively, Q_{vi} is the squeeze flow of the hydrostatic bearing pad $N^{\circ}i$.

$$Q_{vi} = S_a \dot{h}_i$$

(4)

$$Q_{xi} = \int_0^A dx \int_0^{h_i} u_{xi} dy;$$

(5)

$$u_{xi} = \frac{1}{2\mu} \frac{\partial P}{\partial x} (y - h_i)y$$

(6)

$$Q_{zi} = \int_0^B dz \int_0^{h_i} u_{zi} dy;$$

(7)

$$u_{zi} = \frac{1}{2\mu} \frac{\partial P}{\partial z} (y - h_i)y$$

(8)

Where u_{xi}, u_{yi}, u_{zi} are the flow velocities in the x_i, y_i, z_i directions, respectively.

$$Q_n = \frac{\pi d_c^4}{128 \mu L_c} (P_s - P_{ai})$$

(9)

The negative electrorheological fluid

In this study a negative electrorheological fluid which was reported by Boissy et al [9]. They investigated a suspension of polymethylmethacrylate PMMA (particles diameter $\phi \approx 15 \mu m$ and conductivity $\sigma_s = 10^{-14} S/m$) dehydrated during 40 hours in vacuum, dispersed in a mixture of two liquids ($\sigma_L = 3 * 10^{-10} S/m$), Ugilec T^* (a weakly polar solvent) and mineral oil $TF50^*$ in proportion such as to have a liquid density equal to that of the solid phase. They found that the electric field has a strong influence and for a volume fraction of 30%, the viscosity of the suspension can be decreased by a factor up to about 5.

Fig.3 shows the relationship between the viscosity and the electric field for the negative electrorheological fluid studied by Boissy et al [9].

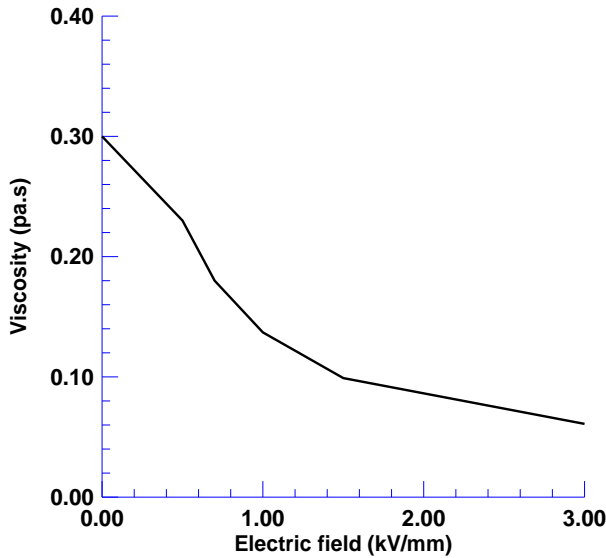


Fig.3. Variation of viscosity with electric field in negative electrorheological fluid.

Analytical results and discussions

The analytical method is used for the calculation of the characteristics by considering the particular assumption of infinitely long journals.

At the point of operation, when the hydrostatic squeeze film damper is in the center position, the following relations are obtained:

$$h_i = h_0, P_{ri} = P_{r0}, \beta_i = \beta_0$$

Where h_0, P_{r0}, β_0 are the film thickness, the recess pressure and the pressure ratio, respectively, at the center position of the hydrostatic squeeze film damper. h_i, P_{ri}, β_i are the film thickness,

the recess pressure and the pressure ratio of the hydrostatic bearing pad N°i.

The bearing characteristics are set as follows:

- Bearing pad length , $A=0.1524 m$ and $B=0.0254 m$;
- Recess dimension ratio, $a/A=0.5$ and b/B , is 1;
- The pressure supply, P_s , is 0.1 MPa;
- The viscosity, μ , is 0.05 Pa.s;

Film thickness analysis

As seen in fig.4, the film thickness is studied according to the pressure ratio at the point of operation as the electric field applied $E=0$ kV/mm. This figure shows that the film thickness decreases when the pressure ratio increases.

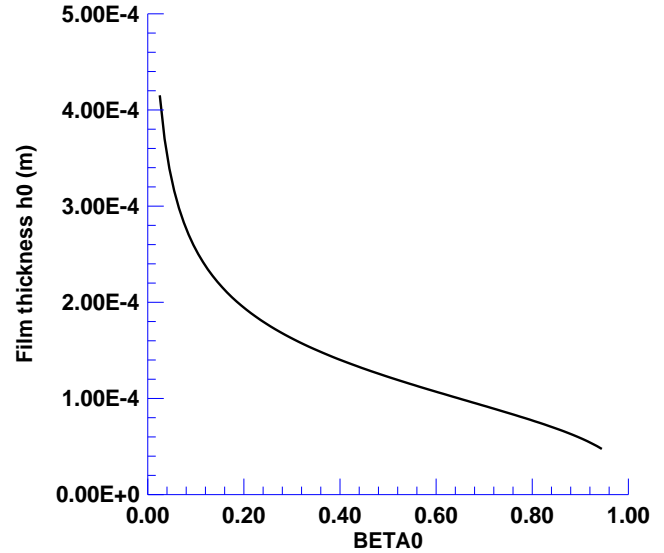


Fig.4. Film thickness versus pressure ratio

Static characteristics analysis

Fig.5 shows the effect of eccentricity ratio and of the electric field on the carrying load capacity. This curve shows that the load capacity increases when the pressure ratio increases. It must be noticed that the electric field has no effect on the load capacity. Fig.6 shows the effect of the eccentricity ratio on the flow rate requirement at the point of operation for different electric fields. The flow rate increases when the electric field increases because the viscosity of the NER fluid decreases when the electric field increases, and as a result, the flow increases since it is inversely proportional to the viscosity.

Dynamic characteristics analysis

Fig.7 shows the influence of eccentricity ratio and of the electric field on the stiffness coefficient at the point of operation. As seen in Fig. 7, there is no effect of electric field on the stiffness coefficient because it is independent to the viscosity. Fig.8 shows the effect of the eccentricity ratio for the different electric fields on the damping coefficient. This curve shows that the damping coefficient increases when the eccentricity ratio increases.

es. On the other hand, the damping coefficient decreases when the electric field increases since it is proportional to the viscosity.

creases and this leads to an increase in the flow rate requirement.

- The stiffness coefficient is not influenced with the application of the electric field.
- The damping coefficient decreases when applying an electric field.

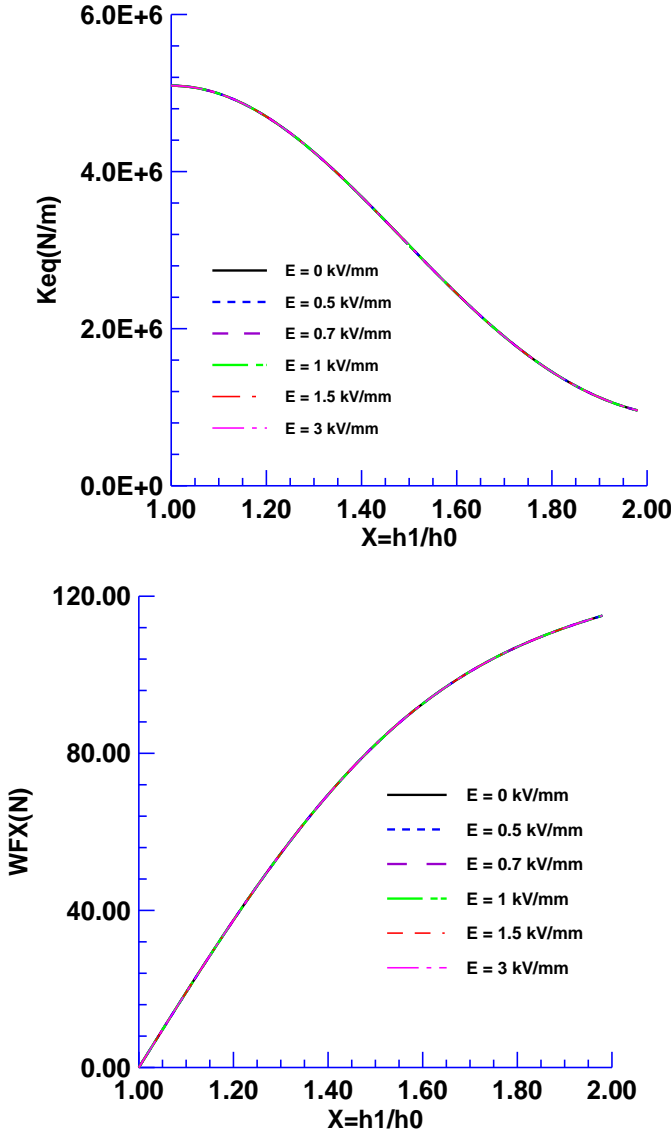


Fig.5. Carrying load capacity versus eccentricity ratio for different electric field.

Conclusions

A linear modeling was performed using analytical methods in order to investigate the effect of negative electrorheological fluids on carrying load capacity, flow, and the dynamic characteristics (stiffness and damping coefficients) of a four-pad hydrostatic squeeze film damper HSFD using a capillary restrictor-type hydraulic resistances . The results can be summarized as follow:

- The electric field has no effect on the carrying load capacity.
- When an electric field is applied, the viscosity of the negative electrorheological fluid de-

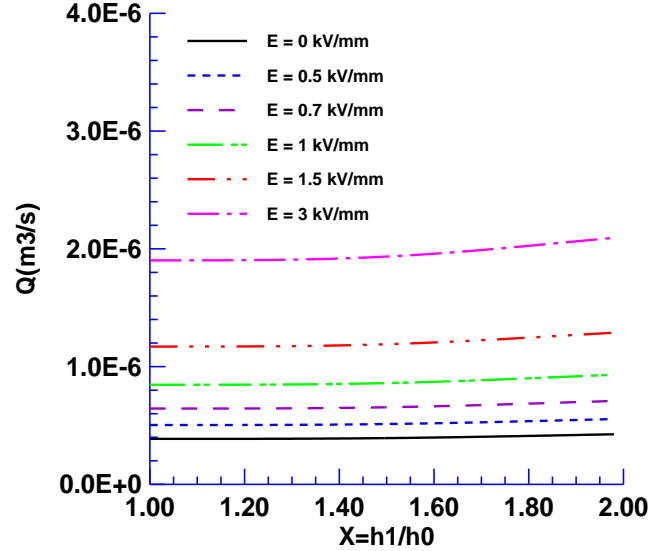


Fig.6. The flow rate versus the eccentricity ratio for different electric field.

Fig.7. The stiffness coefficient versus the eccentricity ratio for different electric field.

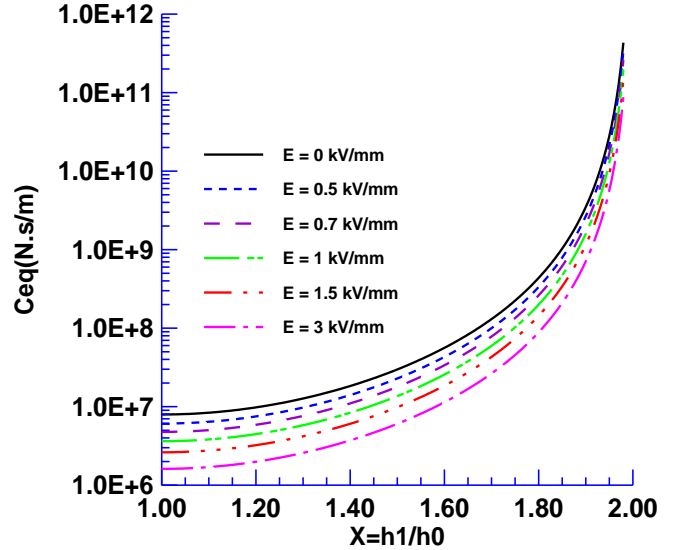


Fig.8. Damping coefficient versus the eccentricity ratio for different electric field

References

[26] Seungchul Lim, Sang-Min Park, Kab-II Kim, AI vibration control of high-speed rotor systems using electro-

- rheological fluid, *Journal of Sound and Vibration* 284 (2005) 685–703.
- [27] A.P. Gast and C. F. Zukoski, Electro-rheological fluids as colloidal suspension, *Adv. Colloid Interface Sci.* 30 (1989), 153-202.
- [28] H. Conrad and A. F. Sprecher, Characteristics and mechanisms of electro-rheological fluids, *J. Stat. Phys.*, 1994, 64, 1073.
- [29] T.C. Halsey, Electro-rheological fluids, *Science* 258 (1992) 761.
- [30] J. H. Block and P. Rattray, Recent developments in ER fluids, in *Progress in Electrorheology*, edited by K.O.Havelka and F.E. Filisko (Plenum Press, New York, 1995), p. 19-42.
- [31] W.M. Winslow, Method and means for translating electrical impulses into mechanical force, U.S. Patent 2417850, 1947.
- [32] T. Hao, Electro-rheological suspensions, *Adv. Colloid Interface Sci.* 97 (2002), 1-35.
- [33] W. Wen, X. Huang, S. Yang, K. Lu and P. Sheng, The giant electro-rheological effect in suspensions of nanoparticles, *Nat. Mater.*, 2003, 2, 727.
- [34] C. Boissy, P. Atten and J.N. Foulc, On the negative electro-rheological effect, *J. Electrostatics* 35 (1995), 13-20.
- [35] Bouzidane A. and Thomas M., An electro-rheological hydrostatic journal bearing for controlling rotor vibration, *Computers and Structures* 86 (2008) 463–472.
- [36] Young Gun Ko and Ung Su Choi, Negative electrorheological fluids, *J. Rheol.* 57(6) (2013) 1655-1667.
- [37] H. Kimura, K. Aikawa, Y. Masubuchi, J. Takimoto, K. Koyama, T. Uemura, 'Positive' and 'negative' electro-rheological effect of liquid blends, *J. Non-Newtonian Fluid Mech.*, 76 (1998) 199–211.
- [38] L. Lobry, E. Lemaire, Viscosity decrease induced by a DC electric field in a suspension, *J. Electrostat* 47 (1999) 61-69.
- [39] Tetsu Mitsumata, Kousuke Sugitani, Negative Electrorheological Effect of Silicone Gels Containing Barium Titanate, *Macromol. Rapid Commun.* 2004, 25, 848–852.
- [40] Cetin, B., H. I. Unal, and O. Erol, The negative and positive electrorheological behavior and vibration damping characteristics of colemanite and polyindene/colemanite conducting composite, *Smart Mater. Struct.* 21, 125011 (2012).
- [41] W. A. Bullough and N. Jakeman, *ELECTRO-RHEOLOGICAL (ER) DEVICES - properties, performance and applications*, 1998.
- [42] [17] S. B. Choi, Y. T. Choi, E. G. Chang, S. J. Han, C. S. Kim, Control characteristics of a continuously variable ER damper, *Mechatronics* 8 (1998) 143-161.
- [43] Limu Wang, Xiuqing Gong, and Weijia Wen, Electrorheological fluid and its applications in microfluidics, *Top Curr Chem* (2011) 304: 91–115.
- [44] Han, Y.-M., and S.-B. Choi, Control of an ER haptic master in a virtual slave environment for minimally invasive surgery applications, *Smart Mater. Struct.* 17, 065012 (2008).
- [45] Nikolajsen, J. L. and Hoque M. S., An Electroviscous damper, N89-22898 (1990) 133-141.
- [46] Pecheux B., Bonneau O. and Frêne J., Investigation about Electro-Rheological Squeeze Film Damper Applied to Active Control of Rotor Dynamic, *International. Journal of Rotating Machinery*, Gordon and Breach Science Publishers, 1997, vol. 3, No.1, pp. 53-60.
- [47] Young-Kong Ahn, Shin Morishita and Bo-Suk Yang, Directionally Controllable Squeeze Film Damper Using Liquid Crystal, *KSME International Journal*, Vol. 12. No. 6, 1998, pp. 1097-1103.
- [48] P.G. Nikolakopoulos, C.A. Papadopoulos, Controllable high speed journal bearings, lubricated with electrorheological fluids. An analytical and experimental approach, *Tribology International* 31 (1998) 225–234.
- [49] G. Z. YAO AND Y. QIU, vibration control of a rotor system by disk type electrorheological damper, *Journal of Sound and Vibration* (1999) 219(1), 175-188.

Local Search Heuristic for Multiple Knapsack Problem

BALBAL Samir
 Computer science Department,
 USTOMB,
 Oran,Algeria
 belbelsamir@gmail.com

LAALAOUI Yacine
 IT Department, Taif University,
 Taif, Kingdom of Saudi Arabia
 y.laalaoui@tu.edu.sa

BENYETTOU Mohamed
 Computer science Department,
 USTOMB, Oran,
 Algeria
 med_benyettou@yahoo.fr

Abstract—In this paper we will present a heuristic method to solve the Multiple Knapsack Problem. The proposed method is an improvement of the IRT heuristic described in [2].the experimental study shows that our improvement leads some gain in time and solution quality against IRT, MTHM, Mulknab and ILOG CPLEX.

Keywords— Multiple Knapsack Problem; Local Search; heuristic;

XII. Introduction

The Multiple Knapsack Problem (MKP) is a variant of the knapsack problem (KP) whose resolution is much more difficult, the fact that we have this problem in areas as different application than the economy, industry, transport, cargo loading and distributed computing, gives it a great practical interest [1].

Viewpoint Artificial Intelligence, the problem of Multiple Knapsack is strongly NP-complete. This means that the resolution of this problem cannot be done in polynomial time. In other words, an exact algorithm is required for optimal resolution.

The objective of this work is to improve the performance of a heuristic proposed by IRT Laalaoui [2], and solve the problem of multiple Knapsack in a way we approached using local search.

I. Presentation of the Multiple Knapsack Problem

The Multiple Knapsack Problem (MKP) is a generalization of the standard 0-1Knapsack Problem where instead of considering only one knapsack, one tries to fill m knapsacks of different capacities [3]. Consider a set $N = \{1... n\}$ of items to be loaded into m knapsacks of capacity c_i with $i \in \{1, ... m\}$. Each item $j \in N$ is characterized by its weight w_j , and its profit p_j and its decision variable x_{ij} which is worth 1 if the item j is loaded into the knapsack i and 0 otherwise. It is then to find m disjoint subsets of N (where each subset corresponds to filling a knapsack) that maximize the total profit made by the sum of the selected items. The mathematical formulation of the problem MKP is as follows:

MKP

$$\begin{cases} \max \sum_{i=1}^m \sum_{j=1}^n p_j x_{ij} \\ \text{s.t. } \sum_{j=1}^n w_j x_{ij} \leq c_i, \quad i \in \{1, \dots, m\} \\ \sum_{i=1}^m x_{ij} \leq 1, \quad j \in \{1, \dots, n\} \\ x_{ij} \in \{0, 1\}, i \in \{1, \dots, m\}, j \in \{1, \dots, n\}. \end{cases} \quad \dots \dots \dots (1)$$

Where p_j , c_i and w_j are positive integers.

In order to avoid any trivial case, we make the following assumptions.

- All items have a chance to be packed (at least in the largest knapsack):

$$\text{Max}_{j \in \{1..n\}} w_j \leq \text{Max}_{i \in \{1, \dots, m\}} c_i \quad \dots \dots (2)$$

- The smallest knapsack can be filled at least by the smallest item:

$$\text{Min}_{j \in \{1..n\}} w_j \leq \text{Min}_{i \in \{1, \dots, m\}} c_i \quad \dots \dots (3)$$

- There is no knapsack which can be filled with all items of N :

$$\sum_{j=1}^n w_j > \text{Max}_{i \in \{1, \dots, m\}} c_i \quad \dots \dots (4)$$

II. resolution method of MKP

The approaches proposed in the literature to solve the problems of the family of the backpack are either exact methods or heuristics. The exact methods are able to solve a problem to optimality but in exponential time [4]. Heuristic methods provide an approximate solution, good quality in reasonable periods of time [4]. Heuristics are either simple heuristic or meta-heuristics.

1. The exact method

The exact methods proposed in the literature to solve problem MKP are based on the Branch-and-Bound (B &B).

- Ingargiola and Korsh [5] proposed a branch-and-bound algorithm which used a reduction procedure based on dominance relationships between pairs of items.
- Hung and Fisk [6] proposed a method based Branch and Bound with depth-first strategy as a journey. The upper bounds are obtained using Lagrangian relaxation, with a decreasing scheduling capacity c_i .

- The algorithm of Martello and Toth [7] improves proposed by Hung and Fisk with the calculation of upper bounds using surrogate relaxation and taking the minimum of the Lagrangian upper bounds and surrogate relaxation method.
- Martello and Toth[8] proposed an algorithm (bound and bound) algorithm improves the Martello and Toth[7]a powerful base of B&B to solve the MKP. This algorithm, called MTM (Method Martello and Toth), applies heuristics Greedy, which involves solving a series of problems with m single Knapsack.
- Pisinger[9] improved the algorithm MTM by incorporating an efficient algorithm for calculating higher and better reduction rules for determining the items that can be set to zero terminals and a method that attempts to reduce the ability of backpacks. This new algorithm is called Mulknap. Power Mulknap located in allocating 100000 items in one second. So Pisinger has succeeded with Mulknap resolve cases problems with very large ($n = 100\ 000$, $m = 10$) in a second. But at the same time it fails to resolve cases in smaller problem ($n = 45$, $m = 15$), when the ratio n/m is between 2 and 5 ($2 \leq n/m \leq 5$).
- Fukunaga and Korf [10] proposed the bin-completion method is a technique based

Heuristic: MTHM

Input: n, p_j, w_j, y_j, z, c_i

Output: y_j, z

Begin

[Initial solution] : Procedure GREEDYS

[Rearrangement]

[First improvement]

[Second improvement]

End

branch- and-bound. It uses the strategy depth first. Each node of the search tree represents a maximum possible allocation for a particular knapsack member.

- A.Fukunaga[11] improved bin-completion method in the case of relatively large bodies ($n = 100$). But the ratio n/m is the major problem in all existing algorithms.

2. Existing solvers

There are many solvers have been developed for solving the problem of the backpack. We distinguish between free software and commercial software. Commercial software often has superior performance to the free solvers. There are two principal existing business software is: The commercial solver IBM ILOG CPLEX and XPRESS-MP solver. There exist also two principal free software are: GLPK and Boob ++.

3. Heuristics

Heuristic methods have been proposed for the problem of multiple bag back in order to find good solutions within a reasonable time, heuristic MTHM, CRH and IRT are proposed to solve the problem MKP.

- The heuristic (MTHM) of Martello and Toth [12] is a very efficient heuristic to solve the problem MKP It takes place in stages present in the following Figure.

Fig. 1 : Heuristic MTHM

- The heuristic RCH described by Lalami et al. in [13] is a heuristic with a polynomial time complexity for solving the MKP. Unfortunately, this heuristic resolve any problems that could be solved using optimality Mulknap i.e. instances of problems with a large n/m ratio, which is where the Mulknap gives the best results in less second. The authors fail to describe the interesting case of problems with a small ratio n/m .
- In [2], Laalaoui proposed a heuristic to solve the problem completely dependent exchanges found in MTHM and also to increase the efficiency of the latter method (improved profit). This new heuristic integrates three simple heuristics (Replace-One-By-One, Replace-Two-By-One and Replace-One-By-Two) with MTHM by two different techniques: the first technique is simple (SRT) and the second iterative (IRT).

4. Metaheuristics Methods

Among the proposed literature to solve the problem MKP methods that uses genetic algorithms metaheuristic methods, methods are located: HGGGA (Hybrid Grouping GA) [14], WCGA (Weighted Coding GA) [15], Ugga (Undominated Grouping GA) [16] and Representation-RSGA (Switching GA) [17].

III. Local search heuristic for MKP

Local Search is used by many metaheuristic. It is about making incremental improvements to the current solution through a basic transformation until no improvement is possible. The solution is called local optimum found with respect to the transformation used, as shown in Fig.2.

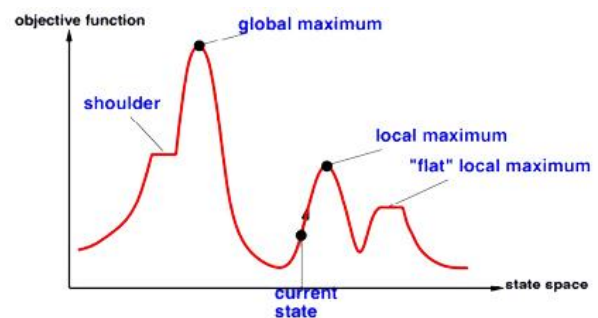


Fig. 2 : Local Search

Technically, the local search consists of a series of transformations of the solution to improve it every time. The current solution S is replaced by a better solution $S' \in N(S)$ in its vicinity. The process stops when it is no longer possible to find-improving solution in the vicinity of S , such that the algorithm written Fig. 3

Fig. 3 : Algorithm for Local Search

Our proposal to solve the problem MKP with local search method is using the following steps:

- Step 01: initial solution;
- Step 02: Perturbation solution
- Step 03: improve the solution;
- Step 04: repeating the process a number of times.

1. Initial solution

For the initial solution of this method we will use the IRT technique written by Y. Laaloui in [2].

2. Perturbation solution

We know that one of the disadvantages of IRT and MTHM is the lack of randomness .This drawback severely limits the ability to better search space exploration.

In our new technical we introduce some randomness to the solution of step disturbance. The principle of perturbation solution is to randomly remove one item or several items of the solution as mentioned in the procedure Perturbation.

3. Improve the solution

For the third step the procedures for exchanging items is applied (Replace-One-By-One, Replace-Two-By-One, Replace-One-By-Two) and the steps are repeated for a number of times. The figure (Fig .4) shows the general algorithm of the method of local search for MKP.

```

Algorithm Local Search Heuristic for MKP ;
Inputs :  $n, p_j, w_j, y_j, z, i, \bar{c}_i$ 
Outputs :  $y_j, z$ 
Begin
01. MTHM
02. Replace-Two-By-One
03. Replace-One-By-Two
04. Replace-One-By-One
05. if(  $prev\_z < z$  )
06.      $prev\_z = z$ ;
07.     goto step 02.
08. if( $tmpz == z$ )
09.      $tmpz = z$ ;
10. for ( $j = 1; j \leq d; j ++$ )
11.      $tmpx[j] = x[j]$ ;
12. for ( $j = 1; j \leq b; j ++$ )
13.      $tmpcr[j] = cr[j]$ ;
14. else
15.      $z = tmpz$ ;
16. for ( $j = 1; j \leq d; j ++$ )
17.      $x[j] = tmpx[j]$ ;
18. for ( $j = 1; j \leq b; j ++$ )
19.      $cr[j] = tmpcr[j]$ ;
20. if( $testmore \leq nbrest$ )
21.     Perturbation()
22.      $testmore = testmore + 1$ 
23.     goto step 02.
End.
```

Fig. 4 :Local Search Heuristic for MKP

```

Algorithm: Local Search
Input: S
Output : N
best ← true

While best = true do
    best ← false

for (S' ∈ N(S)) do
    if (S' is best of S)
        S ← S'
        best ← true

return
```

IV. Experimental Results

To measure the effectiveness of our work, we have implemented in C programming language, this choice is justified by the speed of the language. And we used the system Linux (Ubuntu) as a platform for development, since it is widely used in the academic community, and to use shell scripts. The technical Mulknep work is written in C¹³ .While the code of the implementation MTHM is written in FORTRAN¹⁴and we converted to C using the f2c converter.

We used the optimization tool IBM ILOG CPLEX commercial solver version 12.2.5. All techniques are established in the same environment using the GCC compiler. All tests were performed on a 2.2 GHz Intel Core Duo 2 processor with 2GB of RAM. We have used A. Fukunaga's data-set which was used in [16][17]. This

¹³<http://www.diku.dk/Pisinger/codes.html>

¹⁴<http://www.or.deis.unibo.it/staff-pages/Martello/cvitae.html>

benchmark is a set of 12 problem instances, four instances in each one of the three types: strongly correlated, weakly correlated and multiple subset-sum. The number of knapsacks is 100; the number of items is 300 in each problem instance.

Results of our experimental study are shown in tables 1, this contains a comparison to IRT, MTHM, Mulknep techniques and IBM ILOG CPLEX solver on a data-set from literature [16,17], It is clear that the method attendant gives a result better than Mulknep and CPLEX solver either as a solution or as a time over the local search method for MKP improves the results obtained by the IRT technique with a time greater than the time of the latter method, although it remains our proposal novella usable in real time because time does not exceed one second.

TABLE 1 : RESULTS ON UNCORRELATED,STRONGLY CORRELATED AND MULTIPLE SUBSET-SUM INSTANCES COMPARED TO IRT ,MTHM ,MUMKNAP TECHNIQUES AND IBM ILOG CPLEX SOLVER . TIME COLUMNS SHOW THE TIME IN SECONDS.

Uncorrelated instances											
	MTHM		IRT		Mulknep		Cplex		Local		
	Z	T	Z	T	Z	T	Z	T	Z	T	
S	806	0	83	0	84	1	84	1	84	0	
S	778	0	79	0	80	1	80	1	79	0	
S	723	0	73	0	74	1	74	1	75	0	
S	755	0	76	0	78	1	78	1	78	0	
Strongly correlated instances											
	MTHM		IRT		Mulknep		Cplex		Local		
	Z	T	Z	T	Z	T	Z	T	Z	T	
S	699	0	75	0	74	1	75	1	75	0	
S	681	0	76	0	76	1	76	1	76	0	
S	629	0	71	0	70	1	71	1	71	0	
S	673	0	72	0	72	1	72	1	72	0	
S	711	0	77	0	76	1	77	1	77	0	
S	661	0	73	0	73	1	73	1	73	0	
S	669	0	74	0	74	1	74	1	74	0	
S	704	0	75	0	74	1	75	1	75	0	
S	688	0	75	0	75	1	75	1	75	0	
S	720	0	78	0	78	1	78	1	78	0	
Multiple subset-sum instances											
	MTHM		IRT		Mulknep		Cplex		Local		
	Z	T	Z	T	Z	T	Z	T	Z	T	
S	747	0	75	0	74	1	74	1	75	0	
S	762	0	76	0	76	1	76	1	76	0	
S	707	0	70	0	70	1	70	1	70	0	
S	722	0	72	0	72	1	72	1	72	0	

V. Conclusion

In this article we described an improvement of IRT technique. The proposed method succeeds to give better results compared to IRT, Mulknep and CPLEX with reasonable.

The future work on this new heuristic approach includes a depth experimental study in large-scale data-sets.

References

[50] M. Lalami,M. Elkihel, D. Baz and V.Boyer, "A procedure-based heuristic for 0-1 Multiple Knapsack Problems", International Journal of Mathematics in Operational Research, vol. 4, No. 3, pp. 214-224, 2012.

[51] Y. Laalaoui, "Improved Swap Heuristic for the Multiple Knapsack Problem" IWANN 2013, Part I, LNCS 7902, pp. 547-555, 2013.

[52] S. Martello, P. Toth. "Knapsack problems: algorithms and computer implementations". J Wiley. 1990.

[53] J. Dréo, A. Petrowski, D. Taillard, P. Siarry" Métaheuristiques pour L'optimisation difficile" ,Eyrolles (Editions), November 2003

[54] G. Ingargiola and J.F. Korsh, " An algorithm for the solution of 0-1 loading problems", Operations Research, 23(6):1110--1119, 1975.

[55] M.S. Hung and J.C. Fisk, " An algorithm for the 0-1 multiple knapsack problem", Naval Research Logistics Quarterly, 571--579, 1978.

[56] S. Martello and P. Toth., "Solution of the zero-one multiple knapsack problem",European Journal of Operational Research, 4, 1980.M. Young, The Technical Writer's Handbook. Mill Valley, CA: University Science, 1989.

[57] S. Martello and P. Toth., "A bound and bound algorithm for the zero-one multiple knapsack problem", Discrete Applied Mathematics, vol. 3, pp. 275--288, 1981.

[58] D. Pisinger,"An exact algorithm for large multiple knapsack problems", European Journal of Operational Research, vol. 114, pp. 528--541, 1999.

[59] A. Fukunaga, R.E Korf, "Bin Completion Algorithms for Multicontainer Packing, Knapsack, and Covering Problems", Journal of Artificial Intelligence Research, vol. 28, pp. 393--429, 2007.

[60] A. Fukunaga, "A branch-and-bound algorithm for hard multiple knapsack problems", Annals of Operations Research, vol. 184, N. 1, pp. 97--119, 2011.

[61] S. Martello and P. Toth., "Heuristic algorithms for the multiple knapsack problem", Computing, vol. 27, pp. 93--112, 1981.

[62] M. Lalami,M. Elkihel, D. Baz and V.Boyer,"A procedure-based heuristic for 0-1 Multiple Knapsack Problems, International Journal of Mathematics in Operational Research, vol. 4, No. 3, pp. 214--224, 2012

[63] E. Falkenauer, "A hybrid grouping genetic algorithm for bin packing", Journal of Heuristics, pages 2:5 - 30, 1996.

[64] R. Raidl, "The multiple container packing problem: A genetic algorithm approach with weighted codings", ACM SIGAPP Applied Computing Review, pages 22 - 31, 1999.

[65] A. Fukunaga., "A new grouping genetic algorithm for the multiple knapsack problem", In Proc. IEEE Congress on Evolutionary Computation, pages 2225--2232, 2008.

[66] A. Fukunaga and Satoshi Tazoe, "Combining Multiple Representations in a Genetic Algorithm for the Multiple Knapsack Problem", In Proc of the 11th IEEE Congress on Evolutionary Computation, pages 2423 - 2430, 2009.

Electronic properties of SrAl₂H₂ for hydrogen storage

K. Khodja^{1,*} and Y. Bouhadda^{1,**}

¹Unité de Recherche Appliquée en Energies Renouvelables, URAER, Centre de Développement des Energies Renouvelables, CDER, 47133, Ghardaïa, Algeria
Email: *khodja_kh@yahoo.fr, **bouhadda@yahoo.fr

Abstract—In this paper we report the SrAl₂H₂ electronic structure which is a zintl phase hydride in frame of the density functional theory (DFT) using the plane wave and pseudopotential method. We discuss the chemical bond nature using total and partial density of states (DOS) and also we calculated the enthalpy formation of the SrAl₂H₂, the phonon frequencies and the thermodynamic functions for hydrogen storage.

Keywords: Hydrogen Storage, Zintl Phase, Metal Hydride, Electronic Properties, Density Functional Theory.

Introduction:

Many metals and intermetallic compounds exhibit the ability to absorb and react with hydrogen. Recently aluminum-derived hydrides have been considered as an alternative method for hydrogen storage, because they offer the improved energy density.

Hydrogen materials with Al–H bond such as SrAl₂H₂ have received more attention those last years for their high capacity of storage [1, 2].

Gingl et al. [3] discovered that SrAl₂H₂ is a Zintl-type hydride. This compound is synthesized by exposing the intermetallic SrAl₂ to hydrogen gas under 50bar and rising the reaction temperature slowly from 100 to 200°C [3]. It's crystallizes with trigonal structure in $P\bar{3}m1$ space group (see Figure 1-a).

Alkali metal aluminum hydride can absorb and desorb large amount of hydrogen reversibly at moderate conditions.

In order to optimize the hydrogen storage in SrAl₂H₂ compound several experimental and computational works have been realized. Gingl et al. [3] have studied the hydrogenation of SrAl₂ by X-ray powder diffraction and found that the reaction proceeds in three steps. Orgaz et al. [5] investigated the electronic structure of SrAl₂H₂, Ca₃SnH₂, and Ca₅Sn₃H by means of the full-potential linearized augmented-plane-wave method. They found the SrAl₂H₂ and Ca₅Sn₃H hydrides are metallic and Ca₃SnH₂ is a small-gap semiconductor. The bonding characteristics

study of SrAlSiH, SrAl₂H₂, SrGa₂H₂ and BaGa₂H₂ using DFT calculations were done by Subedi et al. [6]. Their results indicate that in SrAl₂H₂ the Al layers are nominally neutral i.e not polyanionic.

In this study, all the computations have been done using the ABINIT code [7] based on pseudopotentials and plane waves in density functional theory (DFT) [8]. Fritz–Haber–Institute GGA pseudopotentials [9] are used to represent atomic cores. The enthalpy formation is calculated using LDA approximation of Troullier and Martins [10]. The electronic wave functions were expanded in plane waves up to a kinetic energy cutoff of 40 hartree and a 6 × 6 × 6 grid for k-point was used.

The aim of this work is to contribute to the investigation of the zintl phase hydride SrAl₂H₂ by calculating and analyzing the electronic properties and enthalpies formation of this compound.

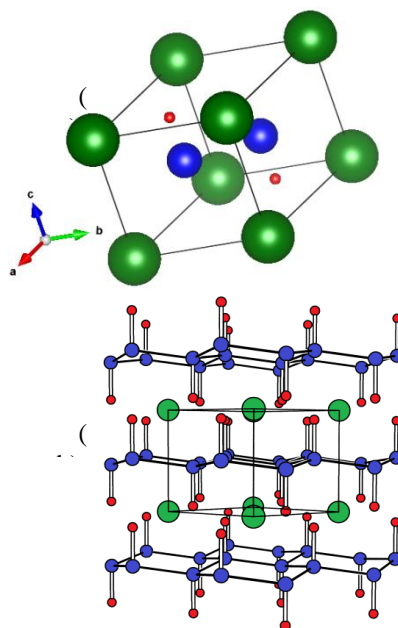


Figure 1: SrAl₂H₂ structure (green: Sr, blue: Al, red: H), (a) our work, (b) taken from ref [3]

Results and discussions

Crystal structure

The crystal structure of SrAl₂H₂ is known and occurs in a trigonal space group $P\bar{3}m1$ (164) with Sr (0, 0, 0), Al (1/3, 2/3, 0.4608) and H (1/3, 2/3, 0.0964) and has a cell parameters of a=4.5283(Å), c=4.7215(Å) which are experimentally determined [3]. The relaxed structure obtained in this study is in good agreement with the reported structure from the experiments [3] (a=4.5949(Å) and c=4.7909(Å), Al (1/3 2/3 0.4570), H (1/3 2/3 0.0849)). Also the lattice constants of Sr and Al which have a fcc structure are taken from reference [11].

Al atoms are arranged as a slightly puckered graphitic layer. Additionally each Al atom is coordinated to one hydrogen atom. In SrAl₂ the puckered Al hexagonal layers are connected by a long Al-Al interlayer bonds which are cut in SrAl₂H₂ and terminated by hydrogen atoms (see Figure 1-b).

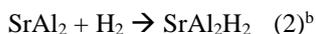
In Table I, we reported the bonding distances of each element that composes the SrAl₂H₂ compound.

Bondings	Distance (Å)
Sr-Al	3.4396
Sr-H	2.6838
Al-H	1.7826
Al-Al	2.6846
H-H	4.7809

Table 1: Bonding distance in SrAl₂H₂

The formation energy (enthalpy formation)

We have take into account two reactions related to the formation of the zintl phase hydride SrAl₂H₂:



To calculate the formation heat of the reaction (1) we subtracted the total energies of the pure elements Sr, Al and the hydrogen molecule from their hydride SrAl₂H₂.

Table 2 contains the total energy and the formation enthalpy computed of SrAl₂H₂ for two different reactions. The total energy of the hydrogen molecule is -31.4020 (eV) and has been also calculated. The heat formation of the second reaction is much less than the first one, making the reaction (2) more favorable for the formation of SrAl₂H₂ compound.

Elements	Total Energy (eV)	Enthalpy Formation (kJ/mol)
Sr	-576.4821	-

Al	-64.0722	-
H ₂	-30.8229	-
SrAl ₂	-712.3662	
SrAl ₂ H ₂	-743.6903	795.1257 ^a 48.3584 ^b

Table 2: Calculated heat of formation of SrAl₂H₂

Electronic structure

The total and the partial densities of state for SrAl₂H₂ are plotted in "Fig. 2" and "Fig. 3" which are similar to that obtained previously by Orgaz and Aburto [5], Subedi and Singh [6]. The electronic structure is metallic without the energy gap. We can also say that SrAl₂H₂ is weakly metallic because the DOS reach a value of 0.0016 (states/eV/cell) at the Fermi level (-0.3129 eV).

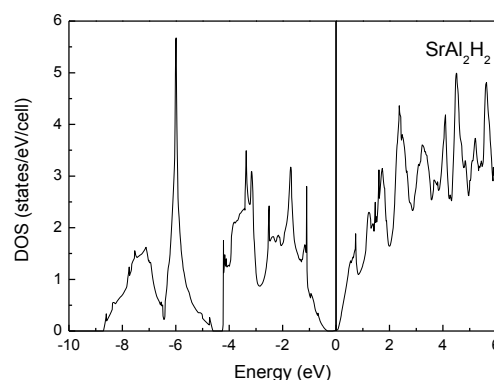


Figure 2: The total density of state of SrAl₂H₂

In Figure 2 at the bottom of energy scale, we can see two peaks; the first concerns the H-s/Al-s bonding interaction. This is followed by a second peak mainly produced by the H-s states, where a non-negligible and small Al-s,p orbital contribution is present. This can be seen in the PDOS plots of Figure 3. The second part of the DOS plot is well separated from the first. Two main contributions appear in increasing order of energy. First, there is a complex H-s/Al-s orbital interaction including small Sr-d and Al-p contributions. This is completed by the Al-p states up to the Fermi energy. The PDOS of Sr has a very small contribution to the valance band from the region -10 (eV) to 0.

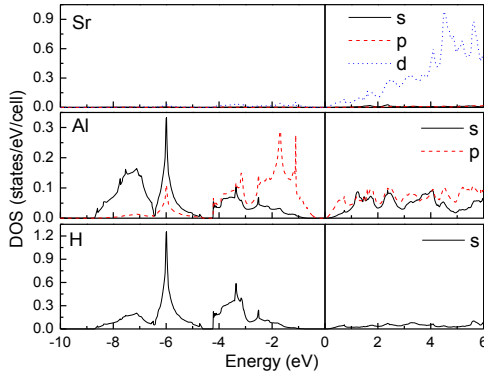


Figure 3: Partial density of state for SrAl₂H₂

The dynamical Properties

Phonon frequencies were subsequently obtained using the linear-response method, which avoids the use of supercells and allows the calculations of the dynamical matrix at arbitrary q vectors. These were later employed to obtain by interpolation, the phonon frequencies at arbitrary points in reciprocal space and the phonon-dispersion relations. The phonon densities of state (DOS) could be obtained from the phonon-dispersion curves.

The phonon dispersion curves for SrAl₂H₂ along several high-symmetry lines are plotted in “Fig. 4”. These results agree qualitatively with phonon DOS of SrAl₂H₂ reported by Subedi et al. [6] using linear response as implemented in the QUANTUM-ESPRESSO package [6], and by Lee et al. [12] using direct method with supercells and plane-wave basis set in the VASP code [12].

Firstly, it can be noticed the presence of four separate bands due to a large mass difference between H atoms and (Sr, Al) atoms. Secondly, the SrAl₂H₂ is dynamically stable since throughout the Brillouin zone all phonon frequencies are positive. The phonon frequencies are in the range of 0-1080 cm⁻¹.

It is noticed also the existence of frequency gap between optical and acoustical modes due to the mass difference between Sr and Al atoms. The frequency-gap between the acoustic and optical branches depends on the mass difference.

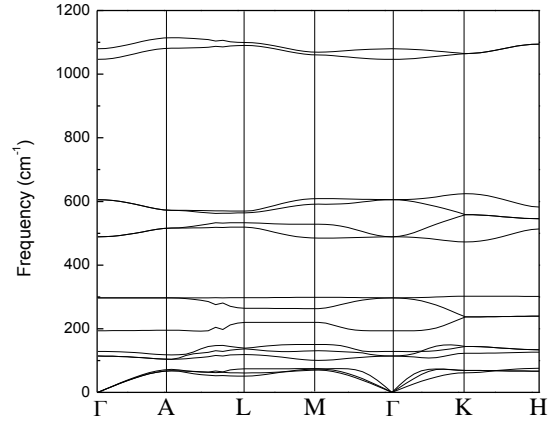


Figure 4: Calculated phonon dispersion curves along symmetry lines for SrAl₂H₂

Thermal properties

Thermodynamic functions of SrAl₂H₂, could be determined by the whole phonon spectrum. In the present study, the phonon contribution to the Helmholtz free energy F , the internal energy E , the entropy S and the constant-volume specific heat C_v , at temperature T , are calculated using the harmonic approximation [13]:

$$F = k_B T \int_0^{\omega_{\max}} \ln(2 \sinh(\frac{\hbar \omega}{2k_B T})) g(\omega) d\omega \quad (1)$$

$$E = \frac{\hbar}{2} \int_0^{\omega_{\max}} \omega \coth(\frac{\hbar \omega}{2k_B T}) g(\omega) d\omega \quad (2)$$

$$S = k_B \int_0^{\omega_{\max}} \left[\frac{\hbar \omega}{2k_B T} \coth(\frac{\hbar \omega}{2k_B T}) - \ln(2 \sinh \frac{\hbar \omega}{2k_B T}) \right] g(\omega) d\omega \quad (3)$$

$$C_v = k_B \int_0^{\omega_{\max}} \left(\frac{\hbar \omega}{2k_B T} \right)^2 \csc^2 \left(\frac{\hbar \omega}{2k_B T} \right) g(\omega) d\omega \quad (4)$$

Where:

k_B is the Boltzman constant. ω_{\max} is the largest phonon frequency.

$g(\omega)$ is the normalized phonon density of states with $\int_0^{\omega_{\max}} g(\omega) d\omega = 1$.

The obtained results are shown in “Fig. 5”. When temperature increases; the calculated free energy F for SrAl₂H₂ decreases gradually. However, the calculated E and S increase continually. F and E at zero temperature represent the zero-point motion [11] and the calculated value is 34.127 kJ/mol.

The calculated C_v exhibits the expected T^3 power-law behavior C_v at lower temperatures, for higher temperatures reaches a classic limit of 123.365 J/mol.cell.K, in good agreement with

the classic law of Dulong-Petit at higher temperatures.

Unfortunately, no experimental values of C_v for SrAl_2H_2 are found. Our calculated values can be seen as a prediction for future investigations.

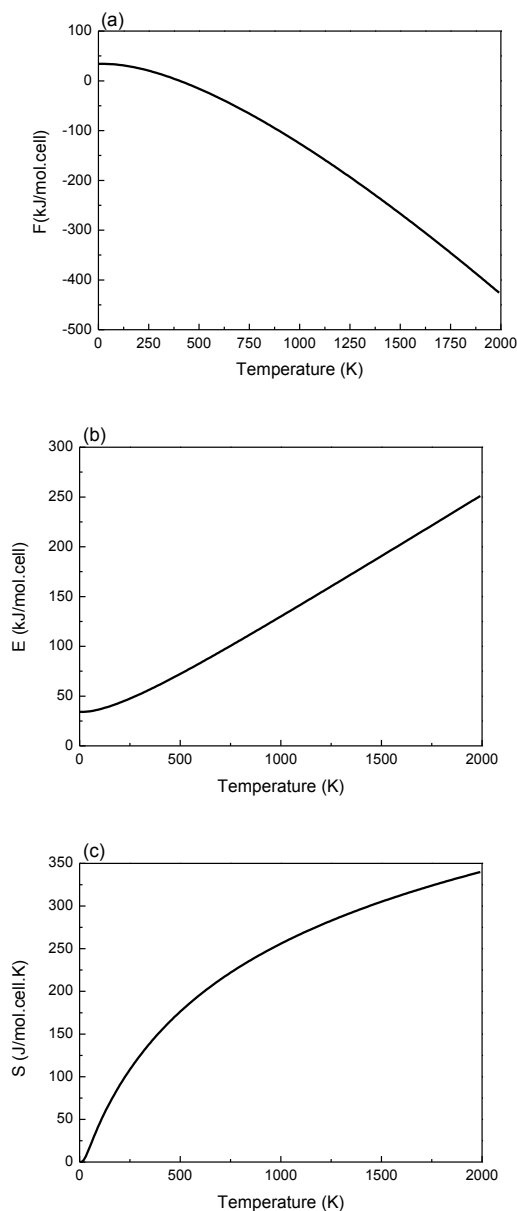


Figure 5: The calculated phonon contribution to the Helmholtz free energy F (a), the internal energy E (b), the entropy S (c) and the constant-volume specific heat C_v (d)

Conclusion

In this work we report the electronic structure calculations for SrAl_2H_2 compound using the ABINIT code. The electronic structure is obtained from GGA, generalized gradient approximation. Formation energy for SrAl_2H_2 is calculated for two different possible reaction pathways. This allowed us to know that is better to synthesize our compound from the precursor material SrAl_2 than from each element that composes the zintl phase hydride. Also from the plot of the DOS, we noted that SrAl_2H_2 has no gap which means that our compound is a metallic and the valence band is dominated by hydrogen atoms. The phonon frequencies and phonon density of states at the Brillouin zone have been obtained using the density functional perturbation theory. No experimental values of the thermodynamic functions for SrAl_2H_2 compound have been reported in the literature; thereby the calculated values could be used for future studies.

References:

- [1] B. Bogdanovic, R. A. Brand, A. Marjanovic, M. Schwickardi, J. Tölle, J. Alloys. Compd, Vol. 302, pp. 36-58, 2000.
- [2] K. J. Gross, G. Sandrock, G. J. Thomas, J. Alloys. Compd, Vol. 330, pp. 691-695, 2002.
- [3] F. Gintl, T. Vogt, E. Akiba, "Trigonal SrAl_2H_2 : the first Zintl phase hydride", J. Alloys. Compd, vol. 306, pp. 127-132, 2000.
- [4] B. Bogdanovic and M. Schwickardi, J. Alloys. Compd, 253-254: 1-9, 1997.
- [5] E. Orgaz and A. Aburto, "Bonding Properties of the New Zintl-Phase Hydrides", Int. J. Quantum. Chem, vol. 101, no. 6, pp. 783-792, 2005.
- [6] A. Subedi and D. J. Singh, "Bonding in Zintl phase hydrides: Density functional calculations for SrAlSiH , SrAl_2H_2 , SrGa_2H_2 , and BaGa_2H_2 ", Phy. Rev. B, vol. 78, pp. 1-7 (045106), 2008.

- [7] X. Gonze, J.M. Beuken, R. Caracas, F. Detraux, M. Fuchs, G.-M. Rignanese, L. Sindic, M. Verstraete, G. Zerah, F. Jollet, M. Torrent, A. Roy, M. Mikami, Ph. Gohsez, J.Y. Raty, D.C. Allan, " First-principles computation of material properties: the ABINIT software project", *Comput. Mater. Sci.*, Vol. 25, no. 3, pp. 478-492, 2002.
- [8] W. Kohn, L.J. Sham, "Self-Consistent Equations Including Exchange and Correlation Effects", *Phys. Rev.*, Vol. 140, no. 4A, pp. A1133-A1138, 1965.
- [9] M. Fuchs, M. Scheffle, *Comput. Phys. Comm.* 119 (1999) 67
- [10] N. Troullier, J. L. Martins, "Efficient pseudopotentials for plane-wave calculations", *Phys. Rev. B*, Vol. 43, No. 3, Jan. 1991, pp. 1993-2006.
- [11] C. Kittel, *Introduction to Solid State Physics*, John Wiley & sons Inc., USA: 2005.
- [12] M. H. Lee, O. F. Sankey, T. Bjorling, D. Moser, D. Noreus, S. F. Parker, and U. Häussermann, *Inorg. Chem.* 46, 6987, 2007.
- [13] C. Lee, X. Gonze, *Phys. Rev. B* 51, 8610, 1995.

Study of structural, electronic and optical properties of the chalcopyrite Ag-GaSe₂

M.Azzouz^{a*}, D Kadri^a, B.Djebour^a, D.Karoum^a, R Ascari^a

Electronic Microscopy Laboratory USTO, department of physics, BP1505 El m'naouar, Oran, Algeria.

(*):E-mail : azzouz moh@yahoo.fr

Abstract-Ternary compounds with structures of the family of chalcogenide chalcopyrite I-III-VI₂ (I = Ag, III = Ga, VI = S, Se) form an extensive semiconductor materials group with diverse optical and electrical properties. Ternary alloys with this composition are well known for their potential applications in the industry of electronic devices and photovoltaics. From a structural point of view, they crystallize with a tetragonal symmetry in the space group I42d (No. 122). The objective of the present work is to predict the structural properties, such as lattice parameter, bulk modulus as well as its derivative compound AgGaSe₂ and their mechanical and electronic properties such as band structure and optical properties using the first principle methods (FP-LMTO).

1. Structural properties:

The fundamental state properties of our material were obtained by the use of a mathematical calculation based on the FP-LMTO method, by a GGA treatment of the exchange energy and correlation. The commonly used procedure to determine the structural properties in the vicinity of equilibrium consists in evaluating the total system energy for different values of c/a at constant volume (see Figure 1). Finally we calculated the total system energy for various values of network parameter for a constant c/a (see Figure 2). The obtained results are then adjusted to the Murnaghan state equation [1].

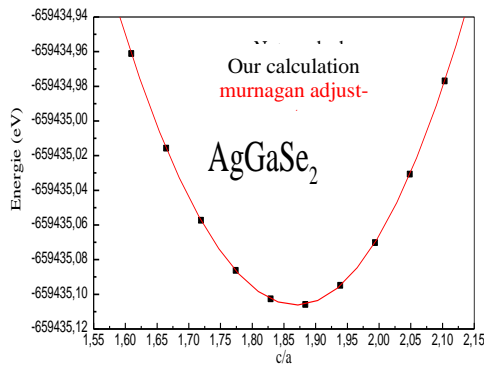


Figure (1): variation of the total energy as a function of c/a of the Ag-GaSe₂ compound with the FP-LMTO-GGA approximation.

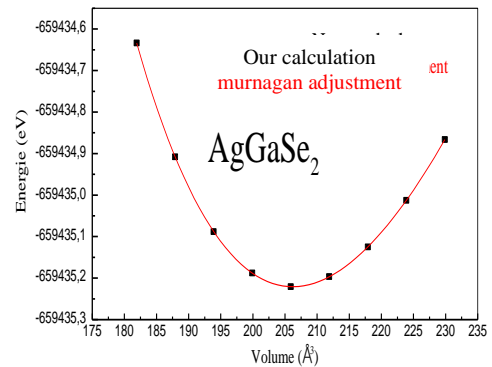


Figure (2): variation of the total energy based on the volume of the AgGaSe₂ compound with the FP-LMTO-GGA approximation.

Table (1): Setting parameters a (Å), c (Å), c/a, u (Å) stiffness modulus B0 (GPa), its derivative B' chalcopyrite AgGaSe₂, compared with experimental, theoretical and other work values.

com- pound	method	a(Å)	c(Å)	c/a	u(Å)	B(GPa)	B'(GPa)
Ag- GaSe ₂	Our GGA calcula- tions	6.0473	11.277 1	1.8648	0.27788		
	other calculations ^a	6.0579	11.294 3	1.8644	0.2788	53.07	4.0076
	theory ^c	6.0629	11.228 4	1.852	0.2794	50.7	5.02
	Experience ^b	5.985	10.904	1.822	0.272	63.8	4.00

Ref^a [2] ,Ref^b [3], Ref^c[4].

2-Elastic properties:

The mechanical stability of crystals has been the subject of extensive theoretical studies. The systematic study of the stability of the network was made by Born and Huang who formulated the criterion of stability. This criterion is expressed in terms of the elastic constants Cij which in the case of our material, is given by:

$$C_{11}, C_{33}, C_{44}, C_{66} > 0, (C_{11}+C_{12})C_{33} > 2C_{13}^2, C_{11} > |C_{12}|, C_{66} > 0, C_{44} > 0$$

It is clear from the above expressions that the condition on the criteria for this chalcopyrite mechanical structure stability is satisfied for all three materials.

Table (2): The elastic constants Cij (GPa) calculated for AgGaS₂.

material	methods	C11	C12	C13	C33	C44	C66
AgGaSe ₂	our calc	74.55	43.30	36.090			32.57028
	Experi- ence ^d	6 89.8	6 65.7	5 45.1	50.44067 58.0	33.8303 21.7	13.3 52.9
	theory ^e	86.4	55.2	52.9	72.4	20.3	21.62
	theory ^f	74.95	41.03	43.03	59.57	30.10	

Ref^d [5], Ref^e [6],Ref^f[7]

3-Electronic properties:

In solid state physics, band theory is a model of energy values that can electrons acquire from within a solid. We calculated the energy bands of chalcopyrite AgGaSe₂, using the FP-LMTO method. The material has the following topology.

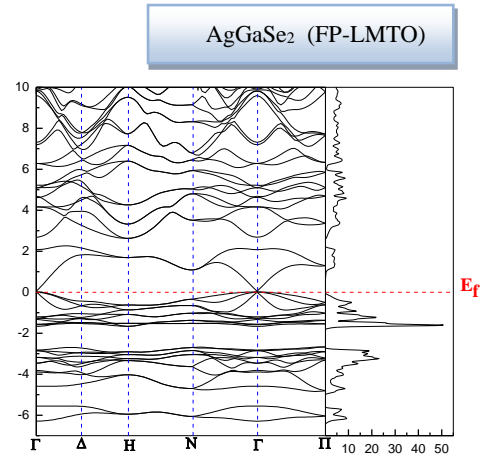


Figure (3): band structure AgGaS₂ obtained by FP-LMTO.

For this material the maximum of the valence band and the minimum of the conduction band are at the same level even at high symmetry point Γ , resulting in a direct gap. The experimental values available to us for this material show a significant underestimation of the energy gap. This was predictable since we have been using the GGA [8]. It is well estab-

lished that GGA underestimate gap energy values due to the fact that they have simple shapes that are not sufficiently flexible to accurately reproduce the energy exchange and correlation.

The energy gap and valence band widths calculated for these compounds are shown in Table 3

Table (3): energy gap AgGaSe₂.

	method	Energy gap
AgGaSe ₂	FP-LMTO	0.04201
	Expeience	1.73 ^e
Ref ^s	[9]	

4-Optical properties:

Figure (4) shows the real and the imaginary part of the dielectric function at normal pressure for a radiation lower than 20 eV for the Ag-GaSe₂ compound. By using the calculated band structures, it would be interesting to identify the inter band transitions that are responsible for the structure of $\epsilon_2(\omega)$.

The analysis of the absorption spectrum shows that the energy threshold of the dielectric function is around 0.394 eV for AgGaSe₂. This energy value corresponds to the static dielectric constant $\epsilon_1(0)$, which is given by the lower limit of $\epsilon_1(\omega)$. It has to be noted that we did not take into account the phonon contribution to the effect of the optical dielectric screen calculated at normal pressure of 9,799 for the AgGaSe₂.

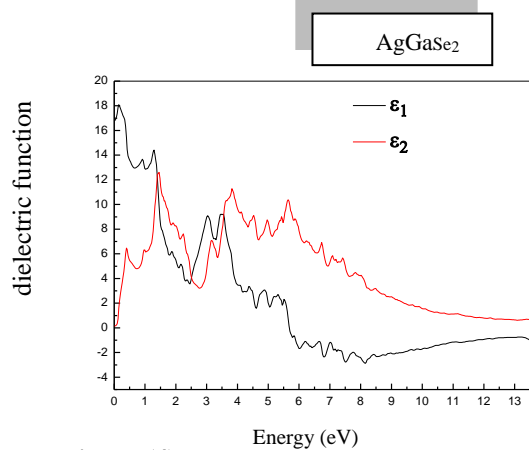


Figure (4): the real part and imaginary part of the dielectric function of AgGaSe₂.

Conclusion:

We have set an objective thorough out this work which mainly consist in determining the structural, electronic, mechanical and optical properties of the chalcopyrite AgGaSe₂, for this purpose we have used the (FP- LMTO) method.

Our results for the structural properties such as lattice parameters (a0 and c0) and internal parameter (u), modulus and its

derivative are in good agreement with the experimental input values. The elastic coefficients predicted by

Table (4): refractive index and static dielectric constants of composite AgGaSe₂.

compound	n	ε0
AgGaSe ₂	3.1304	9.79969

the Mehl models show that our materials are stable in this structure phase. As far as the band structure is concerned we have used the GGA approach.

The latter gives a better topology of the band structure and the values of gap energy we then have optimized the refraction index and dielectric constants.

Values are less than those given by experimental work, which is evident with the use GGA functional. As far as the density state is concerned, we reported contributions of states of each band strips

References:

[1] F. D. Murnaghan, Proc. Natl. Acad. Sci. USA, 30, 5390 (1944).
 [2] J. L. Shay and J. H. Wernik, Ternery Chalcopyrite Semiconductors : Growth, Electronic Properties and applications, Pergamon Press, Oxford, (1974).
 [3] S. Chen, X. G. Gong and S.-H.Wei, Phys. Rev. B 75, (2007) 205209.
 [4] S. Chen, X.G. Gong, S.-H. Wei, Phys. Rev. B 75 (2007) 205209.
 [5] Mesures de vitesse des ondes ultrasons (Ultrasonic wave velocity measurements),
 [6] Ultrasoft pseudopotentials, GGA. TAB.
 [7] T. Ouahrani et al. / Physica B 405 (2010) 3658–3664
 [8] Shouxin cui, Journal of Alloys and Componds 484 (2009) 597.
 [9] B. Tell, H.M. Kasper, Physical Review B 4 (1971) 4455

INDEX OF AUTHORS

A. Chikhaoui	01
A. Mokhtari	01
S. Kharroubi	07
Y. Dahmani	07
O. Nouali	07
A. Tiffour	15
M. Belarbi	15
H. Ouabel.....	19
H. Ouabel.....	26
I. Zouaneb.....	30
M. Belarbi.....	30
N. Abed.....	44
H. Zahloul.....	44
B. BALBAL.....	50
Y. LAALAOUI.....	50
M. BENYETTOU.....	50
K. Khodja.....	54
Y. Bouhadda.....	54
M.Azzouza.....	59
D.Kadria.....	59
B.Djeboura.....	59
D.Karouma.....	59
R Ascaria.....	59

COPYRIGHT AGREEMENT



iwmcs2014@gmail.com

Upon execution of this contract by all parties, it becomes a legally contract. Therefore, please read this contract carefully before signing. Print this contract, Fill the gaps, scan the agreement and send it to iwmcs2014@gmail.com .

Manuscript

Title

Manuscript offered for presentation and publication at

The author(s) must warrant that the manuscript named above that has been submitted to iwmcs 2014 for the publication in the name of article, **IS ORIGINAL**, and has been created by the written permission of the copyright holder for all images, tables, screenshots, graphics, etc.

The author(s) in consideration of the publication named above must understand that:

✓ This manuscript represents the first original publication for a material and not a wholly copy or a part from another work or material.

✓ The Author(s) must represent all the copyrights and the author(s) waives and assign any claim to iwmcs 2014 for the use of any and all rights in the manuscript.

✓ Only the publisher may permit others to publish, make recordings or mechanical renditions, publish club book and micro-film editions, and other electronic versions, quote, and otherwise utilize this work and material based on this work.

✓ This agreement shall be binding upon the parties, successors, assigns and personal representatives.

✓ This agreement represents the entire understandings between parties that the subject matter cannot be modified without the permission of the parties for the manuscript.

✓ This agreement whenever used upon to be construed shall be governed by the laws of the publisher country.



Authors

Name _____ Signature _____ Date _____

Address _____

_____ City/State/Country _____

E-mail _____ Phone _____ Fax _____

Name _____ Signature _____ Date _____

Address _____

_____ City/State/Country _____

E-mail _____ Phone _____ Fax _____

Name _____ Signature _____ Date _____

Address _____

_____ City/State/Country _____

E-mail _____ Phone _____ Fax _____

Name _____ Signature _____ Date _____

Address _____

_____ City/State/Country _____

E-mail _____ Phone _____ Fax _____

Name _____ Signature _____ Date _____

Address _____

_____ City/State/Country _____

E-mail _____ Phone _____ Fax _____

IMPORTANT NOTE

This agreement must be signed and dated and submitted with the complete manuscript to be presented on iwmcS 2014 So print out a copy from this agreement and complete in ink and return it via this E-mail address iwmcS2014@gmail.com . Please note that as this is a legally binding contract.

MONMAJ

This journal concerns both the national and international scientific community and will be primarily focusing on Models and Optimisation of Systems. Systems will be utilized in different applications for example, Web technologies, Information Systems, Decision Systems, Embedded Systems, Control-command Systems and Real-time Systems. Space of journal is also dedicated to mathematical analysis like functional spaces, polynomial computing etc.

Submissions

Papers are invited with interest on the related areas. Each paper should follow the **IEEE format** with title, author's names, affiliation, email addresses, an up to 150 words abstract, and a two columns with 6 single spaced pages and with font size at 10 pts. All papers are submitted electronically in PDF format and in **English language** only and be mailed tomomaj@univ-tiaret.dz or momajournal@gmail.com

LIM Laboratory

Computer Science Department
Faculty of mathematics and computer science
Ibn Khaldoun University of Tiaret Algérie

This journal concerns both the national and international scientific community and will be primarily focusing on Models and Optimisation of Systems. Systems will be utilized in different applications for example, Web technologies, Information Systems, Decision Systems, Embedded Systems, Control-command Systems and Real-time Systems. Space of journal is also dedicated to mathematical analysis like functional spaces, polynomial computing etc.

Submissions

Papers are invited with interest on the related areas. Each paper should follow the IEEE format with title, author's names, affiliation, email addresses, an up to 150 words abstract, and a two columns with 6 single spaced pages and with font size at 10 pts. All papers are submitted electronically in PDF format and in English language only and be mailed to momajournal@gmail.com

LIM Laboratory

Computer Science Department
Faculty of mathematics and computer science
Ibn Khaldoun University of Tiaret - Algeria